Fully developed fires in ”low-energy” and ”energy-efficient” buildings

Kārlis Livkišs

Department of Fire Safety Engineering and Systems Safety
Lund University, Sweden

Report 5382, Lund 2012

HOST UNIVERSITY: Lund University

FACULTY: Faculty of Engineering

DEPARTMENT: Department of Fire Safety Engineering and Systems Safety

Academic Year 2011-2012

Fully developed fires in “low-energy” and “energy-efficient” buildings

Kārlis Livkišs

Supervisor: Prof. Patrick van Hees

Master thesis submitted in the Erasmus Mundus Study Programme

International Master of Science in Fire Safety Engineering

Fully developed fires in “low-energy” and “energy-efficient” buildings

Kārlis Livkišs

Report 5382
ISSN: 1402-3504
ISRN: LUTVDG/TVBB—5382--SE

Number of pages: 95
Illustrations: 41

Keywords
Fire, energy conservation, low-energy buildings, vacuum insulating panels.

Sökord
Fire, energy conservation, low-energy buildings, vacuum insulating panels.

Abstract:
Buildings use approximately 40% of the total amount of the consumed energy in EU and USA. New design approaches and materials are used to reduce the energy consumption for space heating, ventilation, lightning and other domestic necessities. There is a need to investigate effect of these design features on the fire safety.
Increased compartment size can contribute to the fire duration and non-uniform heating of the structural elements. Bigger window areas increase probability of a fuel controlled fire. Advanced glazing systems show better performance, when exposed to high temperatures. Building materials can contribute to the fire load inside a fire compartment. Boundary material properties influence the probability of a flashover and the fire room temperature.
Vacuum insulation panel (VIP) is a state-of-the-art building insulation solution. Bench scale tests were conducted with the VIP samples, consisting of a flammable protective envelope and an incombustible siliceous core. 71-129kW/m2 HRR peak was estimated with the total burning time of approximately 75 seconds. The total released energy was estimated to be 1.6-4.1MJ/m2. Degradation of the core material and increased rate of the heat flow through the sample was observed after exposure to the high heat flux.

Brandteknik och Riskhantering
Lunds tekniska högskola
Lunds universitet
Box 118
221 00 Lund

brand@brand.lth.se
http://www.brand.lth.se

Telefon: 046 - 222 73 60
Telefax: 046 - 222 46 12

Department of Fire Safety Engineering
and Systems Safety
Lund University
P.O. Box 118
SE-221 00 Lund
Sweden

brand@brand.lth.se
http://www.brand.lth.se/english

Telephone: +46 46 222 73 60
Fax: +46 46 222 46 12

DISCLAIMER

This thesis is submitted in partial fulfilment of the requirements for the degree of *The International Master of Science in Fire Safety Engineering (IMFSE)*. This thesis has never been submitted for any degree or examination to any other University/programme. The author declares that this thesis is original work except where stated. This declaration constitutes an assertion that full and accurate references and citations have been included for all material, directly included and indirectly contributing to the thesis. The author gives permission to make this master thesis available for consultation and to copy parts of this master thesis for personal use. In the case of any other use, the limitations of the copyright have to be respected, in particular with regard to the obligation to state expressly the source when quoting results from this master thesis. The thesis supervisor must be informed when data or results are used.

30-04-2012

Abstract

Buildings use approximately 40% of the total amount of the consumed energy in EU and USA. New design approaches and materials are used to reduce the energy consumption for space heating, ventilation, lightning and other domestic necessities. There is a need to investigate effect of these design features on the fire safety.

Increased compartment size can contribute to the fire duration and non-uniform heating of the structural elements. Bigger window areas increase probability of a fuel controlled fire. Advanced glazing systems show better performance, when exposed to high temperatures. Building materials can contribute to the fire load inside a fire compartment. Boundary material properties influence the probability of a flashover and the fire room temperature.

Vacuum insulation panel (VIP) is a state-of-the-art building insulation solution. Bench scale tests were conducted with the VIP samples, consisting of a flammable protective envelope and an incombustible siliceous core. 71-129kW/m^2 HRR peak was estimated with the total burning time of approximately 75 seconds. The total released energy was estimated to be 1.6-4.1MJ/m^2. Degradation of the core material and increased rate of the heat flow through the sample was observed after exposure to the high heat flux.

Kopsavilkums

ES un ASV ēku uzturēšanai izmanto aptuveni 40% no kopējā enerģijas patēriņa. Inovatīvi būvniecības risinājumi un materiāli ļauj samazināt enerģijas patēriņu apkurei, ventilācijai, apgaismei utt. Ir nepieciešamība pārskatīt šo jauninājumu ietekmi uz būvju ugunsdrošību.

Palielinot ugunsdrošības nodalīju platību, jāņem vērā tā ietekme uz ugunsgrēka ilgumu un neviendabīgu būvelementu apsildīšanu. Lielāka ēkas stiklotās daļas platība palielina varbūtība, ka ugunsgrēku kontrolēs degvielas daudzums, nevis pieejamais skābeklis. Uzlabotas stikloto daļu sistēmas ir izturīgākas ugunsgrēka apstākļos, ierobežojot skābekļa iekļuvi ugunsgrēka telpās. Būvmateriālu degšanas īpašības ietekmē telpas ugunsslodzi. Sienu materiālu termiskās īpašības ietekmē vispārēja uzliesmojuma iespējamību un telpas temperatūru ugunsgrēka laikā.

Vakūma izolācijas paneļi (VIP) ir šodienas augstākais sasniegums izolācijas jomā. Testi ar kona kalorimetru ir veikti, lai pārbaudītu VIP paraugus, kas ir veidoti no degtspējīga apvalka un nedegoša silicija iekšienes. 71-129 kW/m^2 siltumenerģijas maksimālā vērtība ir noteikta un degšanas ilgums aptuveni 75 sekundes. Kopējais sadegšanas siltums ir aptuveni 1.6 – 4.1 MJ/m^2. Testa rezultāti uzrāda iekšējās daļas sadrupšanu un termisko īpašību pasliktināšanos.

Table of contents

1 List of symbols and abbreviations

1.1 List of symbols

$A_o -$ *area of opening* (m^2)
$A_T -$ *total surface area* (m^2)
$A_t -$ *total enclosures surace area* (m^2)
$A_v -$ *ventilation opening area* (m^2)
$c_p -$ *thermal capacity at constant pressure* (kJ/kg/K)
$c_s -$ *solid thermal capacity* (kJ/kg/K)
$C -$ *coefficient of natural convection*
$C_d -$ *discharge coefficient*
$D -$ *enclosure depth* (m)
$E -$ *heat of combustion per unit mass of oxygen* (kJ/kg)
$g -$ *gravitational acceleration constant* (m/s^2)
$H_o -$ *height of opening*(m)
$H -$ *enclosure height*(m)
$h_k -$ *effective heat transfer coefficient* ($W/m^2/K$)
$h_{eq} -$ *averaged ventilation opening height* (m)
$H_{ui} -$ *net calorific value*(MJ/kg)
$h -$ *convective heat transfer coeffcient* ($W/m^2/K$)
$I_w -$ *radiative intensity*(W/m^2)
$k -$ *thermal conductivity* (W/m/K)
$k_s -$ *solid thermal conductivity*(W/m/K)
$\dot{m}_a -$ *mass of incoming air* (kg)
$M_{k,i} -$ *mass of combustable material* (kg)
$M_{o2} -$ *molecular weight of oxygen* (g/mol)
$M_{air} -$ *molecular weight of air* (g/mol)
$\mathrm{Pr} -$ *Prandl number*
$\dot{q_C} -$ *rate of heat release due to combustion*(kW)
$\dot{q_L} -$ *rate of heat loss due to replacement of hot gases by cold* (kW)
$\dot{q_W} -$ *rate of heat loss through the walls, ceiling and floor* (kW)
$\dot{q_R} -$ *rate of heat loss by radiation through the openings*(kW)
$\dot{q_B} -$ *rate of heat storage in the gas volume*(kW)
$\dot{q''}_c -$ *convective heat flux* (kW/m^2)
$\dot{q''}_r -$ *radiative heat flux* (kW/m^2)
$Q_{fi,k} -$ *fire load* (kJ)
$\dot{Q}_{FO} -$ *critical heat release rate for flashover to occur* (kW)
$Re -$ *Reynolds number*
$RH -$ *relative humidity* (%)
$t -$ *time*(s)
$T -$ *temperature* (K of C^o)
$U -$ *rate of heat loss through material per unit of surface area and unit temperature* ($W/m^2/K$)
$W -$ *enclosure width* (m)
$x -$ *coordiante*

$\alpha - thermal\ diffusivity$ (m/s^2)
$\alpha - expansion\ factor\ (chapter\ 6.4.1)$
$\delta - thickness$ (m)
$\Delta T - change\ of\ temperature$ (K or C^o)
$\varepsilon -\ emissivity$
$\lambda - rate\ of\ heat\ loss\ through\ matrial\ per\ unit\ \ thickness\ and\ unit\ temperature$ (W/m/K)
$\rho - density$ (kg/m^3)
$\rho_\infty -\ density\ at\ initial\ conditions$ (kg/m^3)
$\rho_s -\ solid\ density$(kg/m^3)
$\rho_a -\ air\ density$(kg/m^3)
$\psi_i -\ factor\ for\ assesing\ protected\ fire\ loads$
$\vartheta - temperature$(K or C^o)

1.2 List of abbreviations

BREEAM –Building research establishment environmental assessment method
CFD –computational fluid dynamics
DNS – direct numerical simulation
EPS –expanded polystyrene
EU –European Union
FDS – Fire dynamics simulator
HRR – heat release rate
LEED – leadership in energy and environmental design
LES – large eddy simulation
OSB – oriented strand board
PUR -polyurethane
PIR - polyisocyanurate
USA – United States of America
VIP – vacuum insulation panel
XPS – extruded polystyrene

2 List of tables and figures

3 Introduction & Objectives

3.1 Introduction

This master thesis is written at the department of fire safety engineering and systems safety at Lund University during the spring of 2012. The thesis objective is to investigate design solutions used to reduce building energy consumption and their impact on fire safety. The thesis is focused on a fully developed stage of enclosure fires. Part of the thesis is dedicated to investigate vacuum insulating panel (VIP) behaviour at high temperatures.

3.2 Background

Sustainable development is an attempt to meet the needs of the present generation without compromising the ability of future generations to meet their own needs [1].

The construction sector contributes to about 40% of total energy consumption and 35% of carbon dioxide emissions, which is argued to contribute to climate change [2]. Attempts to reduce finite recourse consumption and CO_2 emissions have been done by developing new design solutions. Improving building envelope thermal properties, optimizing glazing areas and orientation and increasing air-tightness are some of the measures, taken to reach this goal. The result is a set of innovative buildings, whose design often do not fit into settled limits of traditional fire safety codes.

This thesis will have a focus on a stage of fully developed fires. Fully developed fires are characterised by peak heat release rate (HRR) of combustion. It is assumed that fully developed fire conditions are not tenable for occupants, therefore human life and safety is not directly concerned at this stage. Fully developed fires are of concern regarding to possible fire spread to other buildings or within the building. Two fire spread mechanisms are identified: destructive and convective [3; 4]. Fire can spread between compartments because of loss of the integrity of the compartment bounding structures (destructive fire spread) or by convection of unburned combustible fuel volatiles (convective fire spread) [3; 4].

The estimation of thermal loading is essential to design structures for resisting destructive fire spread. Traditionally standard and parametric fire curves are used to characterise thermal loading to structures. However many limitations are exist for these fire models (opening factors, boundary properties, enclosure dimensions etc.).

3.3 Objectives

This thesis has the following objectives:

1. to make a systematic summary of often used design solutions for reducing the building energy consumption and to discuss their possible impacts to fully developed fire conditions;

2. To recognise the gaps in understanding enclosure fire behaviour and to relate it to existing and future trends in building design;
3. To investigate the behaviour of vacuum insulation panel (VIPs) in fire conditions and to recognise specific issues regarding to a fully developed fire stage.

3.4 The thesis content

This thesis is divided in 3 parts:

- ✓ Chapter 4: "Sustainability and fire safety" describes principles of "low-energy" and "energy-efficient" buildings and current methods for modelling enclosure fires. This part is a basis for further discussions in chapter 5 and 6;
- ✓ Chapter 5: "Design solutions and its impact to fire safety" list most often used measures to reduce energy consumption in buildings and discusses possible related fire safety issues. This chapter is made as a literature review. It is written to meet previously posed objectives 1 and 2;
- ✓ Chapter 6: "Bench-scale tests with vacuum insulation panels" describes performed tests with VIPs. This chapter is made to meet the previously posed objective 3.

3.5 Methodology

The thesis chapter 4 and 5 are made mostly by literature review, but other methods are used as well to reach the thesis objectives. In chapter 5.5.3 hand calculations are performed to estimate increase of fuel load in compartment, when combustible insulation is considered. In chapter 5.5.5 the simulations with CFD program FDS5 are performed to point-out the importance of boundary thermal property changes in fire conditions. The input data for simulations are presented in appendix A. Chapter 5.5.5.4 presents hand calculations, performed to estimate the heating of steel I section in the temperature regimes simulated with FDS5. Assumptions and final results of these calculations are presented in the thesis. Table with extended results is presented in appendix B.

Chapter 6 is made as a report for the experimental part of this thesis. Objectives, methodology and results are presented for bench-scale tests, performed with cone calorimeter (ISO 5660). The tests are conducted with Vacuum insulation panels (VIPs) samples.

3.6 Limitations

This thesis will discuss fully-developed fires. Necessary conditions for reaching this stage (fuel load and available ventilation) will be assumed.

This thesis will identify possible issues during a fully developed fire stage. However, it is not an aim of the thesis to suggest solutions, how to deal with these problems.

The thesis also investigates behaviour of vacuum insulation panels in fire conditions. The author has not been able to find any references about similar tests in available literature sources. The tests should be seen as a first assessment of behaviour of VIPs in fire conditions.

4 Sustainability and fire safety

4.1 Low-energy and energy-efficient buildings

Buildings use about 40% of the total consumed energy in USA and European Union, from which almost half is used for space heating [5; 6; 7]. In 1997, about 25% of total energy consumption in EU was used for space heating [6]. In the first quarter of 2010 50% of UK energy consumption was due to domestic and service sectors [8].

Concept of sustainability can be seen as protecting that what physically sustain us [9]. Based on this principle, each ongoing and future project should minimise its environmental impact. Sustainability is a process, which is focused to reach this particular goal. Driving forces for sustainability are economical and environmental considerations.

Environmental or green building is a building that is designed to reach an optimal environmental performance in terms of ecological loading and indoor environmental quality [10]. This performance should be evaluated throughout the full life cycle of a building, starting from defining the need of building up to recourse recycling and land usage after demolition.

Abel [11] points out two ways to look at buildings that are improved to reduce energy consumption.

1. "Low energy buildings" – buildings whose ultimate goal is not to consume any "purchased energy";
2. "Energy-efficient buildings" – where decrease of energy consumption is motivated economically.

Number of solutions used in "low-energy" buildings might not be suitable for "energy-effective" buildings [11].

Following design strategies are applied in "low-energy" and "energy-efficient" building design [10]:

1. Reducing demand of energy for:
    1.1. Space heating
    1.2. Electricity;
    1.3. Water heating etc.;
2. Utilization of renewable energy sources;
3. Efficient usage of fossil fuels.

Most energy for building necessities is used for space heating and cooling. Figure 4.1 presents consumed energy amounts by percentage for different building necessities for residential buildings in USA.

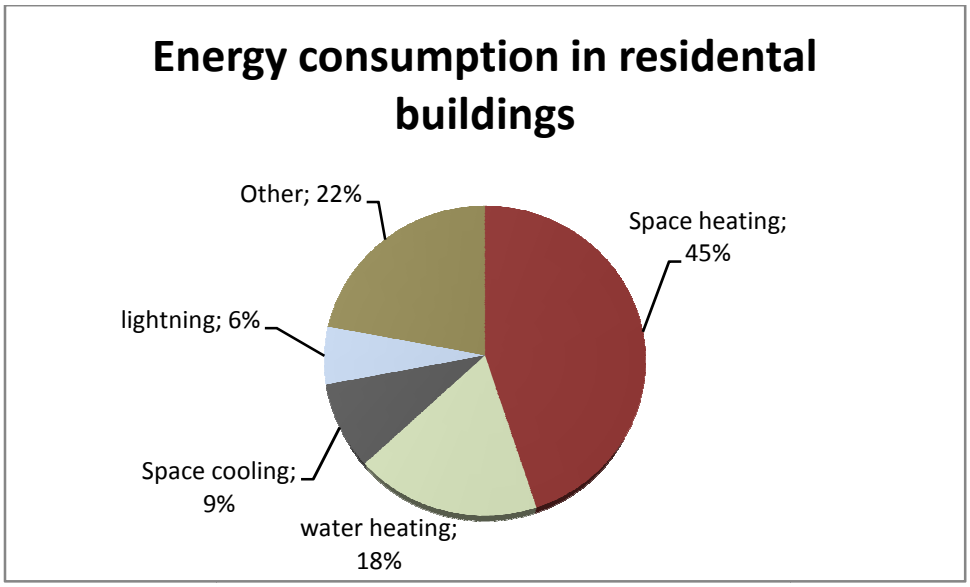

Figure 4.1: Energy consumption by Btu in residential buildings in USA (reproduced from Buildings energy databook [7]).

Depending on country there are different criteria to be reached in order for building to be recognised as a *Green building*. It is generally accepted that the buildings typically use 30kWh/m2 to 15 kWh/m^2 energy per year for space heating [5; 12].

A Classification of the building (depending on climate, area, occupancy type etc.) allows to determine the optimal energy saving measures at the early stages of the project [10]. Following passive and active measures are most often used in "low-energy" and "energy-efficient" buildings [13]:

- ✓ Using advanced insulation (thickness or materials);
- ✓ Using improved glazing and glazing frames;
- ✓ Improving air-tightness;
- ✓ Applying advanced design measures, like optimising glazing areas and orientation, Space optimization;
- ✓ Using heat recovery techniques (from ventilation, domestic hot water);
- ✓ Using heat extraction techniques (solar collectors, heat pumps, from domestic appliances).

A number of projects have been started in order to reduce energy consumption in the building sector. France is performing renovation in all its public buildings to reduce energy consumption by almost 40% in 2020. The renovation plan is carried out in Germany, showing the energy consumption reduction of 50% for the refurbished buildings. Low – energy housing project „Stenlose South", consisting of 750 dwellings has been developed in Danish municipality of Egedal [14] The EU aims to reduce its CO_2 emission by 20 % by the year 2020 compared to the 1990 level [14]. Pursuit to sustainability will continue.

Different environmental parameters are used to evaluate the building performance: energy savings, efficiency of water usage, CO_2 emissions, improved

indoor air environment quality, and stewardship of recourses and sensitivity to their impacts throughout the world. Rating systems include Building Research Establishment Environmental Assessment Method (BREEAM), Leadership in Energy and Environmental Design (LEED)[15; 16; 17] etc. *Green buildings* also should have a positive social impact and they should be "future-proven" in order for it to be usable for longer lifespan [16].

Risk factors (fire, other natural hazards) have often been bypassed in the *Green building* performance analysis [15; 16]. The idea of Green building is largely replaced by idea of energy savings and indoor environment quality in normal operation conditions, without considering its operation in abnormal conditions. It can result in new building solutions, which would be beneficial from energy consumption point of view, but might have a negative impact from the perspective of fire safety (fire development, smoke movement, fire load, fire spread, evacuation or activities of rescue services). Researchers also note that the risk events lead to higher carbon emissions during the building life cycle [16].

Historically, building fire safety has been mainly based on experience and thus it would be usable only in certain limits of validated construction solutions. Innovation is a core of sustainability concept therefore fire safety should be dealt with engineering methods.

4.2 Description of fully developed enclosure fires

4.2.1 Enclosure fire

Commonly the enclosure fire development is divided into stages according to Walton and Thomas [18]:

- ✓ Ignition;
- ✓ Growth;
- ✓ Flashover;
- ✓ Fully developed fire;
- ✓ Decay.

An enclosure fire might go through all of these stages or it might not reach the flashover, thus skipping the fully developed fire stages. Figure 4.2 presents temperature – time relation in compartment fire.

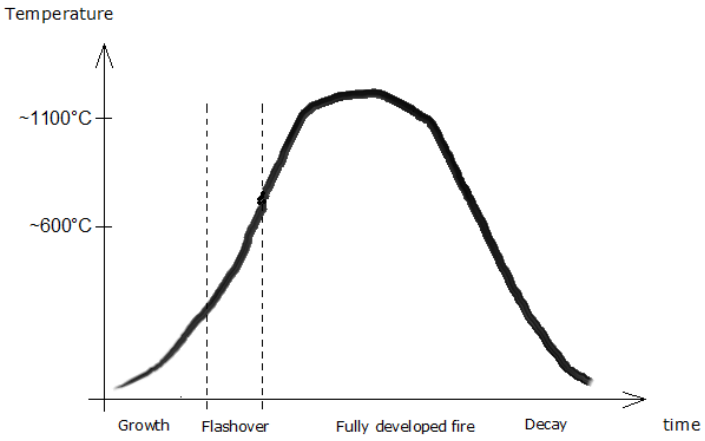

Figure 4.2: Time-temperature curve throughout enclosure fire development.

An enclosure fire scenario involves ignition and generation of smoke immediately after it. Most often, smoke rises to ceiling level due to the buoyant forces. After reaching the ceiling, it follows the path of least resistance, spreading along the ceiling (ceiling jet).

Meanwhile the flaming region radiates energy to the area around it and more fuel get involved in combustion. The pyrolysis rate, HRR and the temperature of the smoke layer in the enclosure increases. At a certain moment the heat flux from the smoke layer and the enclosure boundaries begins significantly affect the fuel bed. At this stage, if sufficient outlet of smoke is not provided, the smoke level reaches flames and the fire self extinguishes due to the lack of oxygen.

If openings are available, the smoke layer reaches the soffit of an opening and starts to exit the enclosure. If openings are sufficiently large, height of the smoke layer stabilizes under top of the opening when a steady state is reached. Hot combustion gases leave the enclosure above a certain level, called the neutral plane. Cold ambient air enters the enclosure under the neutral plane and provides the fire with oxygen. The temperature of the smoke layer and boundaries rises up

to a point when the radiated heat flux can ignite all the fuel in the compartment. This process is called flashover and it is followed by a fully developed fire stage.

A fully developed fire is characterised by a peak HRR, burning rate and temperature in the enclosure. At this stage gas temperatures in a fire compartment can reach 1100 °C or more [19].

It is assumed that people can't survive flashover, so human life is not of concern within the fire room at this stage. Main issue concerning to a fully developed fire is the possible fire spread, thereby endangering people outside of the fire room. Fire can spread to nearby buildings or within the building. Two mechanisms of fire spread are identified [4]:

- ✓ Fire spread by structural destruction and collapse;
- ✓ Fire spread by convection of unburned fuel volatiles.

Fully developed fires are divided into Regime I and Regime II.

Regime I is a fully developed fire, which is controlled by the available oxygen. This occurs in enclosures with relatively small opening areas. In this arrangement, the HRR is determined by the amount of incoming air. The unburned gases might leave the compartment through an opening and burn outside, creating external flaming. Traditionally, Regime I is deemed to be the worst case scenario.

Regime II is a fully developed fire, which is controlled by the amount of available fuel. This occurs in enclosures with relatively large openings. Thus by increasing the opening size in an equivalent enclosure, the fire will change from Regime I to Regime II at a certain point. If the fire is going to be ventilation controlled is also depending on enclosure, fuel load, type and arrangement [20].

Very often fully developed fires are assumed to be ventilation controlled (Regime I), which is valid for the case where relatively small openings provide oxygen. In this case, incomplete combustion generates unburned gases, which escape through the opening and might ignite. This process causes flames to stick out the openings during a fully developed fire [21]. This process is referred as convective fire spread. It is noted to be the most often cause of fire spread between the compartments [4].

Most of the models assume that all the combustion takes place within the enclosure (standard and parametric fire curves, Magnusson –Thelandersson [22] etc.). This assumption leads to the highest thermal loading to structures, thus the higher probability of fire spread by structural destruction. If the structures are not sufficiently resistant, it can lead to fire spread by structural destruction.

The timescale of the pre-flashover and fully developed fire phases are in order of minutes. The typical duration until flashover is observed to be 5-20 minutes, and typical duration of the fully developed fire phase is about 30 minutes [4,3]. However, these durations are determined by fuel load, fuel type, fuel characteristics and dimensions of enclosure.

4.2.2 Flashover

It is assumed that no person in the fire room can survive flashover, thus predicting flashover is important to establish the maximum available time for egress.

A flashover marks the beginning of the fully developed fire. Concept of flashover involves thermal instability created by the initial fire, which results in full room involvement in the fire. The processes involved in flashover are explained by Thomas [23].

Most common definitions of a flashover are [19]:

- ✓ The transition from a localized fire to the general conflagration within the compartment when all the fuel surfaces are burning;
- ✓ The transition from fuel controlled fire to a ventilation controlled fire;
- ✓ The sudden propagation of flame through the unburned gases and vapours collected under ceiling.

Established criteria allow analysing the probability of flashover and fully developed fire stage. This probability is also depending on the enclosure characteristics. Established criteria are mostly thermal i.e. smoke layer temperature, or radiative heat flux to floor. But it can be also qualitative – i.e. flames emerging from openings (Hagglund 1974) [19].

Waterman carried out series of experiments in late 1960s in order to study flashover [24]. From the performed experiments, which involved burning furniture in a compartment 3.64x3.64x2.43 m^3, he concluded that a heat flux of about 20kW/m^2 is necessary for flashover to occur [19]. In this case the flashover criterion was established as ignition of paper targets.

In several other studies (Hagglund, 1974 and Fang 1975) a corresponding ceiling temperature of approximately T=600°C for flashover to occur was observed[19].

It is also noticed that flashover would occur with lower gas temperature, if compartment height is smaller. Flashover has been reported to occur at T=450°C in small scale experiments (room height 1m) [19].

Babrauskas derived an equation from energy balance equations for predicting critical HRR for flashover to occur:

$$\dot{Q}_{FO} = 750 A_o \sqrt{H_o} \qquad (4.1)$$

With following assumptions [18]:

- ✓ The fire is ventilation-controlled, heat release rate is determined by incoming air flow in the compartment;
- ✓ Energy is lost by radiation up to 40% of the walls;
- ✓ Flashover is assumed to occur when the smoke temperature reaches 873K or 600 °C degrees;
- ✓ Specific heat of air c_p=1.0kJ/(kgK);
- ✓ Emissivity of the hot gasses ε=0.5.

The method by McCaffrey, Quintiere and Harkleroad suggests the following expression, presented by Karlsson and Quintiere in book "Enclosure fire dynamics" [21]:

$$\dot{Q}_{FO} = 610(h_k A_T A_o \sqrt{H_o})^{1/2} \quad (4.2)$$

Where:

$$h_k = \frac{k}{\delta} \quad \text{for} \quad t \geq \frac{\rho c \delta^2}{4k} \quad (4.3)$$

And

$$h_k = \sqrt{\frac{k\rho c}{t}} \quad \text{for} \quad t \leq \frac{\rho c \delta^2}{4k} \quad (4.4)$$

With the following assumptions [21,18]:

- ✓ T_g=T_s Cooling of boundaries is neglected;
- ✓ Flashover is assumed to occur when smoke temperature difference ΔT=500°C
- ✓ The rise in temperature is applicable between 20 and 600°C degrees;
- ✓ The method assumes loss of energy by gases moving out from the opening. The equation is not applicable in cases when significant time is required for the smoke layer to reach an opening;
- ✓ Burning is assumed to be in the middle of the enclosure;
- ✓ Properties of ambient air are assumed as follows: c_p=1.0kJ/(kgK) and ρ_a=1.18 kg/m^3.

It can be concluded that the critical HRR for flashover to occur is depending on the dimensions of openings and enclosure and thermal inertia value of the boundary materials($\sqrt{k\rho c}$).

4.2.3 Post flashover fire modelling

For engineering purposes, fire models are required to be balanced between accuracy and simplicity. They must be sufficiently accurate to serve its purpose and simple enough to be usable in a systematic way. Most developed models are partly theoretical and partly empirical. It is suggested, that enclosure fire models might be fully empirical, if the limits of correlations would be acknowledged and the engineers would never go beyond them [23]. However available experimental data range is rather narrow to be directly used for most real life situations. Most tests are performed in unrealistically small enclosures with almost a quadratic shape. Mostly cellulosic fuel is used and the number of measurement devices is limited [25].

One of the most commonly used fire models during all stages of the compartment fire is the methodology by Magnusson and Thelandersson [22]. It has also served as a basis for EN1 parametric fire curves [26]. This method gives estimation of gas temperature-time relation as a function of the fire load density, the opening factor of the compartment, and the thermal properties of the bounding surfaces [21]. The main weakness of the suggested solution from Magnusson-Thelanderson is the fact that it assumes an uniform temperature distribution in the fire compartment

(suited for ventilation-controlled fires in relatively small compartments of almost quadratic shape).
The Magnusson - Thelandersson method uses energy balance equation:

$$\dot{q_C} = \dot{q_L} + \dot{q_W} + \dot{q_R} + \dot{q}_B \quad (4.5)$$

Where:
$\dot{q_C} - \ rate\ of\ heat\ release\ due\ to\ combustion\ (kW)$;
$\dot{q_L} - \ rate\ of\ heat\ loss\ due\ to\ replacement\ of\ hot\ gases\ by\ cold\ (kW)$;
$\dot{q_W} - \ rate\ of\ heat\ loss\ through\ the\ walls, ceiling\ and\ floor\ (kW)$;
$\dot{q_R} - \ rate\ of\ heat\ loss\ by\ radiation\ through\ the\ openings\ (kW)$;
$\dot{q_B} - \ rate\ of\ heat\ storage\ in\ the\ gas\ volume\ (kW)$.

Following assumptions have been made [19]:

- ✓ The combustion is complete and takes place entirely within the confines of the compartment;
- ✓ The temperature is uniform within the compartment at all times;
- ✓ A single surface heat transfer coefficient may be used for the entire inner surface of the compartment;
- ✓ The heat flow to and through the compartment boundaries is one-dimensional, corners and edges are ignored and the boundaries are assumed to be infinite slabs.

Advanced thermal insulation is the primary measure to be taken to reduce energy consumption for space heating. So it is clear that for the purpose of this thesis a particular interest exist for the calculations for heat loss through boundaries (term $\dot{q_W}$). Rate of the heat losses through the compartment boundaries, is determined by solving the general equation of heat conduction in the one-dimensional case under non-steady flow conditions. Temperature depending thermal properties, evaporation of occluded water and possible structural transformations are taken in account [22].

Energy balance equations were solved and satisfactory results were obtained when compared with the experimentally measured values. Obtained data was compared to 4 test series observations [22]. The test results were in acceptable agreement with calculations, however limited usage of different boundary materials and solutions should be noted.

The results of the Magnusson and Thelandersson methodology are summarised in a series of time-temperature curves, which were presented for 7 types of enclosures (type A to type G) [22]. This presentation allows for a systematic and simple way to determine gas temperatures for equivalent enclosures. Although curves are made to be functions of opening factor and fuel load density, wall properties are implemented in the concept “enclosure type”. From examining results of Magnusson and Thelandersson analysis, it can be concluded that more insulating solutions leads to higher maximum temperatures and a longer cooling phase.

4.2.4 Parametric fire curves

For design purposes the EN1 parametric fire curves are widely used to estimate gas temperatures in the fire compartment. The parametric fire curves divide an enclosure fire into 2 phases: heating and cooling phase. The heating phase follows the principles of the standard fire curve and is expressed by natural logarithms, but, unlike the standard fire curve, it is adjusted according to ventilation, fuel load density and material properties. Parametric fire curves have been based on the results of the method by Magnusson and Thelandersson.

As stated by EN1 [26], parametric fire curves can be used with the following limitations:

- ✓ The fire compartment area is limited up to 500 m^2 and 4 m height;
- ✓ The opening factors, expressed as $\frac{A_v\sqrt{h_{eq}}}{A_t}$, must be between 0.02 and 0.2. No ceiling openings;
- ✓ The b factor, characterising thermal properties of boundaries must be within $100 \leq \sqrt{k\rho c} \leq 2200$ ($\frac{J}{m^2 s^{\frac{1}{2}} K}$).

It is also important to note that the parametric fire curves do not directly take in account the properties of boundary materials as a function of temperature. It is allowed to use thermal properties at ambient temperature [26].

4.2.5 Fire Dynamics Simulator (FDS)

An engineering alternative is to use computational fluid dynamics (CFD) modelling programs, for example Fire Dynamics Simulator (FDS). FDS is a CFD model suited for fire driven fluid flow calculations. The model is developed to numerically solve a form of Navier-Stokes equations, appropriate for low-speed, thermally driven flow. A grid divides the computational volume into control volumes. Calculations are being performed for each control volume for a certain time step [27].

Simulations can be performed as a direct numerical simulation (DNS) or a large eddy simulation (LES). In DNS calculations the control volume is small enough to directly resolve all the significant physical phenomena taking place within it. DNS would allow solving fluid dynamics from first principles, thus suggested to give representative results. It however requires much computer capacity and it is not used for most engineering problems. Instead LES uses sub-grid scale models (for example the Smagorinsky form of large eddy simulations for turbulence [27]). LES allow saving computer power and time, however a number of measures must be taken to ensure reliability, reproducibility and validity of the calculations.

FDS is suited to resolve the fluid flow, but regarding to the enclosure impact on the gas temperatures heat transfer within boundaries is of interest. New materials, with more extreme thermal properties, are developed to be used in construction of "low-energy" and "energy-efficient" buildings. FDS, as well as other CFD models, must ensure that heat transfer processes within boundaries are handled with certain accuracy and all the common materials can be appropriately modelled.

In FDSv5 heat conduction is assumed only in the direction normal to the surface and is resolved by the following equation[27]:

$$\rho_s c_s \frac{\partial T_s}{\partial t} = \frac{\partial}{\partial x} k_s \frac{\partial T_s}{\partial x} + \dot{q}_s''' \quad (4.6)$$

The source term, $\dot{q}_s'''$, consists of chemical reactions and radiative absorption [27].

It is assumed, that radiation from gases is absorbed within an infinitely thin layer at the surface of a solid. Net radiative heat flux is defined as sum of incoming and outgoing components:

$$\dot{q}''_r = \dot{q}''_{r,in} - \dot{q}''_{r,out} \quad (4.7)$$

Considering, that in a real case radiation penetrates the solid in a certain depth, radiation transport within the solid is accounted as the source term $\dot{q}_s'''$ [27].

In Large Eddy simulation (LES) [27] calculations of the convective heat flux to a surface is obtained from a combination of natural and forced convection correlations.

$$\dot{q}''_c = h\Delta T \ (\frac{W}{m^2}) \quad (4.8)$$

Where:

$$h = \max[\ C|\Delta T|^{\frac{1}{3}},\ \frac{k}{L}0.037\ Re^{\frac{4}{5}}Pr^{\frac{1}{3}}] \quad (4.9)$$

C is a coefficient of natural convection; C=1.52 for horizontal surface, C=1.31 for vertical surface. k – thermal conductivity of gas. Considering that the Re number is proportionally related to the characteristic length, L, the heat transfer coefficient is weakly related to L. L=1m is used for most of the calculations.

The conductivity and volumetric heat capacity of the solid are defined as:

$$k_s = \sum_{\alpha=1}^{N_m} X_a k_{s,a} \quad (4.10) \quad ;$$

$$\rho c = \sum_{a=1}^{N_m} \rho_{s,a} c_{s,a} \quad (4.11)$$

Where

N_m – $number\ of\ components\ of\ material$

$\rho_{s,a}$ – $component\ density$

X_a – $volume\ fraction\ of\ component\ a$

On the exposed surface and back surface, the following boundary condition is applied:

$$k_s \frac{\partial T_s}{\partial x}\ (0,t) = \dot{q}''_c + \dot{q}''_r \quad (4.12)$$

If the back surface is assumed to be perfectly insulated, the following boundary condition is applied:

$$k_s \frac{\partial T_s}{\partial x} = 0 \quad (4.13)$$

Flashover tests have been conducted and compared between FDS v5.4.3 and SIMTEC simulations by Li, Yan, Zong, Sunden and Liao [28]. Four tests (1.2x1.2x1.2m compartment) were performed with different fuel bed areas and types: gasoline and polyethylene. Two of the tests actually reached a post-flashover stage and the conclusion was made that the experiment results are in a reasonable agreement to both CFD codes, with expectation of the flame zone regions [28].

FDS is a highly user dependant model. Comparing to hand calculations, it requires more input data. Thus it much more relies on the knowledge and the ethics of the user. The Validity and reliability of a CFD programme must be demonstrated for each case. Obtained results are dependent on grid size, but resolving smaller grid size requires more resources.

Chapter 5.5.5 presents simulations done with FDSv5. The objective of the simulations is to estimate the impact of the temperature dependent boundary conductivity on the gas temperatures. The above presented equations 4.6 to 4.13 should be taken in consideration to interpret the results of chapter 5.5.5.

5 Design solutions and its impact to fire safety

Different design strategies are used in buildings in order to:

- ✓ Reduce heat losses through the building envelope (increased the air-tightness, increased the insulation, using advanced window solutions);
- ✓ Benefit from available, natural energy sources (using the solar panels and heat pumps, optimisation of the window areas and orientation, using the double-skin facades, optimisation of the building space);
- ✓ Recover the heat from ventilation and waste water.

This thesis discusses few of these design strategies and measures: increasing air tightness, increasing insulation, optimisation of space, optimization of windows and using the double-skin facades.

5.1 Air tightness

5.1.1 Description

Air infiltration in buildings is of a concern because of the following reasons [29]:

- ✓ Air infiltration reduces the performance of an installed thermal insulation, thus affecting energy demand. Air infiltration accounts for 25-50% of the heating/cooling demand in residential buildings and 15%in commercial buildings[29];
- ✓ Moisture carried by infiltration might have a long term impact on the structural elements;
- ✓ It affects indoor air quality and distribution of air pollutions.

Air infiltration is created by pressure gradients across the building envelope due two main reasons:

- ✓ wind;
- ✓ stack effect (often governing factor for high rise buildings).

Existing ventilation might furthermore contribute to the above mentioned factors.

It can be argued that air infiltration depends on the workmanship of constructors. Estimated air change depending on the envelope construction is presented in the table 5.1. Average residential building air tightness falls into the "medium" category [29].

Table5.1: Characteristic air-infiltration amounts in buildings depending on the air-tightness level.

Tightness of envelope construction	**Average winter air changes per hour**
Tight	0.2 – 0.6
Medium	0.6 – 1.0
Loose	1.0 – 2.0

5.1.2 Fire safety

The thesis is focused on fully developed enclosure fires. For a fire to reach a fully developed stage, air exchange in the fire enclosure is required as described in chapter 4.2.1. Air exchange might be provided by a broken window or another opening. For a window to break during the fire growth phase, sufficiently high energy release must be built up.

It is unknown what air-infiltration levels would be enough to support the fire during its growth stage, if the enclosure without openings is considered. However it is reasonable to assume that by increasing the air-tightness of a building the probability for a fire to reach a fully-developed stage decreases. On the other hand, if additional openings in the building envelope are provided (broken windows) then effect of air infiltration might be neglected.

In normal operation conditions increased air-tightness results in reduction of air currents inside building due to stack effect and wind. In a case of a fire, a similar effect might be considered only if the building envelope is left intact (oxygen to the burning is provided from inside the building through an opened door). In this case predicting smoke movement in buildings might have less uncertainty, because some unknown factors have been eliminated.

Harmathy [3] suggests that limiting air drafts in a building would result in higher gas temperatures in a fire compartment. It would increase potential for loss of structural resistance during the fire. Harmathy also suggests that limiting air-drafts would decrease potential for convective fire spread [3].

The smoke movement in buildings is governed by stack effect, wind pressure, buoyancy created by fire and HVAC systems [19]. Additional effects might occur because of piston effect [30]. The air movement in a building is complex and it is not obvious up until what extend reducing the stack effect and wind influence would have an effect on a fire.

5.2 Window sizes and orientation

5.2.1 Description

In normal exploitation conditions, windows have a negative impact on the energy balance within a building, because glazing solutions have worse thermal properties compared to wall solutions. It also requires introducing additional junctions between the envelope and the window frame. These junctions may cause thermal bridges which might lead to air infiltration.

Glazing is beneficial from health and esthetical considerations. Glazing also allows using natural lighting and gains from solar radiation, thus reducing electricity consumption. Using glazing in an urban environment benefits for general appearance of a city.

It has been suggested that by optimizing the glazing orientation and size, a compromise can be found between energy losses and benefits of having windows. A generally accepted measure for residential buildings is to create large south facing windows and smaller windows facing north. This measure is supported by suggestion that south facing glazing would increase solar energy gains, while smaller windows on the north would have minimal impact on heat loss.

A study on window orientation and size effect on energy consumption in green terrace residential houses was carried out in Sweden in 2005 [31]. The study also shows that using energy – effective windows on the south facade is more effective than having just highly insulating wall. It is also suggested that the area of glazing facing north might be increased with no significant effect on energy consumption. It can be concluded that window sizes and orientation are still to be optimized for residential houses.

On the other hand, glazing areas in modern office buildings are increasing to reach high levels of daylight and attractive building appearance. In order to reduce heat losses, windows in office buildings often are made so that occupants couldn't open them.

5.2.2 Fire safety

Generally the design trend is to increase glazing areas of buildings. In residential buildings, a suggested optimization method is to increase window sizes on the south facade and decrease them on the north facade.

Fire models, including the parametric fire curves, require input data regarding to ventilation conditions. In real life situations assumption about ventilation is made based on glazing areas. The commonly accepted assumption is that glazing will fail when exposed to thermal loading or it will be destroyed by interaction of rescue services. A number of studies have been carried out about loss of window integrity in fire conditions [32].

The relation between energy release rate from combustion and used oxygen is explained by W.M. Thornton in 1917 and later measured by Huggett in late 1970s, as described by Janssens [65]. This discovery allowed to make the necessary assumptions and to correlate the enclosure fire energy release rate with incoming air (and thus with opening dimensions) for ventilation-controlled fires. If the opening area is increased, the fire goes from ventilation-controlled fire (Regime I) to fuel-controlled (Regime II). In a fuel controlled fire, the opening area will not have a direct impact to the HRR from the fire.

Large opening sizes result in non-uniform temperature distribution vertically [20], thus uniform room temperature can no longer be a valid assumption. There might be a need to consider non-uniform heating of structural elements.

The opening factor, given as $\frac{A\sqrt{H_o}}{A_t}$ is used in EN1 parametric fire curves. EN1 parametric fire curves are stated to be valid in range of $0{,}02 \leq \frac{A\sqrt{H_o}}{A_t} \leq 0{,}20$. A survey in University of Edinburgh [33] has shown that sometimes these limits are not representative for real of buildings. Inspection of 28 university buildings in campus "Kings Buildings" reveal that 32 out of 3055 rooms had opening factors out of range. Trend to increase glazing would furthermore bring buildings outside the restrictions of EN1 parametric fire curves.

Also integrity of glazing systems in fire conditions must be evaluated. Resistance of triple glazed windows is still to be evaluated. It is noted that some advanced glazing systems are very difficult to brake for rescue purposes [34].

5.3 Double skin facades

5.3.1 Description

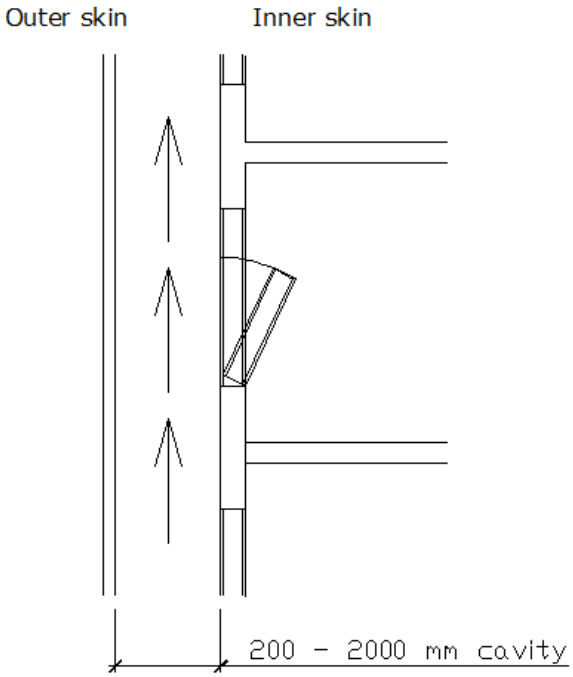

Figure 5.1: Scheme of a multi storey double skin facade

A Double-skin facade is an engineering solution, designed to increase the efficiency of ventilation and gains from solar radiation. Double-skin facades are becoming more popular for modern office building design. A list of buildings with double glazing facades is given by H.Poirazis [35].

Double-skin facades consist of an entirely glazed outer building envelope and an inner envelope, which might be fully or partly glazed. Walls of the inner envelope should allow accumulating of heat in order for the design to work. The distance between the facades is usually between 20cm to 2m [35].

Air in between the building skins is heated by solar radiation. Air circulation is ensured by stack effect. The heat is then transmitted to the inner skin by convection. A process in double skin facades involves optical, thermodynamics and fluid dynamics. Calculations for air flow, temperature in different height and daylight simulations have been attempted, but a complete system is extremely difficult to model [36; 37]. For these reasons energy saving effectiveness of this design is unclear.

5.3.2 Fire safety

There are multiple types of double-skin facades. Horizontal and vertical partition in between both building skins might or might not exist. If no partition exists along building height, this design is called multi storey double skin facade (figure 5.1) [36].

Extensive studies have not yet been done to estimate if and up until what extend double skin facades might have impact on fire safety. It might be suggested that if partitions does not exist along building height, then in principle vertical compartmentation of a building is lost. This might provide possible mean of smoke and flame spread in between building floors. Outer skin might act as a physical barrier, which does not allow for combustion gases to escape outside the building and possibly bending flame tip closer to inner facade. Furthermore natural stack effect might promote this process.

It is suggested that the glazed space could be used for fire escape [36]. This suggestion however would be invalid if compartmentation of this building part is not provided. Furthermore psychological aspects should be considered.

5.4 Floor layouts

5.4.1 Description

The usage of large floor spaces and open atria interconnecting stories for commercial, office and assembly occupancy type buildings is a common trend today. This solution is beneficial from a perspective of light distribution and natural ventilation. Air conditioning and lightning together account for about two thirds of the total energy consumption in a modern office building during its utilization [38]. It is also suggested, that the natural light benefits human health, compared to the artificial light, which is corresponding to the concept of sustainability.

5.4.2 Fire safety

Large spaces provide more flexibility for the interior design. Lightweight separation walls, reaching up until the suspended ceiling, are often used. This solution leaves a void in between suspended ceilings and the actual ceiling, which is often used for cables and air-ducts. The entire compartment should therefore be considered without having any passive physical barriers. Issues of fire fighting in this arrangement include need for evacuation of the entire fire floor. Differences in wall arrangements between the building stories and air drafts created by the HCAV system arrangements are creating issues during the fire fighting operations [39].

Most existing post flashover fire models assume a uniform temperature distribution in the fire compartment [23]. This assumption is made for a ventilation controlled fire in relatively small, quadratic shape compartments, but there is no reason to believe that it's valid also for large or deep compartments (rooms whose depth is significantly larger then width and height).

Researchers argue that the uniform temperature assumption is not valid for fires in real buildings [40; 25; 41; 42]. Nevertheless, a standard fire test requires to test the building structures in furnaces keeping uniform temperatures, so a large part of structural fire safety is based on this assumption.

Stern et al. [25; 43] argues that higher degrees of non-uniformity are to be expected in real building fires and that the standard or parametric fire curves are unsuitable to characterise them considering the aim – to predict thermal loading effect on structures. Analysis by Majdalani and Torero notes, that the high values of the enclosures depth to height ratio lead to non-uniform temperatures distribution horizontally [20].

The uniform enclosure temperature assumption is argued to be fairly representative for relatively small compartments and that is why it is used in EN1 parametric fire curves. The parametric fire curves are allowed to be used up to limits of 500 m^2 for floor area and 4m for enclosure height. A survey done at University of Edinburgh (UK) campus Kings Buildings indicates that dimensions (floor area and height) for 21 of 3055 rooms at the campus does not fall into

required limitations of parametric fire curves [33]. Engineers are forced to apply the standard and parametric fire curves on the compartments, for which these curves are clearly not applicable.

Bigger compartment size results in enclosure fire that is less affected by the enclosure boundaries. There is a lower probability that the fire would reach the flashover as indicated by McCaffrey, Quintiere and Harkleroad in expression 4.2, presented by Karlsson and Quintierein in the book "Enclosure fire dynamics" [21]:

$$\dot{Q}_{FO} = 610(h_k A_T A_o \sqrt{H_o})^{1/2} \quad (4.2)$$

The fire growth will be slower, as it would be less affected by the smoke layer and boundaries. Fire duration would be longer, as it takes more time to consume all fuel step by step moving around the compartment space. Uneven heating of structural elements is expected, which is not considered in the standard fire resistance assessment.

In their studies, Moinuddin and Thomas [42] have tested fire conditions in the enclosures whose depth is significantly larger then width and height. Dimension ratios $D/H \approx 13$ and $D/W \geq 2$ were used in fire tests, where D – depth, H-height and W – width of enclosure. 16 fuel trays with methylated spirits were placed in rows of two throughout the compartment. A narrow wall was used as an opening. The researchers report, that immediately after ignition of the rear tray, the flame moved to the front trays, near the opening. When fuel in the front trays was burnt out, the fire moved to the next row of trays, further away from the opening. In some cases the flame stayed near the opening even after the front trays had no fuel left.

A design approach, referred as "travelling fires", is suggested by Stern-Gottfried et.al. [43; 44]. The methodology divides the fire compartment in "near field" (flaming region of the fire, with relatively high temperature) and "far field" (representing gases away from the flaming region, with relatively cool temperature).

5.5 Thermal insulation

5.5.1 Description

Building thermal insulation is defined as materials or solutions, which minimise rate of heat flow through insulated surface [45]. Thermal insulation of a building envelope is argued to be the most important and primary measure for reducing the energy consumption for space heating. The performance of a building envelope is depending on thermal properties of the envelope components and material ability to absorb and emit solar heat [45].

The rate of a heat flow through a unit surface area of all components, with unit temperature difference between surfaces is called "coefficient of heat transmission" or "U-value". U-value is measured in W/(m²K). Lower U-value means that less energy is lost through the surface. This is a common criterion to evaluate the insulation performance [46].

Requirements for minimum U-values for the components of a building envelope are included in the national building regulations (see table 5.2.). In real design cases, it is not unusual to use more advanced solutions.

Table5.2: Required minimum U-values of building components in northern Europe cities, April 2007. Used by permission of EURIMA [46].

Requirements and/or recommendations on component level			existing requirements					
			U-value [W/m²K]					
			Wall		Roof		Floor	
City	Country	ISO 3166-1 country code	low	high	low	high	low	High
Copenhagen	Denmark	DNK	0,20	0,40	0,15	0,25	0,12	0,30
Aalborg	Denmark	DNK	0,20	0,40	0,15	0,25	0,12	0,30
Tallinn	Estonia	EST	0,25	0,25	0,16	0,16	0,25	0,25
Helsinki	Finland	FIN	0,25	0,25	0,16	0,16	0,25	0,25
Oulu	Finland	FIN	0,25	0,25	0,16	0,16	0,25	0,25
Ivalo	Finland	FIN	0,25	0,25	0,16	0,16	0,25	0,25
Dublin	Ireland	IRL	0,27	0,37	0,16	0,25	0,25	0,37
Kilkenny	Ireland	IRL	0,27	0,37	0,16	0,25	0,25	0,37
Riga	Latvia	LVA	0,25	0,40	0,20	0,20	0,25	0,25
Klapeida	Lithuania	LVU	0,20	0,50	0,16	0,40	0,25	0,50
Vilnius	Lithuania	LVU	0,20	0,50	0,16	0,40	0,25	0,50
Bergen	Norway	NOR	0,18	0,22	0,13	0,18	0,15	0,18
Oslo	Norway	NOR	0,18	0,22	0,13	0,18	0,15	0,18
Trondheim	Norway	NOR	0,18	0,22	0,13	0,18	0,15	0,18
Tromsö	Norway	NOR	0,18	0,22	0,13	0,18	0,15	0,18
Hammersfest	Norway	NOR	0,18	0,22	0,13	0,18	0,15	0,18
Swinonjscie	Poland	POL	0,30	0,50	0,30	0,30	0,60	0,60
Poznan	Poland	POL	0,30	0,50	0,30	0,30	0,60	0,60
Warschau	Poland	POL	0,30	0,50	0,30	0,30	0,60	0,60
Gdansk	Poland	POL	0,30	0,50	0,30	0,30	0,60	0,60
Goteborg	Sweden	SWE	0,18	0,18	0,13	0,13	0,15	0,15
Stockholm	Sweden	SWE	0,18	0,18	0,13	0,13	0,15	0,15
Umea	Sweden	SWE	0,18	0,18	0,13	0,13	0,15	0,15
Lulea	Sweden	SWE	0,18	0,18	0,13	0,13	0,15	0,15
Kiruna	Sweden	SWE	0,18	0,18	0,13	0,13	0,15	0,15

The U-value can be reduced by increasing the thickness of the insulation layer or by using materials with lower conductivity (λ or k) values. The conductivity value is measured in W/(mK). The required minimum U-values can be achieved with conventional insulation (mineral wool, polystyrene etc) with a thickness of about 15-25 cm for walls. In order to achieve "low – energy" standards conventional insulation with thickness of about 30 to 50 cm is being used [13]. However, if more effective solutions are used (lower conductivity value), required thickness will be less. Decreasing insulation thickness is important for a number of reasons: it allows using lighter envelope solutions; it saves space; increases aesthetics and flexibility for architects.

Currently used and future building thermal isolation materials are presented in table 5.3. The table is made by reviewing work by Lyons [47] and Jelle [48].

Table5.3: Currently used, state-of-the-art and future building thermal isolation solutions [47, 48].

Material/solution	**Typical conductivity values W/(mK)**	**Comments**
Mineral wool	≈0.04	Made from natural or synthetic minerals. Mineral wool includes glass wool (produced from borosilicate), rock wool (produced from diabase or dolerite stone) and ceramic wool. Thermal conductivity varies with temperature, moisture content and mass density. Relatively inert in fire.
Expanded polystyrene (EPS)	0.03-0.04	Made from small spheres of polystyrene (from crude oil) containing an expansion agent, e.g. pentane C_6H_{12}, which expand by heating. Thermal conductivity varies with temperature, moisture content and mass density. Combustible.
Extruded polystyrene (XPS)	0.03-0.04	Produced from melted polystyrene (from crude oil) by adding an expansion gas, e.g. HFC, CO_2 or C_6H_{12}. The polystyrene mass is extruded through a nozzle with pressure release causing the mass to expand. The thermal conductivity varies with temperature, moisture content and mass density. Combustible.
Cellulose	0.04-0.05	Made from recycled paper or wood fibre mass. Boric acid (H_3BO_3) and borax ($Na_2B_4O_7*10H_2O$) are added to improve product properties. Thermal conductivity varies with temperature, moisture content and mass density. Combustible.
Cork	0.04-0.05	The thermal conductivity varies with temperature, moisture content and mass density. Combustible.
Polyurethane (PUR)	0.02-0.03	Formed by reaction between isocyanates and polyols. During the expansion process the closed pores are filled with expansion gases, HFC, CO_2, or C_6H_{12}. Combustible.
Polyisocyanurate (PIR)	0.023-0.025	Usually blown with hydrochlorofluorocarbons (HCFCs). PIR foams are more heat-resistant then

		other organic insulation foams. Combustible.
Vacuum insulating panels (VIPs)	0.004-0.008	Open porous core in several metalized polymer laminate layers. Loss of thermal properties due to aging (water vapour and air diffusion) and puncturing of the VIP envelope. Core material can be combustible or non-combustible. Envelope solutions are combustible.
Gas-filled panels	Experimentally ~ 0.04; much lower theoretical values are calculated	Similar to VIP, but instead of vacuum, gas with lover conductivity then air is used (Ar, Kr, Xe).
Aerogel	Commercially available from 0.013-0.014.	Made from silica dioxide by supercritical drying process.
Nano insulation materials		Similar to VIP, with pore size under certain size (40nm). Product of future. No commercial systems are yet available.

B.P.Jelle has suggested desirable properties for future thermal insulation materials [48]. These properties include:

- ✓ T hermal conductivity of about 0.004 W/(mK) with acceptable increase to 0.005 W/(mK) in 100 years of usage;
- ✓ Variable mechanical properties;
- ✓ Flammability characteristics depending on protection. Toxic gases from materials should be identified.

5.5.2 Material performance in fire

Material performance in fires should be considered from two different perspectives:

1. Material effect on fire conditions within fire room, fire and smoke spread and toxicity of combustion products;
2. Consequences of material damage due to risk factors from economical and ecological perspective.

Classical civil engineering deals with materials at the ambient temperature. In fire conditions material have different properties, determined by thermal loading. Some of them have effect on fire conditions. Properties of material can be divided:

- ✓ Chemical (charring, decomposition, flammability);
- ✓ Physical (bulk density, melting etc.);
- ✓ Mechanical (strength and elasticity);

- ✓ Thermal (conductivity, specific heat etc.).

The above mentioned properties are dependent on temperature and might be significantly different in fire conditions, if compared to ambient conditions.

Most of the "green" building certification systems (like LEED) do not directly consider different risk factors in the construction. This can lead to an approach in choice of the insulation materials, where materials are selected depending on their thermal or economical benefits, with insufficient consideration of their behaviour at elevated temperatures [15].

Problems with insulation materials can be accounted in the following ways [49]:

1. The toxicity of the chemical decomposition products from insulation material;
2. Reaction to fire and the fire load;
3. Automatic suppression approaches;
4. Effect on room temperatures due to the energy loss through the boundaries. Effect on the "fire severity" of exposed elements, because of the radiation from walls.

Number 1 is mostly regarded as an issue for pre-flashover fire stage and is discussed by researchers, especially regarding to polymer insulation [50; 51]. Toxicity will not be discussed in detail in this thesis. Numbers 2,3 and 5 can be associated with all stages of compartment fire. Numbers 2, 4 and 5 contributes to fire growth and temperature peak in compartment. Number 3 contributes to potential fire spread.

The reaction to fire of building thermal insulation will have an impact to the fire development. If insulation materials are combustible it increases the fire load in the compartment, thus increasing the fire duration and/or HRR. This results in higher temperatures in a fire compartment and thermal loading to the structures. In cases when a combustible insulation is put up over the height of several stories, it might provide means for fire spread between compartments.

The energy losses are affected by the thermal properties of the compartment boundaries (see equation 4.4). The boundaries with low thermal inertia ($\sqrt{k\rho c}\ group$) will allow less heat to escape through them. In this case, the probability of flashover will increase (see equation 4.2). Higher gas temperatures within a compartment during the fully developed fire stage are expected for the same reason.

Not all insulation solutions have significant impact on fire conditions. Mineral wool has proven to be relatively inert to fire conditions. On the other hand, combustible insulation rise concerns regarding to the reaction to fire. It is important to note that thermal insulation is not used as a lining material. It is protected by other components (most often by plasterboard or steel sheets). It would make sense to investigate response of the full system rather than separate elements.

5.5.3 Reaction to fire and fire load of insulation materials

Often used combustible building thermal insulation materials are expanded polystyrene (EPS), extruded polystyrene (XPS), polyurethane (PUR) and polyisocyanurate (PIR). Polymers are popular because of its thermal properties and low bulk density.

EPS and XPS are materials that melt in high temperatures. It starts to soften at about 90-100°C, but its melting point can't be exactly determined. Polystyrene reaches flashpoint at 350°C and self ignition temperature at 490°C [50]. PUR is a charring material.

A number of tests and research has been done in order to understand PUR, ESP and XPS performance in fire. Tests have also been carried out to investigate different flame retarding agents influence on PUR/PIR mechanical properties and fire behaviour [52; 53; 54].

Bench-scale fire tests with polyurethane foams have been performed with the cone calorimeter [55]. Conventional polyurethane and solutions treated with flame retarding agents have been compared exposed to heat flux of 45kW/m^2. Results indicated maximum values of HRR to be 162 kW/m^2 to 302 kW/m^2 (294 kW/m^2 for conventional polyurethane). Exceptions were samples whose chemical structure was modified to improve thermal and fire performance, their maximum HRR was 48 -130kW/m^2. These samples were also the only ones that couldn't been ignited with radiative heat flux of 40 kW/m^2.

The EN1 [26] suggests net calorific value for polyurethane to be H_{ui} = 25MJ/kg. Other recourses suggest this value to be 22.6 – 28.0 MJ/kg for rigid forms of polyurethane under well ventilated conditions [56]. Values 35.6-38.2 MJ/kg are proposed for polystyrene foams [56].

Simple hand calculations based on the methodology of EN1 are performed as a part of this thesis, in order to assess increase of the fuel load if PUR foams are used. It is important to note that PUR is not the only insulation material that would increase the fuel load in compartment; it refers to all combustible insulation materials. PUR is chosen as an example because the EN1 offers value of fire load for PUR foams, used in construction.

Equation 5.1 is used to determine the fuel load. The input variables for the calculations regarding to the compartment are presented in table5.4.

The EN1 [26] defines the fire load as:

$$Q_{fi,k} = \Sigma M_{k,i} * H_{ui} * \psi_i = \Sigma Q_{fi,k,i} \quad (5.1)$$

Where,

$M_{k,i}$ – $amount\ of\ combustible\ material\ [kg]$

H_{ui} – $net\ calorific\ value\ [\frac{MJ}{kg}]$

ψ_i – $optional\ factor\ for\ assesing\ protected\ fire\ loads$

Table5.4: Input variables for fuel load density example calculations.

Enclosure size	3x3x3m
Enclosure type	Office
Corresponding fire load density per floor area (EN1)	511 MJ/m^2
Opening dimensions	1x1m

Calculations are done for 6 different thicknesses of insulation layer. Considering that thermal insulation is almost never applied on all surfaces of enclosure, two cases of how the insulation is applied is chosen:

- ✓ Case1 – wall with an opening is insulated with rigid PUR foam boards. This arrangement results in 8m^2 insulated surface area ;
- ✓ Case 2 – wall with an opening and one other wall is insulated with rigid PUR foam boards. This arrangement results in 17m^2 insulated surface area.

The results indicate a significant increase in fire load density if polyurethane insulation is used. Up to 24% increase is estimated if two insulated walls are assumed with insulation thickness 26cm. Results are summarised in table 5.5. and figure 5.2.

Table5.5: Increase in fuel load density if polyurethane foams are used in enclosures.

Desnity of polyurethane foam (kg/m^3) [57]	Thickness of polyurethane plates, m	Mass of polyurethane, kg	Fire load of polyurethane,MJ	Fire load density per total surface area without polyurethane, MJ/m^2	Fire load density per surface area with polyurethane, MJ/m^2	Increase in fire load density, %
	CASE 1, insulated surface area: 8m^2					
30	0.04	9.60	240.00	86.77	88.26	1.71%
30	0.08	19.20	480.00	86.77	89.74	3.41%
30	0.12	28.80	720.00	86.77	91.22	5.12%
30	0.18	43.20	1080.00	86.77	93.44	7.68%
30	0.22	52.80	1320.00	86.77	94.92	9.39%
30	0.26	62.40	1560.00	86.77	96.40	11.10%
	CASE 2, insulated surface area: 17m^2					
30	0.04	20.40	510.00	86.77	89.92	3.63%
30	0.08	40.80	1020.00	86.77	93.07	7.26%
30	0.12	61.20	1530.00	86.77	96.22	10.88%
30	0.18	91.80	2295.00	86.77	100.94	16.33%
30	0.22	112.20	2805.00	86.77	104.09	19.95%
30	0.26	132.60	3315.00	86.77	107.24	23.58%

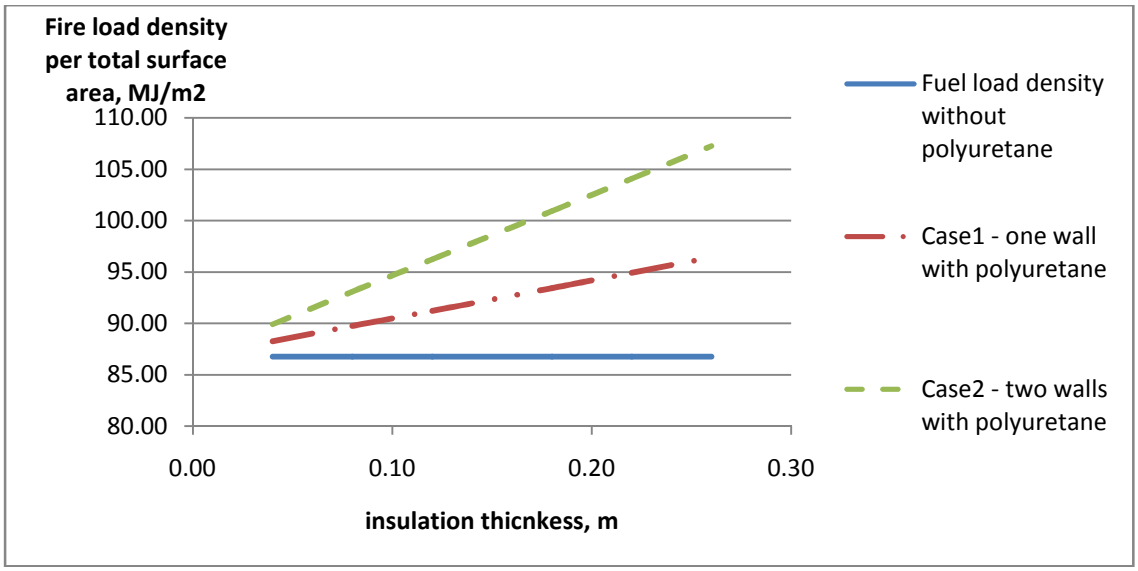

Figure5.2: Enclosure fuel load depending on thickness of polyurethane insulation.

In construction rigid polyurethane is used as part of insulation boards, faced with different materials (metal skins, gypsum, OSB etc.). It can also be used in cavity walls, flooring and roofing. Facings are used to increase fire safety when these materials are used.

Full-scale natural fire tests were done in 2010 with gypsum lined structural insulation panels (SIP), composed of oriented strand board (OSB) facing plates and EPS or PUR insulation [58]. It was observed that the heat was sufficient to melt the EPS, but the plasterboard and OSB governed the overall system performance during the fire. PUR was observed to smoulder, which might raise question about possible ignition after removal of plasterboard. The reduction of the load bearing capacity due to loss of the insulation has been noted for the floor plates. The authors also note a necessity to remove all residual plasterboard, to access and extinguish OSB and insulation [58].

It can be concluded that performance of facing materials is important in enclosure fires. In 2005 full scale tests to determine the performance of gypsum board in real full time fire exposure were carried out by Manzello, Gann, Kukuck and Lenhert [59]. For both gypsum board types, falling out of sections was observed during the cooling phase.

5.5.4 Boundary thermal properties

The energy balance is a commonly used concept, that allows to estimate the fire conditions in an enclosure. The concept predicts the effect of the boundary material thermal properties to the compartment gas temperatures.

The thermal insulation on the outer surface most likely will not affect the fire conditions within a fire compartment, because thermal penetration time for most solutions is longer than fire duration [3]. If however insulation materials are placed

at a certain depth, close to inner surface, its thermal properties will have an effect on the fire conditions. The boundary thermal properties will have the following effects on the flashover and fully developed fire conditions:

- ✓ A smaller critical HRR is required for flashover in a compartment with low thermal inertia values. Flashover will be reached in a shorter time (equation 4.2);
- ✓ A hotter upper layer temperature during a fully developed fire stage is expected in enclosures with boundary materials with low thermal inertia;
- ✓ The boundary lining thermal inertia values are expected to have an effect on the exposure of the structural elements. If the boundaries have lower thermal thermal inertia, the boundary surface would heat up more rapidly and the radiation from them would have more effect on exposed structural elements. This effect is observed in standard furnace tests [19].

A method for the estimation of the fire room temperatures by Magnusson and Thelandersson [22] is used as a basis for the EN1 parametric fire curves, thus there is a need to recognise the assumptions of this analysis. The total coefficient of heat transfer to the boundaries is calculated as consisting of a radiative and convective component. The convective component is assumed to be 20kcal/m^{2}hC ≈ 23W/ m^{2}K. The energy loss through the boundaries is estimated for a one-dimensional case under non-steady flow conditions.

$$c * \rho * \frac{\partial \vartheta}{\partial t} = \frac{\partial}{\partial x}\left(\lambda_x * \frac{\partial \vartheta}{\partial t}\right) \qquad (5.2)$$

The boundary conductivity is treated as being dependent on temperature.

In the EN1 parametric fire curves boundaries are defined as the lining material thermal inertia (parameter$\sqrt{k\rho c}$) at ambient temperature. Parametric fire curves have been compared to the curves of Magnusson and Thelandersson, so indirectly they take in account the change of boundary materials. But because the materials are defined as their initial properties, parametric fire curves are suited only for a certain kind of materials, whose thermal properties are well known. For example, if material A and material B would have the same value of$\sqrt{k\rho c}$ at ambient temperature, these materials would be considered as equal even, if the properties of material A would change much more rapidly as a function of temperature than properties of the material B. Processes like cracking or melting during the fire can significantly increase heat flow rate through the boundaries. The influence of the temperature dependence on the material's conductivity is further discussed in chapter 5.5.5.

The Parametric fire curves have the following limitations of the thermal inertia values of the enclosure boundaries:

$100 \leq \sqrt{k\rho c} \leq 2200$ ($\frac{J}{m^2 s^{\frac{1}{2}} K}$).

For example, unprotected mineral wool has a thermal inertia value below these limits (≈60 J/m^2 /s$^{1/2}$ /K), but steel reaches above the upper limit (≈13000 J/m^2 /s$^{1/2}$) [21].

5.5.5 Temperature dependent boundary properties

5.5.5.1 Objectives and methodology

Simulations with CFD model FDS version 5.5.3. are performed to investigate the fire compartment temperatures, when the conductivity dependence on the temperature is assigned for the boundary materials. The related heat transfer correlations used in FDSv5 are presented in chapter 4.2.5.

5.5.5.2 Simulation set-up

The enclosure and the locations of the temperature measurement devices are presented in figure 5.3. A single enclosure with dimensions of 3.6x2.4x2.4m is modelled. The wall thickness is chosen to be 0.02m.
Two openings at the opposite narrow walls are created:

- ✓ „door" opening of size 1.2x1.5m;
- ✓ „window opening" of size 1.6x1m.

This arrangement results in an opening factor of 0.13 $m^{1/2}$ (according to EN1) [26].

A 1x2m burner is positioned in the middle of the enclosure. The assigned heat release rate per unit area (HRRPUA) is 1000kW/m^2. This arrangement results in a constant 2MW fire. The HRR is settled to be constant and would not be affected by the enclosure boundaries. The openings and the burner were modelled to ensure that the gas temperatures within the compartment reach a value above +600 °C and that all combustion takes place within compartment (no flames reaching out of compartment).

The gas temperatures were calculated by using devices with assigned QUANTITY="TEMPERATURE". These devices are not thermocouples, thus they do not simulate thermocouple error. 3 trees of five devices are modelled on heights of 0.3m, 0.8m, 1.3m, 1.8m and 2.3m (see figure 5.3). The burner size and location is adjusted so that the temperatures are not measured in the flaming region.

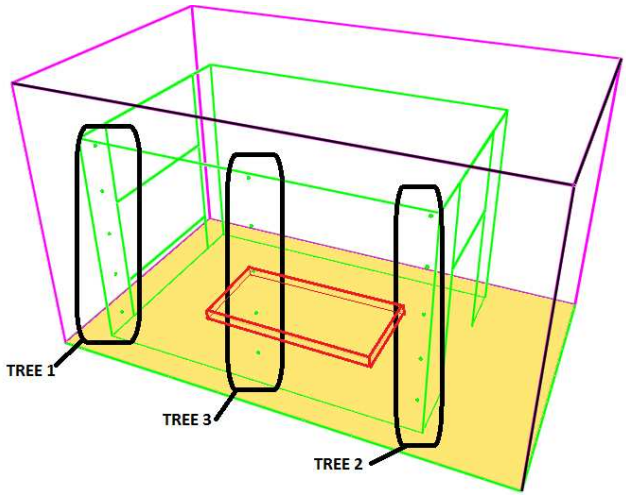

Figure 5.3: Computational domain for done simulations.

The boundary material is referred as „VIP" (see Annex A). This material can represent any existing or future material.

By using the CONDUCTIVITY_RAMP, temperature dependent conductivity values are assigned to the boundary material. The conductivity value at ambient temperature (+20°C) is assigned to be 0.004W/(m*K). Four different scenarios (Case 1-4) are chosen for the conductivity dependence on temperature. Extremes are case 1 and case 4. For case 1 the conductivity changes only very slightly with increase of the temperature. For case 4 the conductivity changes only slightly up until 500°C, then it rapidly increases. The conductivity changes in temperature are presented in table 5.6. and figure 5.4.

Table 5.6: Conductivity changes as a function of temperature for material „VIP".

Temperature, °C	**Conductivity, W/(mK)**			
	CASE1	**CASE2**	**CASE3**	**CASE4**
20	0.004	0.004	0.004	0.004
500				0.005
900	0.0075	0.5	1	60

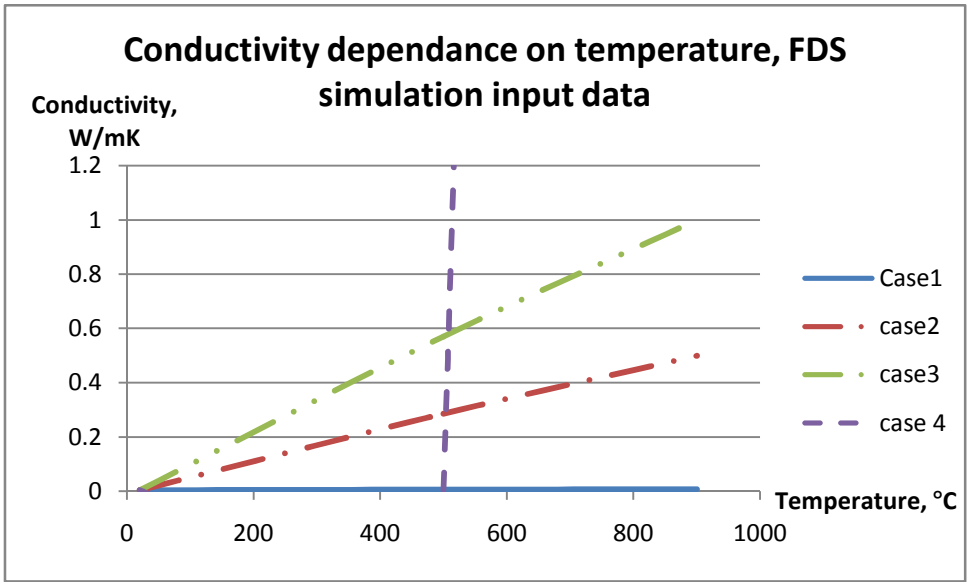

Figure 5.4: The conductivity as a function of temperature for material „VIP".

The same specific heat capacity and density values are assigned for boundaries. The function SPECIFIC_HEAT_RAMP is used to assign c=0.726 kJ/(kg*K) until the temperature reaches T=43C and c=0.915kJ/(kg*K) for T=178°C. The density is assigned to be ρ=192kg/m^3.

5.5.5.3 Results

The simulations have been done for two different grid sizes: 0.1x0.1x0.1m^3 and 0.05x0.05x0.05m^3. Both of these grid sizes are considered to be fine mesh according to FDS Mesh Size Calculator [67]. Both grid sizes showed differences in the absolute measurement values for temperatures, with nevertheless the same

trends. The results obtained with the 0.05x0.05x0.05m^3 grid size are presented in figures 5.5 – 5.7. Results obtained with coarser grid (0.1x0.1x0.1 m^3) are not presented, because it is expected that finer grid leads to more precise results. Making grid even finer was impossible because of limited computer capacity.

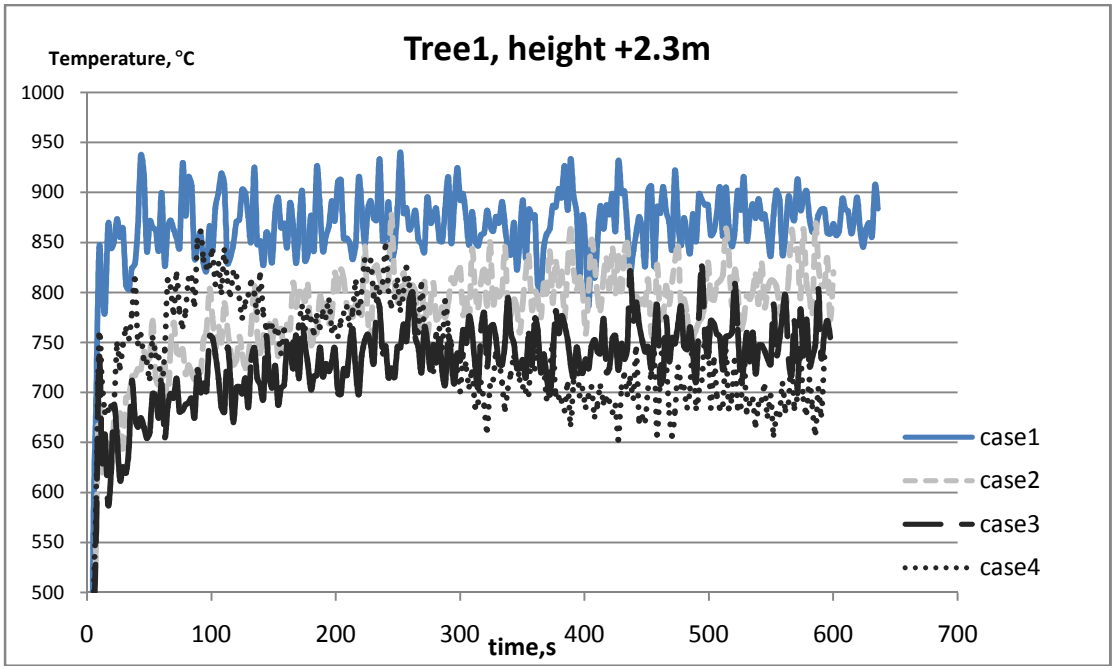

Figure 5.5: Time-temperature at height +2.3m for tree 1

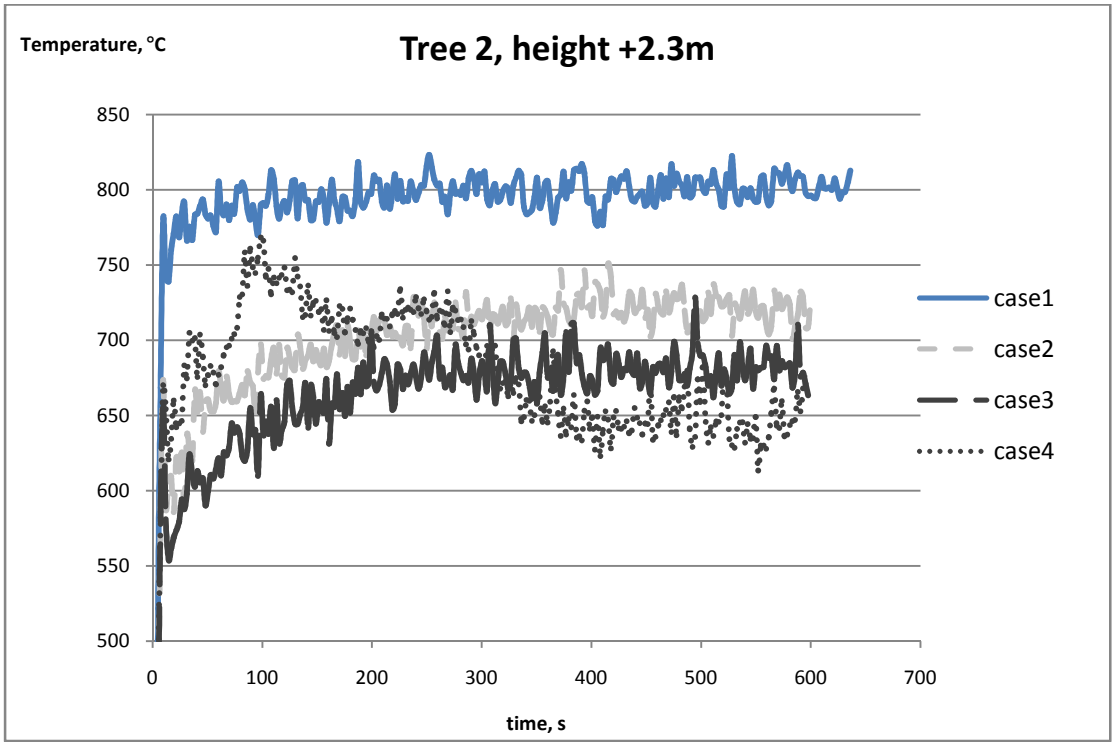

Figure 5.6: Time-temperature at height +2.3m for tree 2

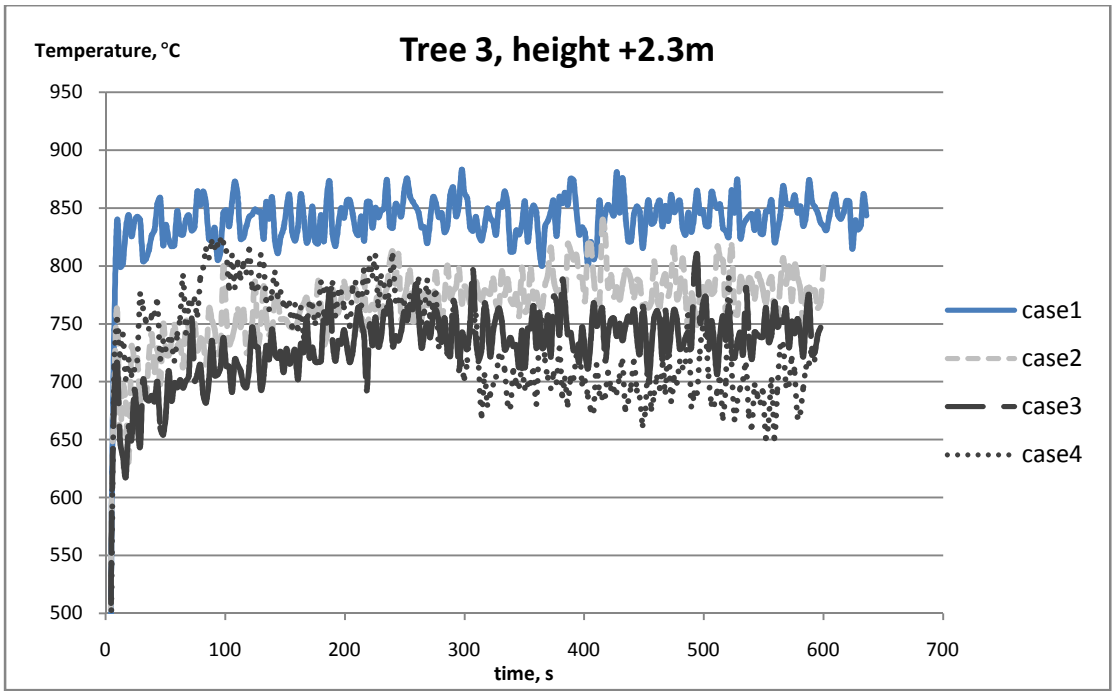

Figure 5.7: Time-temperature at height +2.3m for tree 3

The results show that the loss of thermal properties of boundary materials leads to lower enclosure gas temperatures. A difference of about 150°C degrees is obtained for the later stages of a fire between the extreme cases 1 and 4. Up to 200°C difference is measured on tree1, close to the „window" opening.

A constant HRRPUA value is used in all simulations. It means that the assumption is made that the combustion is not affected by the radiation from the walls. A more realistic fire scenario would involve change of burning rate depending on the thermal inertia of walls. To simulate this scenario pyrolysis model should be used. At this stage, pyrolysis model for FDS is not reliable enough, so it was not used for these simulations.

5.5.5.4 Heating of unprotected steel section

An estimation of the enclosure gas temperatures is done to characterise the thermal loading on the exposed structures. The exposed structures must be capable to withstand the fire conditions until the fire burns out. For steel structures the failure is expected due to loss of strength at high temperatures.

The heating of the unprotected steel section is calculated for presented fire conditions (case1 to case 4). An universal column 254x254x167 (BS4:Part1 2005) will be used for this example (figure 5.8 and tables 5.7 and 5.8)

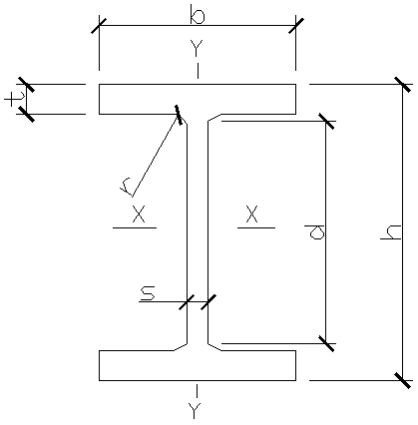

Figure 5.8: Dimensions of the universal column 254x254x167 (BS4:Part1 2005).

Table 5.7: Universal column 254x254x167 (BS4:Part1 2005) dimensions.

Designation	Mass per m	Depth of section	Width of section	Thickness of		Root radius	Depth between fillets	Area of section
				web	flange			
	M	h	b	s	t	r	d	A
	kg/m	mm	mm	mm	mm	mm	mm	cm^2
254x254x167	167.1	289.1	265.2	19.2	31.7	12.7	200.3	213

Table 5.8: Assumed steel properties.

Steel density	Steel specific heat	Emissivity of steel	Convective heat transfer coefficient
ρ_s	c_s	ε_s	h_{conv}
kg/m^3	kJ/kg/K		$kW/m^2/K$
7850	0.6	0.9	0.023

The steel member is heated by the hot gases due to radiation and convection:

$$q''_{total} = q''_{rad} + q''_{conv} \quad (5.3)$$

Where radiation and convective heat fluxes for the 1 dimensional case are equal to:

$$q''_{rad} = \varepsilon_s \sigma \left(T_g^4 - T_s^4\right) \quad (5.4)$$

$$q''_{rad} = h_{conv}\left(T_g - T_s\right) \quad (5.5)$$

The heat flow through a unit surface area of the section is stored in the section volume. If the member is exposed uniformly from all sides this leads to:

$$q_{total}'' * \Delta t \dot{*} A_{surface} = \rho_s c_s \Delta T_s V \quad (5.6)$$

Equation 5.6 describes the body as having lumped capacity properties – conduction in the section is not taken in account and there is no temperature drop over the cross section. This assumption is valid because Bi number for given case is less than 0.1[19]:

$$Bi = \frac{h\frac{t}{2}}{k} = \frac{23 * \frac{0.0317}{2}}{45} = 0.008$$

Combining the equations 5.4, 5.5 and 5.6 allows us to calculate the steel section temperature increase in each time step as a function of gas temperature:

$$\Delta T_s = \frac{A_{surface}}{V}\frac{\Delta t}{\rho_s c_s}\left(h_{conv}(T_g - T_s) + \varepsilon_s \sigma\left(T_g^4 - T_s^4\right)\right) \qquad (5.7)$$

The following simplification can be made:

$$\frac{A_{surface}}{V} = \frac{P_{cross\ section}}{A_{cross\ section}} \qquad (5.8)$$

An excel spread sheet is made to calculate the heating of the steel section during the simulated time for all simulated cases (case 1 to case 4). Results are presented in figure 5.9 and in table in Annex B.

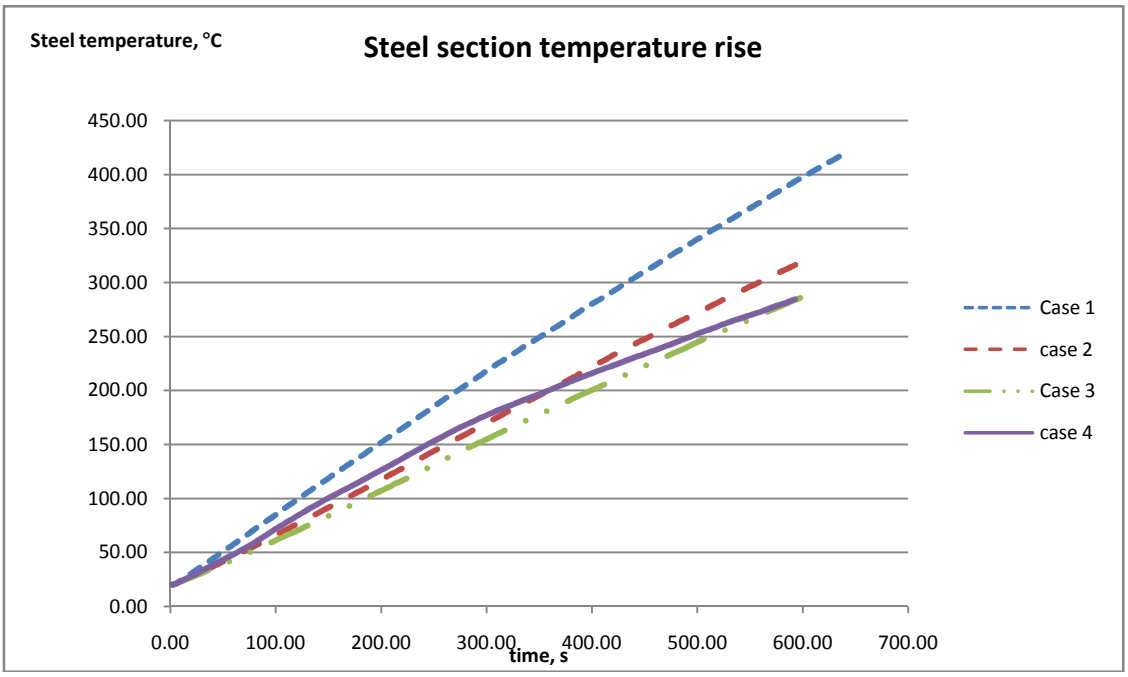

Figure 5.9: Heating of I steel section 254x254x167 in different heating regimes case 1 to case4.

The results indicate significant differences in the steel temperature differences for cases 1 to 4. In case 1 the steel temperature reaches about +400 °C in 600 seconds. In case 3 the steel temperature reaches about +275 °C. In case 4, the steel heats up more rapidly compared to cases 2 and 3. After about 300 seconds heating slows down and after 600seconds the steel temperature is similar to case 3.

Considering that the steel temperature increase is linear for case1 to case3, extrapolation of these results can be performed easily. A common assumption is that the critical temperature for steel is 550 °C, after which steel loses its strength very rapidly. In the heating regime case1 the section will reach this temperature in approximately 825 seconds. In case2 it will occur after about 1030 seconds, in case 3 – 1180 seconds. Considering the heating trend for case4, it is expected that the steel will reach its critical temperature even later in this case.

Calculations show that heating of the structural members are directly affected by the boundary thermal property change as a function of temperature.

The following assumptions and limitations are used in the described calculations:

- ✓ The steel section is heated only by convection and radiation of the hot gases. The radiation from the boundaries is not considered;
- ✓ The steel section is treated as a lumped heat capacity model;
- ✓ A 1-dimensional heat flow is considered;
- ✓ The steel section is modelled as an ideal grey body;
- ✓ The steel properties are temperature independent;
- ✓ The steel section is infinitely long.

5.5.5.5 Discussion and conclusions

The change of boundary conductivity as a function of temperature during the fire can significantly influence the gas temperatures and heating of building structures. In real life situations, the heat transfer through boundaries might be affected by chemical or physical processes (cracking etc.).

The presented simulations exaggerate probable real life scenarios. Using highly isolative boundaries on all compartment surfaces is not a common practice. Usually thermal insulation is used in the building envelope, thus in general only few enclosure surfaces would be composed with highly isolative materials. Sometimes however the insulation can be used also for inner walls to ensure acoustic comfort.

Plasterboard is often used to protect thermal insulation materials. Considering plasterboard properties and relatively short timescales of enclosure fires, plasterboard will most likely govern temperatures in a fire room.

Furthermore the size of the enclosure has a great impact on gas temperatures, which is not discussed in these simulations.

Even considering discussed imperfections, the presented simulations give a proof how sensitive the temperature inside the fire room is when the conductivity changes of the boundary surfaces changes a lot as a function of temperature. This indicates that using initial material thermal inertia values at ambient temperatures might not be a proper way for estimating the fire room temperatures. As discussed previously, “Low -energy” buildings introduce new materials to the construction. The characteristics of these materials should be examined, and their relevance to existing fire safety codes must be evaluated.

6 Bench-scale tests with vacuum insulation panels

6.1 Test objectives

Tests with the cone calorimeter (ISO 5660) were performed to evaluate the behaviour of vacuum insulating panels (VIPs), when exposed to heat fluxes of 30, 40 and 48 kW/m^2. Results could be used:

- ✓ To identify specific characteristics of VIPs in case of a fire;
- ✓ As an input data for CFD models or empirical models to predict fire spread.

6.2 Background

6.2.1 Vacuum insulation panels

Today, the most commonly used thermal insulation materials are mineral wool, polystyrene and polyurethane foams, with conductivity of $\lambda \approx 0.03 - 0.04$ W/m/K. The suitability of vacuum insulating panels (VIPs) for building applications is discussed by a number of researchers [6; 8; 60]. The conductivity of VIPs is about $\lambda \approx 0.008$ W/m/K, depending on the thickness of the insulation. This value is almost five times lower than the conductivity of conventional insulation materials. VIPs allow reaching equivalent insulation level with much thinner building envelope. It provides more flexibility to architects and is especially important in renovation works. VIPs can be applied for internal or external surfaces of buildings [8].

A VIP is a thermal insulation system, consisting of a rigid porous core material and multiple layers of protective envelope. The pore size of the core material is chosen to maintain vacuum below minimum critical level and to physically support the VIPs envelope [8].

The VIP core can be made from[8]:

- ✓ EPS or PUR foams with porous size 30-250 m^{-6} ;
- ✓ fumed silica with porous size of about 300x10^{-9} m;
- ✓ glass fibre.

The VIP envelope consists of a protective layer, a barrier layer and a sealing layer. Polyurethane, polyethylene terephthalane and metalized layers of polymers are used for the envelope [8].

The heat transfer process in VIPs involves convection, solid conduction, gas conduction and radiation. VIPs are designed to suppress convective heat transfer, thus reducing total heat transfer. Its thermal properties are affected by the temperature, pressure, moisture, mechanical impacts and aging [6; 48].

Before 2005, VIPs have been integrated in five different buildings in Germany and Switzerland. It has been concluded that VIPs are suitable for buildings [6]. With several companies, Germany holds a large market share of VIPs supply in Europe. Information about technology, applications and projects, involving VIPs, can be found in website www.vip-bau.de [61], financed by German Federal Ministry of Economics and Technology.

6.3 Methodology

6.3.1 Test description

Bench-scale tests were performed at the fire laboratory of Lund University Physics department during March and April, 2012. VIP samples of size 120x200x20 mm^3 were tested with a cone calorimeter (ISO 5660). The test apparatus (cone calorimeter) is standardized, but the performed tests did not follow standard methodology. The test methodology is described in this chapter.

The tests were designed to measure:

- ✓ HRR (oxygen depletion method);
- ✓ Temperature of the exposed and unexposed surfaces of the sample (measurements done with thermocouples).

6.3.2 Test samples

6 tests were performed with samples of the same VIP solution. The samples were of product "va-Q-vip B", provided by the company "va-Q-tec AG" [68]. All samples were of the same size (200x120x20 mm^3).

The core material of all samples was made from micro-porous silica acid powder and an opacifying agent. According to the manufacturers given information, this core solution is non-combustible. The core of the samples was wrapped in multiple protective layers: 3 layers of metalized polyester (metalized with aluminium), one layer of polyurethane and one layer of black fibreglass. The envelope solution is inflammable.

One of the sample sides had an envelope junction. The side with this junction was used as unexposed side in presented tests.

According to the information by the manufacturer, thermal conductivity at ambient conditions for the test samples is λ=0.007W/m/K. The mass per unit area for a thickness (2cm) is 4kg/m^2. The mass of the sample was therefore calculated m=0.096kg. No information is available about the conductivity, density and specific heat capacity at higher temperatures.

6.3.3 Test set-up

The tests were not standardized because of the size of the test samples. For the tests, samples with dimensions 0.2x0.12x0.02 m^3 were used. Availability of the samples was limited and these dimensions were chosen to be most appropriate for test aims. If VIPs are mechanically impacted they lose their insulation ability, thus the test samples could not be cut in order to fit the standard cone calorimeter sample size.

The sample holder, fitted for the sample size was made. The holder was made from a Promatec ® [62] board and mineral wool (λ_{wool}=0.04W/m/K). The holder ensured the correct position and the stability of the sample beneath the cone heater during the test. The edges of the holder were cut out from a single piece of rigid mineral wool slab. The mineral wool was fixed to a Promatec ® board with hot glue. The mineral wool was also glued to the base of the holder, ensuring insulation of the back side of the sample.

The mineral wool was used to minimise the heat transfer along the sides of the sample. Mineral wool from rolls was used in between the sample and the edges of rigid mineral wool to further reduce thermal bridges and to ensure air-tightness. A schematic view of the sample holder is presented in figure 6.1.

a)

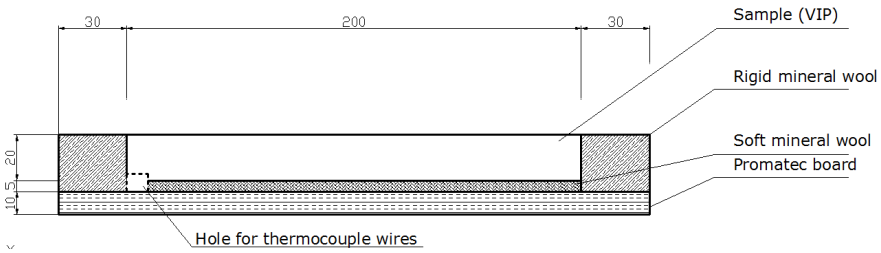

b)

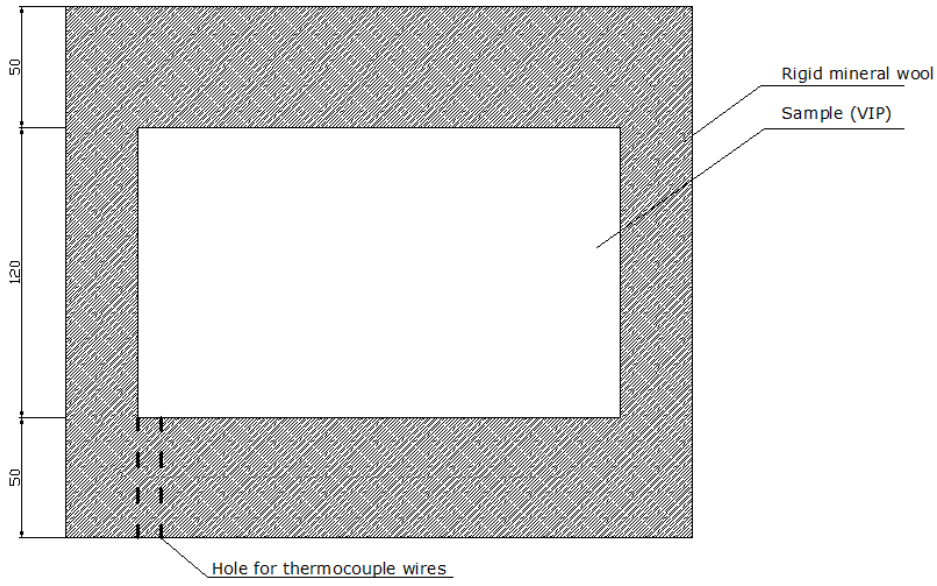

c)

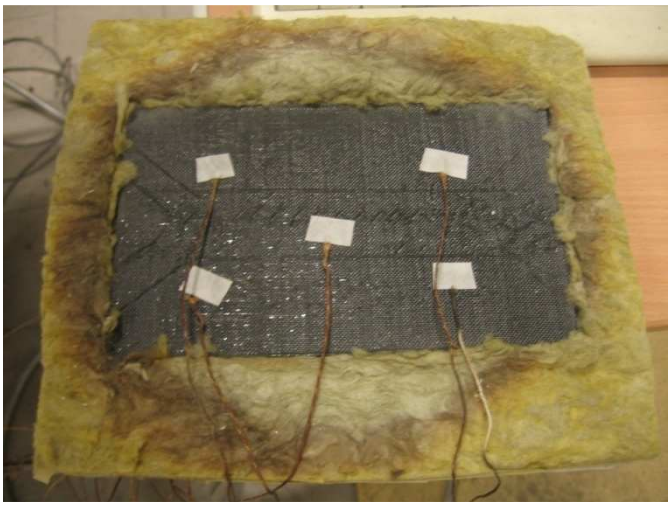

Figure 6.1: A schematic view of the sample holder. a) cross section view from side. b) view from above c) Photo of a sample in the holder.

6.3.4 Measurement devices

12 K-type thermocouples were used to measure the temperature of the sample surfaces. 5 thermocouples were placed on the exposed side and 5 thermocouples are placed on the unexposed side. 2 thermocouples were placed on the side surfaces of a sample. Locations of the thermocouples are presented in figure 6.2.

a) b)

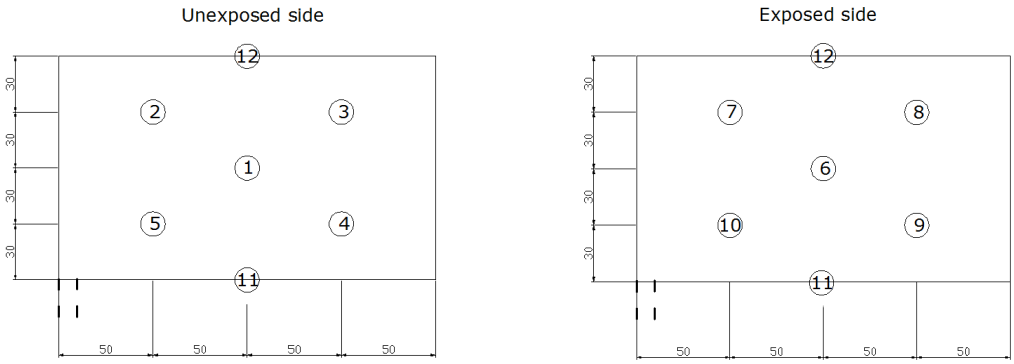

Figure 6.2: Locations of thermocouples on sample surface a) unexposed side. b) exposed side.

The thermocouple wires from the unexposed side were leaving the test holder through a hole in lower side of the rigid mineral wool edges (see figure 6.1). The hole was then filled with mineral wool.

The thermocouple beads were welded and fixed to the sample with a glass fibre tape ("stick-on" method). This method was chosen because it allows fixing the thermocouples without mechanically affecting the samples. Using glass fibre tape is simplest way, which also creates several problems. For example, thermocouples might not be properly fixed and lose their position during the test. Different methods of fixing thermocouples to a surface are discussed by P.R.N.Childs [63].

A gas analyser (Servomex 4000 series) was used to measure the concentration of the combustion gases. HRR was calculated with an oxygen depletion method by using measured concentrations of O_2 and CO_2[64]. HRR was calculated for 5 out of 6 performed tests.

The mass of the samples was measured with scales after the tests. A measurement of one single sample was used as a reference for the initial mass.

The time of ignition and the duration of burning were estimated from the calculated HRR and the temperature of the exposed surface.

Other physical changes or occurring phenomena were observed during and after the tests.

6.3.5 Test conditions

6.3.5.1 Tests

The samples were exposed to heat fluxes of 30; 40 and 48kW/m^2. Heat flux was created by the conical heater, which was set up to a corresponding temperature. The applied heat flux is depending on temperature of cone heater and distance between cone heater and exposed surface. The choice of the cone heater temperature was based on previously done calibrations and a known distance between the heater and the exposed surface (2.5cm). The heat flux was not measured before each test. The cone temperature and corresponding heat fluxes are presented in table 6.1.

Table 6.1: Cone temperature and corresponding heat flux for tests.

TEST NUMBER	**Cone temperature, C**	**Corresponding heat flux in distance 2.5 cm from edge of cone, kW/m^2**
TEST1	725	40
TEST2	725	40
TEST3	650	30
TEST4	650	30
TEST5	775	48
TEST6	775	48

Usually, in cone calorimeter tests, samples with a surface area of 100x100 mm^2 are used. In presented tests the exposed surface size was 200x120 mm^2. It is expected that the applied heat flux is not uniform on the exposed surface.

Two tests were conducted to evaluate the performance of the test-set up and the sample holder. In these tests, Promatec® samples with size 200x120x10 mm^3 were used. Since the sample holder was suited for VIP samples, but Promatec®

samples were thinner, the distance from the cone heater to the surface of the Promatec® samples was more than 2,5cm. As a consequence the actual heat flux is unknown. The distance was kept consistent between both tests. As expected, the test results show a clear transition region of a temperature increase on the unexposed side when the unexposed side reaches 100 °C (see figure 6.3) . This may be explained by changes in the specific heat capacity and water vapour formation. Indirectly it shows that obtained results are logical and predictable. Average (average of the 5 thermocouples on unexposed side) measured temperature on the unexposed side for these tests is presented in figure 6.3.

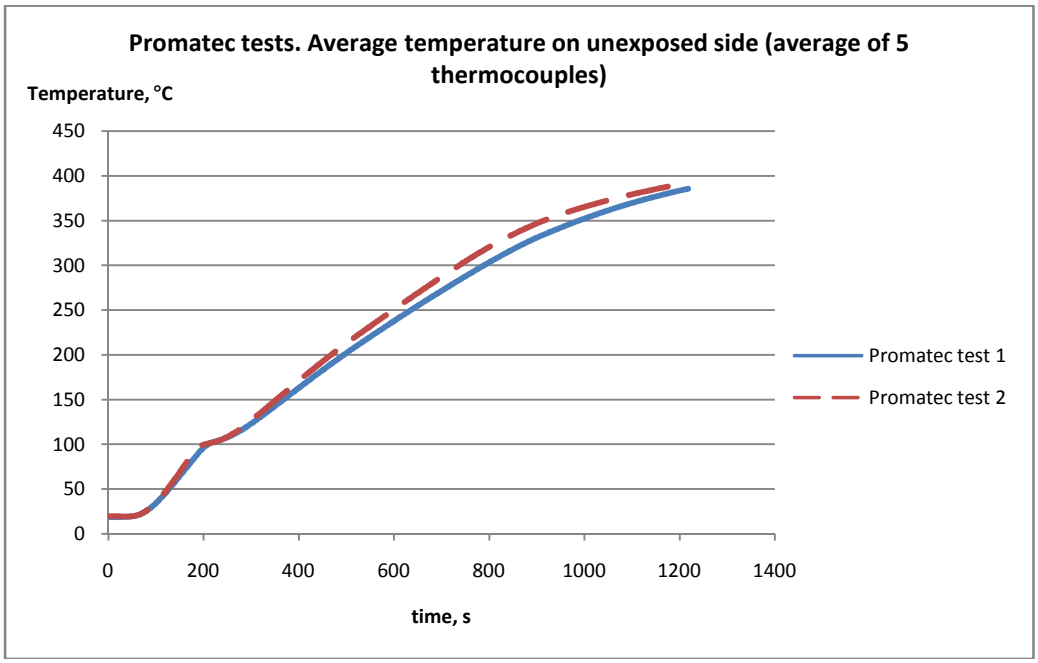

Figure 6.3: Results from tests with Promatec board samples.

6.3.5.2 *Correspondence to real fire conditions*

The test objective was to investigate VIPs performance under flashover and fully-developed fire conditions. Samples were exposed to heat fluxes of 30; 40 and 48kW/m^2. Increasing heat flux above 48kW/m^2 was not done because of technical considerations. This chapter describes the tests conditions in accordance to its objective.

The radiative heat flux of 20kW/m^2 from the smoke layer to the ground is often used as criteria for flashover. This heat flux is enough to ignite a paper (spontaneous ignition). It is also more than enough to ensure piloted ignition for wood [19].

Heat is transferred to a surface of material by convection and radiation. The total heat flux can be calculated by following equations:

$$\dot{q}''_{total} = \dot{q}''_{conv} + \dot{q}''_{rad} \quad (6.1)$$

$$\dot{q}''_{conv} = h * \Delta T \quad (6.2)$$

$$\dot{q}''_{rad} = \sigma \varepsilon T^4 \quad (6.3)$$

Where:

$h - convective\ heat\ transfer\ coefficient. Typical\ values\ are\ 5 - 25 \frac{W}{m^2}$ $for\ free\ convection.$ [19]

$\varepsilon -\ Emmisivity. Typically\ \varepsilon = 0.9$

$\sigma = 5.67 * 10^{-8} \frac{W}{m^2 K^4} Stefan - Boltzman\ constant$

Calculations to determine representative gas temperature for chosen heat fluxes were done with a "Trial and Error" method. Calculations were also done without taking into account convective heat transfer. The results of the calculations are presented in table 6.2.

Table 6.2: Calculations of corresponding gas temperatures for chosen heat fluxes. Calculations are done with a Trial and Error approach and presented with +/- 10C error.

$Heat\ flux, \dot{q}''_{total}$, W/m^2	Temperature if h=5W/m², C	Temperature if h=25W/m², C	Temperature if convective heat transfer is not considered, C
30000	580	490	600
40000	650	570	670
48000	695	620	710

Considering all the arguments mentioned above, it can be suggested that chosen heat fluxes (30, 40 and 48 kW/m²) are representative for a flashover and very early stages of fully developed fires. In later stages of a fully developed fire heat fluxes would be much higher. However for this thesis objective, presented tests would give sufficient information.

6.4 Results

6.4.1 Flammability

In all the tests, spontaneous ignition of the protective envelope took place almost immediately after exposing the samples to the heat flux.

a) b)

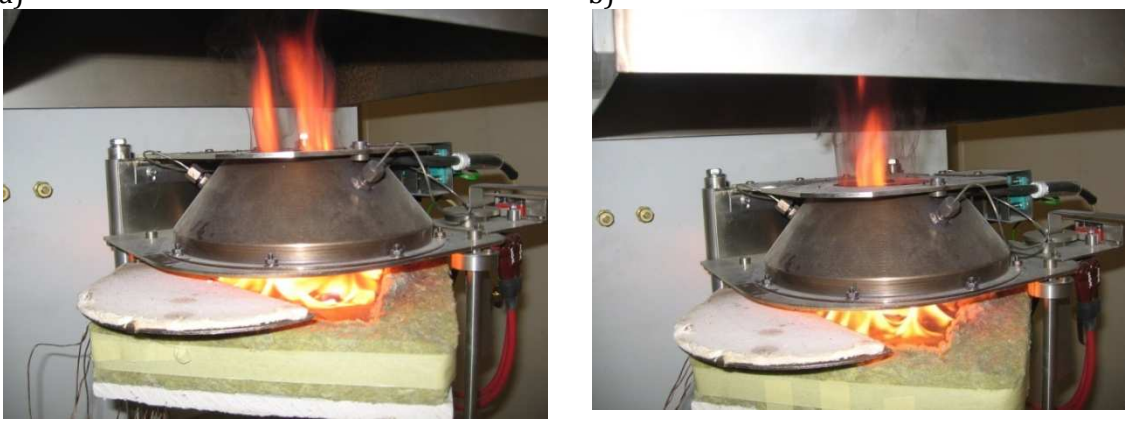

Figure 6.4: Burning of VIP samples a) test2 b) test5.

The HRR was determined with an oxygen consumption method by measured amount of O_2 and CO_2 in combustion gases [65]. O_2 and CO_2 concentrations were measured only for 5 tests (test2 to test6). For this reason results are presented only for these five tests. HRR calculation input variables are presented in table6.3.

Table 6.3: Input variables for HRR calculations with the oxygen depletion method.

Variable	**Symbol**	**Units**	**Value**
Relative humidity	RH	%	60
Heat of combustion per unit mass of oxygen	E	kJ/kg	13100
Expansion factor	α	-	1.105
Molecular weight of oxygen	M_{o2}	g/mol	32
Molecular weight of air	M_{air}	g/mol	28.56

In all the tests, a HRR peak was registered 40 – 50 seconds after the beginning of a test. The burning time was approximately 75 seconds. The peak HRR changed from approximately 3kW for exposure of 48kW/m^2 to approximately 1.6kW for exposure of 30kW/m^2. Considering the sample size, the results indicated a calculated peak HRR about 71 – 129 kW/ m^2. The results of the HRR calculations for tests 2-6 are presented in figure 6.5 and table 6.4.

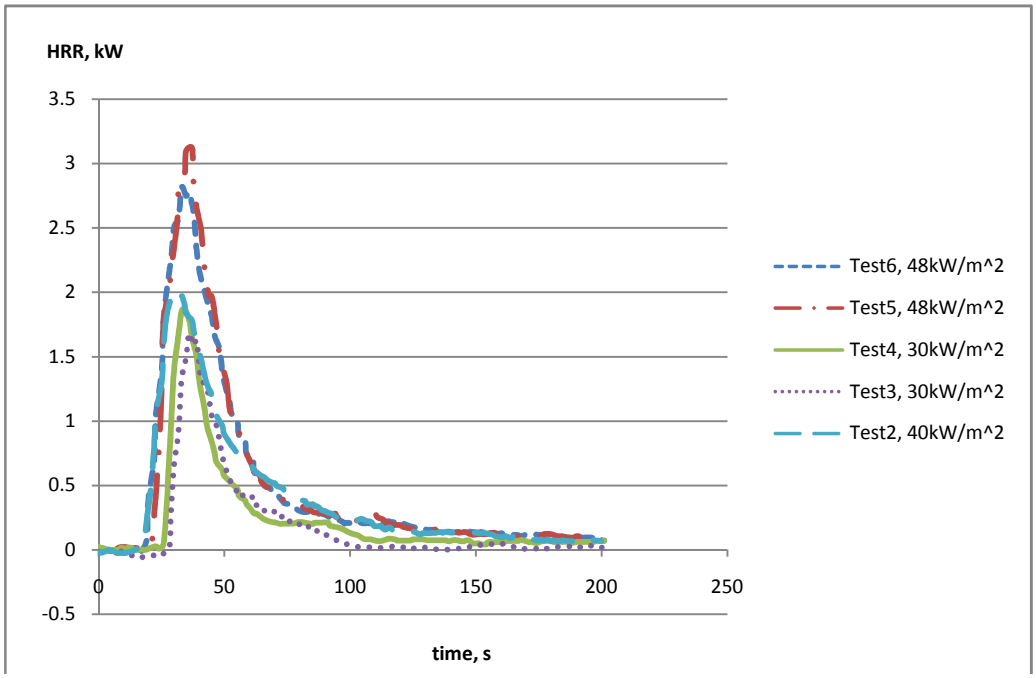

Figure 6.5: HRR measurements of VIP tests.

Table 6.4: Calculated peak HRR for VIP samples 200x120x20 mm^3.

Test number	Peak HRR of sample, kW	Peak HRR per m^2, kW/m^2
2	2	83
3	1.7	71
4	1.9	79
5	3.1	129
6	2.8	117

The total energy release was calculated by integrating a HRR over duration of burning. Results are presented in table 6.5 and figure 6.6.

Table 6.5: Total energy release for VIP samples 200x120x20 mm^3.

TEST	Total released energy, kJ
1	-
2	81
3	39
4	48
5	99
6	98

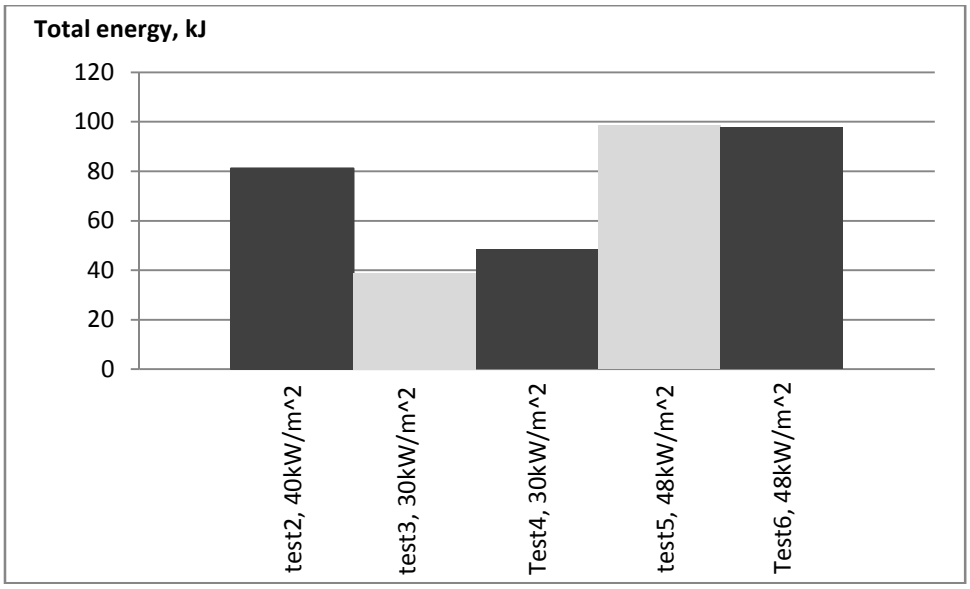

Figure 6.6: Total energy release of VIP samples.

The peak value of HRR and the total released energy was dependent on the applied heat flux. The highest applied heat flux (48kW/m^2) resulted in the highest HRR and the amount total released energy. When a heat flux of 48kW/m^2 was applied, more than two times higher total energy release was calculated, comparing to an applied heat flux 30kW/m^2. This might be explained by suggesting, that more combustibles were involved from protected sides of a sample. Higher heat flux as well would increase the pyrolysis rate (and HRR), but it does not explain increased amount of the total released energy.

6.4.2 Thermal properties

K-type thermocouples were used to measure the temperature of the sample surfaces as presented in chapter 6.3.4.

In all the tests, during the burning several thermocouples on the exposed surface detached from the surface and lost their positions. In two cases, all but one thermocouple was left on the exposed surface. Data taken from the misplaced or detached thermocouples are not taken in account in the following analysis.

The remaining thermocouples showed a fairly uniform temperature distribution over the exposed surface after the burning. A maximum difference of about 100°C was measured in between thermocouples on the exposed surface. The temperature remained rather constant during the remaining test time. The thermocouple measurements from the exposed side are presented in Annex C.

At a certain point during the tests, the temperature of the thermocouples on the sides (11 and 12) raised and become comparable to the exposed surface temperature. After some time, the temperature of the side thermocouples dropped. This might indicate combustion on the sides of the sample, even though they were insulated with mineral wool. The temperature measurements on the sample surfaces are presented in Annex D.

The temperature rise on the unexposed side was observed about 100seconds after the beginning of a test. If the system would be governed by the thickness of a sample, then it is expected that the thermocouple at the middle would show the highest temperature and the most rapid temperature rise. However in 4 of 6 tests, one other thermocouple measurement was higher than the measurement for the middle thermocouple at the unexposed side. This might occur because of heat penetration through insulated sides of the sample holder. If heat conduction would be governed by the envelope of the sample, it would be expected that more than one thermocouple would show a higher temperature then the thermocouple at the middle. In some cases the thermocouple at the middle showed about 50°C higher measured temperature, comparing to other thermocouples on the unexposed side. The thermocouple measurements on the unexposed side are presented in the charts in Annex E.

The surface temperature rise of the unexposed side is presented in figure 6.7.

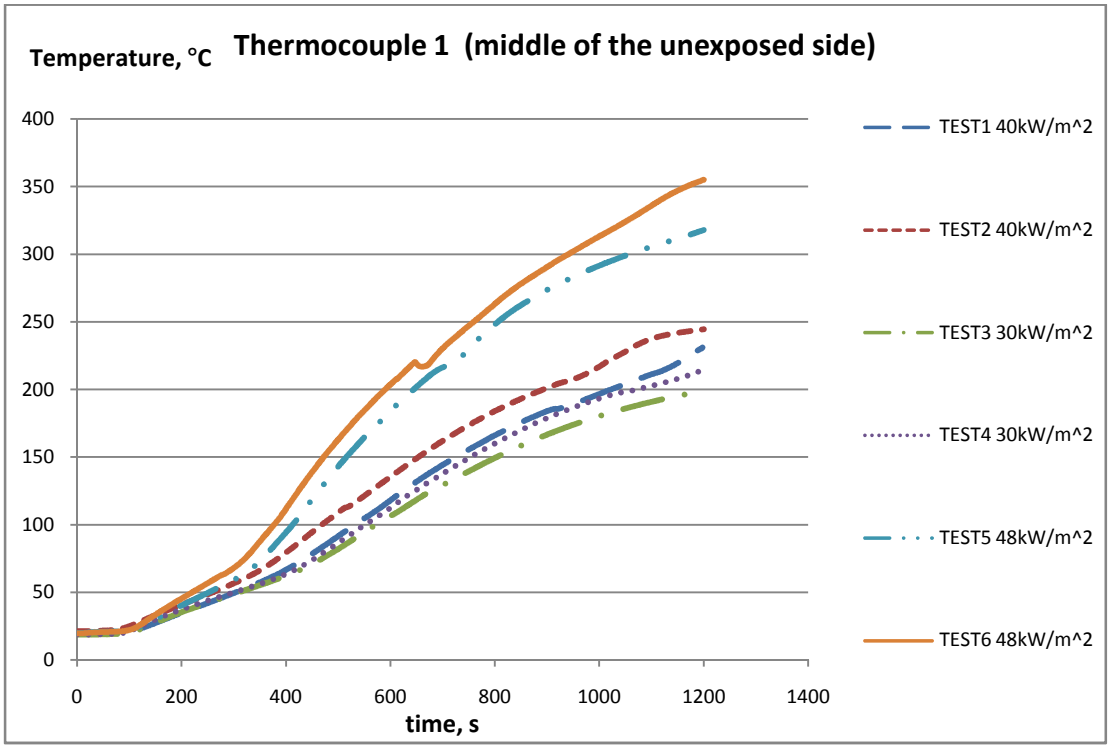

Figure 6.7: Rise of temperature at the middle of unexposed side.

The temperature rise was fairly linear for all the tests, up until the unexposed side reached approximately 60- 70°C. Then the temperature increase become more rapid, indicating changes in heat transport within the samples. This transition phase could be explained by suggesting that at the given temperatures cracking of the core material reached the unexposed side.

After the transition phase, the temperature rise become more rapid, however still more or less linear. Depending on the applied heat flux, the linearity of the temperature rise was slightly lost, when the unexposed side temperature reached 150-250°C.

After the burning, the exposed surface took fairly uniform temperature, which did not significantly change during the tests. It allowed using a constant, instantly applied surface temperature as a boundary condition and solve heat flow as for a semi-infinite solid [66]:

$$\frac{\partial^2 T}{\partial x^2} = \frac{1}{\alpha}\frac{\partial T}{\partial t} \quad (6.4)$$

The boundary and initial conditions are:

$$T(x,0) = T_i$$
$$T(0,t) = T_0 \quad for\ t > 0$$

The Laplace transform technique allows to solve equation as:

$$\frac{T\ (x,t) - T_0}{T_i - T_0} = erf\frac{x}{2\sqrt{\alpha t}} \quad (6.5)$$

Where:

$T\ (x,t) -\ material\ temperature\ after\ time\ t\ and\ atdepth\ x. In\ presented\ case,$ $temperature\ on\ the\ unexposed\ side\ (°C).$

$T_0\ -\ Temperature\ on\ the\ exposed\ side\ (°C);$

$T_i -\ initial\ temperature\ of\ the\ sample. In\ presented\ case, initial\ temperature$ $of\ the\ unexposed\ side\ (°C);$

$x - depth, thickness\ of\ the\ sample;\ x = 0.02\ m\ in\ all\ cases\ \ (m);$

$\alpha - thermal\ diffusivity. \alpha = \frac{\lambda}{\rho c}\ (\frac{m^2}{s});$

$t - time. In\ presented\ case, duration\ of\ analysed\ range, (s)$

Solving equation 6.5 with a "*Trial and Error*" approach, allowed estimating thermal diffusivity value (all the other values are known from the test results). If specific heat capacity and density is assumed to be constant (temperature independent), the conductivity value can be calculated. However, due to the made assumptions and simplifications of the heat transfer physics, this conductivity should be considered as an apparent conductivity and not as the correct, actual conductivity.

The calculated conductivity is not a real value, but rather an averaged value of the temperature range over the thickness of a sample. In the tests the exposed surface temperature (T_o) was not ideally instantly applied and constant. Average values over the time were used for T_o values. Above mentioned considerations make these calculations unsuitable for any real case, nevertheless they can give a first insight in the changes of the VIPs thermal properties when exposed to higher heat fluxes.

For calculation purposes, the temperature rise on the unexposed side was divided into: range 1, range 2 and transmission range (see figure 6.8). This division was made so that temperature rise could be considered linear during range 1 and range 2. It was assumed that during the range 1 and range 2 material properties are constant and the calculations for α and λ were performed.

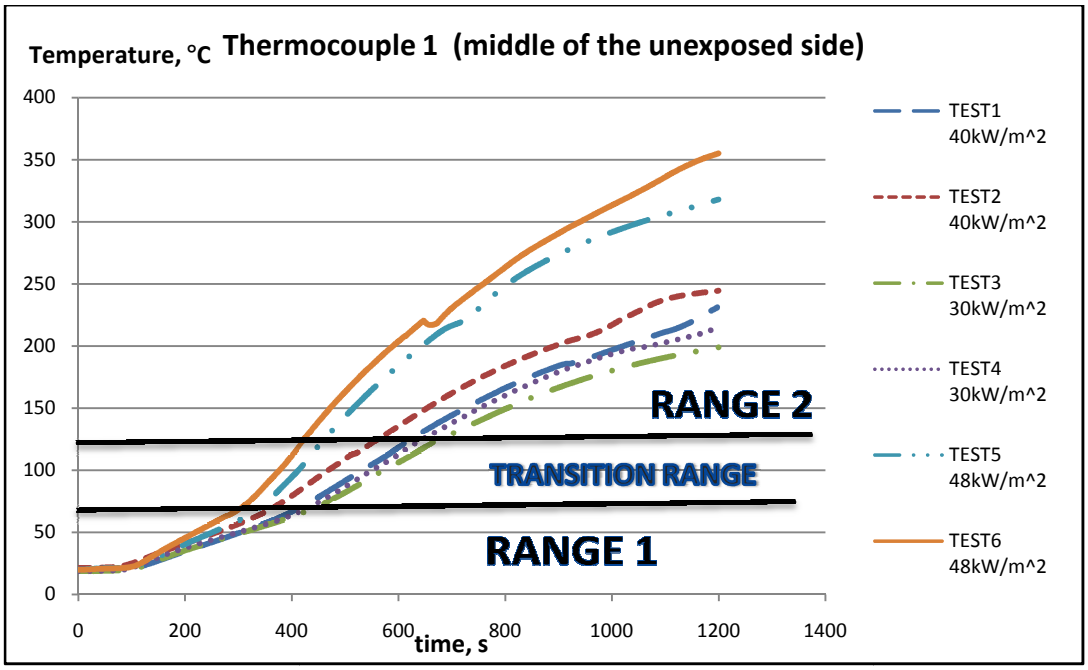

Figure 6.8: Chosen temperature ranges.

It was determined that the range 1 starts at time 0 seconds and ambient temperature was assumed to be 20 °C. Range 2 begun at 350 to 500 seconds after the beginning of the test, depending on tests. At the beginning of range 2, the sample was already pre-heated and the temperature drop over the thickness was established. This temperature drop is not considered in equation 6.5, which creates an additional error in the calculations. Due to this error, it is expected that calculated λ values will be higher than actual values.

The calculations were done by a "*Trial and Error*" approach. The sample density and specific heat values were taken as follows: c_p=800J/kg/K and ρ=190kg/m^3. The conductivity value was changed until both sides of equation 6.5 came to a reasonable agreement. The results for each range (range 1 and range 2) are presented in table 6.6 and in figure 6.9.

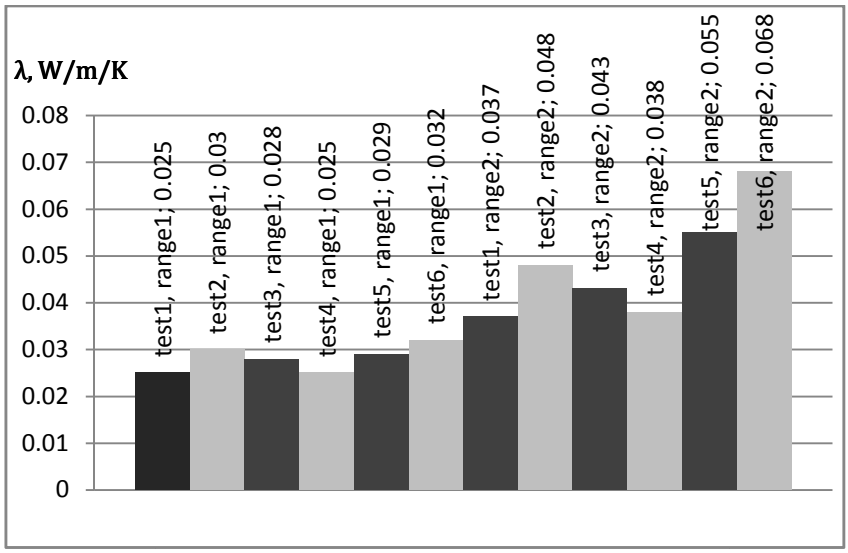

Figure 6.9 λ values calculated for the temperature range 1 and 2.

Table 6.6:. λ and α values calculated for temperature range 1 and 2 for VIP samples.

								Values that must have agreement between	
								Calculated value, with equation 6.5	TEST VALUES, measured with thermocouples
	Test	Time of range	Duration, t	λ,	α,	To	T i	T (x,t)	T (x,t)
	Nr.	second	s	W/m/K	m^2/s	C	C	C	C
Range 1	1	0 - 350 second	350	0.025	1.6E-07	612.7	20	56.9	57.4
	2	0 - 350 second	350	0.03	2.0E-07	551.2	20	67.2	66.2
	3	0 - 400 second	400	0.028	1.8E-07	459.1	20	63.7	62
	4	0 - 400 second	400	0.025	1.6E-07	551.5	20	63.2	63.7
	5	0-300 second	300	0.029	1.9E-07	653.4	20	59	59.5
	6	0-300 second	300	0.032	2.1E-07	659.1	20	68	68.1
Range 2	1	350 - 1200 second	850	0.037	2.4E-07	589.8	57.4	230.7	231
	2	350 - 1200 second	850	0.048	3.2E-07	523.8	66.2	243.8	244.5
	3	500 - 1200 second	700	0.043	2.8E-07	455.1	82.4	199.8	199
	4	500 - 1200 second	700	0.038	2.5E-07	534.8	87	214.7	214.9
	5	400- 1200 second	800	0.055	3.6E-07	643.6	94.4	317.3	318
	6	400- 1200 second	800	0.068	4.5E-07	648.4	111.4	355.6	355.2

Following assumptions were made:

- ✓ A linear temperature drop over the thickness of sample;
- ✓ The conductivity changes linearly over the temperature range.

Then the calculated conductivity was assigned to the temperature at the middle of the sample. In this case, the same conductivity value was assigned for two temperatures (beginning and end of each range). 24 scatter points were obtained and plotted. The results are presented in figure 6.10.

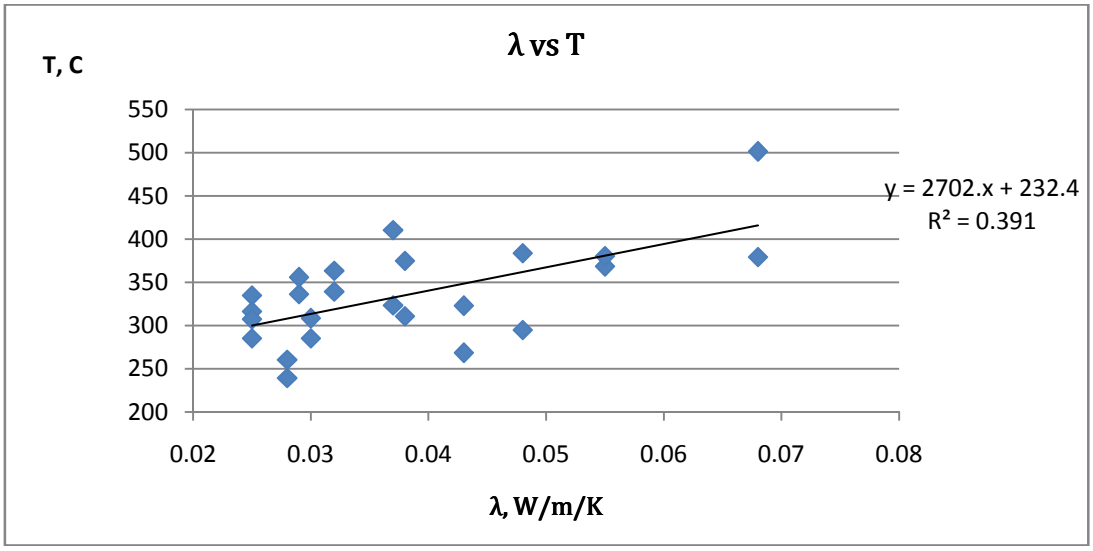

Figure 6.10: Estimated λ values.

6.4.3 Physical properties

In all the tests, the protective envelope of the samples spontaneously ignited and burned for about 75 seconds. The burned surfaces changed colour from black to white.

After 2 of 6 tests, the protective fabric was physically damaged because of exposure to heat. In one case, the junction of the envelope (on unexposed side) was opened (see figure 6.11).

a) b)

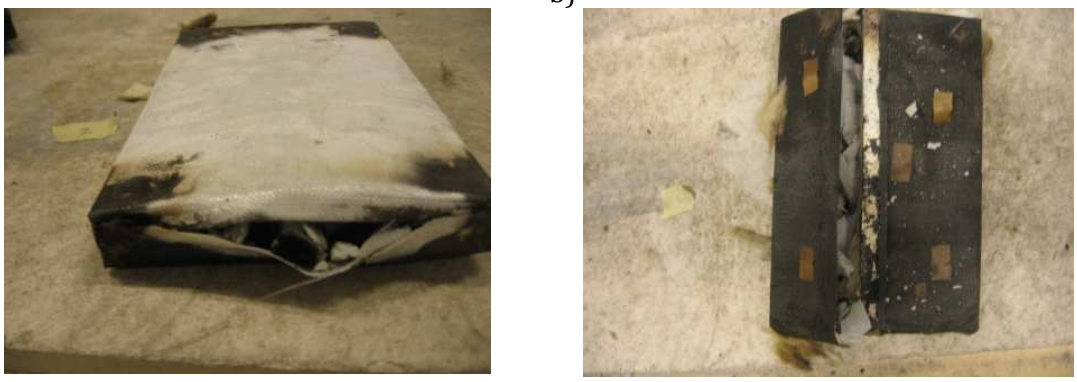

Figure 6.11: Photos of the samples after the tests. a) Test sample 2. Exposed to 40 kW/m2 . Exposed side; b) Test sample 6. Exposed to 48 kW/m2. Unexposed side.

The weight of the undamaged samples was measured after the tests. The weight of a single sample was used as a reference. The sample weight before exposure was measured to be 112.7g. Results are presented in table 6.7.

Table 6.7: Mass after the test and the change of the mass percentage of the VIP samples 200x120x20 mm^3.

Test nr.	**Mass after test, g**	**Change of mass, %**
1	112.1	-0.5
2	Damaged sample	-
3	112.5	-0.2
4	113.2	0.4
5	99.7	-11.5
6	Damaged sample	-

The change of mass of the test samples is insignificant. Test 5 (heat flux 48kW/m^2) shows the greatest mass loss, while tests 3 and 4 (heat flux 30kW/m^2) shows the least mass loss. This might be because the higher heat flux might involve more fuel from the sides of the sample.

By closer inspection of the core material after the tests, it is noticeable that it had become brittle and degraded.

a) b)

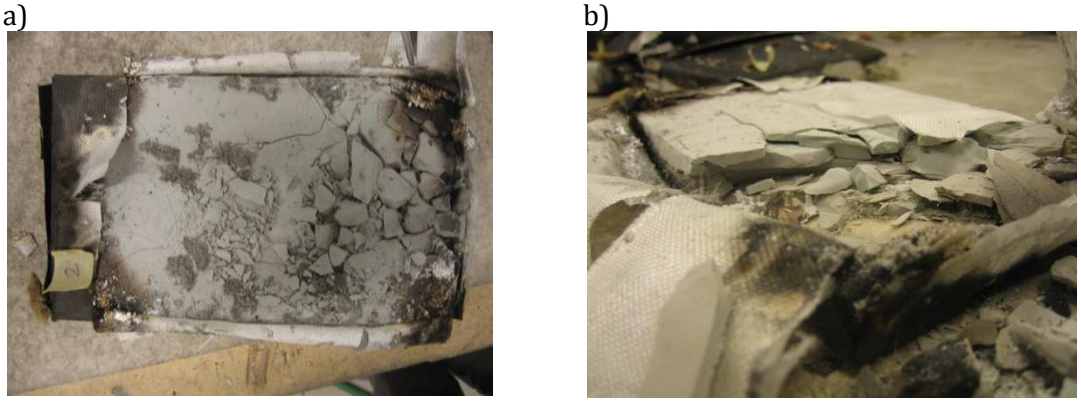

Figure 6.12: Photos of samples after tests, with removed protective envelope. a) Test sample 2. Exposed to 40 kW/m2 . Exposed side; b) Test sample 2 (heat flux 40kW/m2). After removing part of the core material.

6.5 Discussion

6.5.1 Validity

Even with all the measures done, it was impossible to completely eliminate thermal bridges in the experiment set-up system. The sample holder for the tests was made mostly of mineral wool. The thermal properties of a mineral wool are much different than those of VIP. The mineral wool transfers heat at a higher rate, which raises doubts if heat transfer in the performed tests was governed by the VIP sample. Also, it is hard to provide a perfect air-tightness at the edges of the sample. It is unknown to what level the sample holder had effected temperature measurements.

The chosen heat fluxes are representative for flashover and very early stages of a fully developed fire, as discussed in paragraph 6.3.5.1. In later stages of a fully developed fire radiant heat flux levels might be much higher. In this case even more significant material degradation might be expected. In real construction VIPs are protected (by gypsum boards, concrete etc). This protection most likely would not allow VIPs to be exposed to very high heat flux. So the chosen levels might be realistic to be obtained for the later stages of a fully developed fire when the VIP panels would be protected by a protective layer.

The tested VIPs consisted of micro-porous silica acid powder core, 3 layers of metalized polyester (metalized with aluminium), one layer of polyurethane and one layer of black fibreglass. Test results are only valid for this arrangement and materials and not for other compositions of VIPs.

The conductivity measurements (chapter 6.4.2) hold very crude approximations and can't be considered as precise values. Calculated conductivity should be considered as apparent values. Calculations however give first insight to how rapid the change of heat flow is through the VIPs slab and how the thermal insulation changes for higher temperatures.

6.5.2 Errors and uncertainties

The presented test holds following errors and uncertainties:

- ✓ The thermocouple measurement uncertainty. The thermocouple class for the tests was unknown. If thermocouple are assumed to be of class 2, measurement tolerance uncertainties are +-2.5 °C in temperatures -40 to 333°C and +-0.75% in temperatures 333 – 1200°C [63]; These tolerance uncertainties may increase with thermocouple age[63] The age of the thermocouple in the particular tests is unknown, but it was less than 5 years;
- ✓ For surface temperature measurements, thermocouples are required to have a perfect thermal contact with the surface. This might be an source of error in the presented tests as it was difficult to know how good the attachment of the thermocouples is during the test;

- ✓ The thermocouples are expected to be influenced by radiation heat flux from cone and the flames, thus increasing the measured temperature;
- ✓ The thermocouples were fixed to the surface with a thermal tape. The sample is expected to have a higher conductivity then the tape material, thus the tape shouldn't create significant errors in measurement. However a slight deviation from normal situation was created because tape changes convection on the surface;
- ✓ The radiation heat flux was not measured before each experiment, which creates uncertainty in the test conditions;
- ✓ The radiation feedback from the surrounding materials is unknown and increasing with time, as surrounding heats up;
- ✓ The K-type thermocouples are sensitive to electrical noises created by external sources. Although often noise errors are insignificant, it must be recognised. Instrumentation cables should be located in a distance away from possible sources of noise (power cables, electric motors, generators etc.) [63];
- ✓ The response time depends on the thermocouple size [63];
- ✓ The K-type thermocouples are sensitive to hysteresis, especially in temperatures between 300°C and 600°C. This can cause error of several degrees;
- ✓ It is suggested that the electromagnetic force produced in a thermocouple is dependent on pressure. This affect is argued to be small [63];
- ✓ Above 800°C oxidation causes drift for K-type thermocouples [63];
- ✓ Gas analyser measurement errors effect the measured HRR;
- ✓ In the HRR calculations some values are unknown for this particular case. Expansion factor and heat of combustion per mass unit of oxygen were chosen as default values, which might not be representative for this specific materials;
- ✓ In the HRR measurements it was assumed to have a completely dry samples, which introduces some error;
- ✓ In HRR calculations, combustion from insulated side parts and mineral wool might have influence on results;
- ✓ The thermal conductivity estimation procedure holds few crude assumptions as described in chapter 6.4.2.

6.5.3 Conclusions

VIPs allow significantly reducing the thickness of a building envelope, reaching equivalent insulation level, if compared to conventional thermal insulation solutions.

VIPs are often produced with a porous silica based core. This solution is incombustible. Alternatively PUR or glass fibre can be used for the core material. The envelope of a VIP is designed to protect the core from mechanical impacts, air

and moisture infiltration etc. The envelope is usually made with polyurethane and polyethylene components, which makes it combustible.

VIPs lose their insulation if they are mechanically damaged. Because of this reason, VIP samples can't be cut in order to adjust to the standard test size requirements. This will create problems for testing of these panels. VIPs samples for the fire tests will have to be made separately or tests will have to be adjusted to suit available the sample sizes.

The tested VIPs spontaneously ignited under 30kW/m^2 and higher heat fluxes. Ignition occurred after a very short time in the beginning of the tests and burning was governed by the envelope components. Measured peak HRR was about 71-129 kW/m^2. The total energy release was measured to be 39-99 kJ per sample. The amount of the total released energy and the peak HRR was dependent on the applied heat flux. It can be concluded that the fuel load of tested VIPs would not be significant in case of a compartment fire. It must be noted that installing VIPs might also require some additional usage of polyurethane foams to form a joint between two VIPs. This would increase total fuel load in a fire compartment. But it would still be less than if another combustible insulation would be used.

The envelope ignites very easily and fire compartmentation of a building must be considered when VIPs are used in construction. If improperly installed, VIPs could provide means of fire spread between the fire compartments. Special care must be taken if VIPs are installed in renovation and a void is left between VIP and other building components. VIPs would greatly benefit if an incombustible envelope solution would be found.

The core of the tested VIPs was made from porous silica which showed degradation under high heat flux. Because of the material degradation, VIPs loose part of their thermal properties. This also leads to necessity to change VIPs after a fire accident. During a design process, it should be ensured that VIPs are easy to replace.

The loss of conductivity does not seem significant enough to influence fire conditions in a fire compartment. Estimated highest conductivity value was about λ=0.07W/m/K, which is comparable to conductivity of a cork plate at ambient conditions [21]. However more correct determination of the conductivity is necessary to establish exact values. The tested VIPs do not show any sign of charring or melting, mass loss or change of volume. The core material however becomes brittle and its capability to hold its own weight (if large plates are placed vertically) is unknown.

6.5.4 Future research

The presented test results give a first insight to VIPs burning behaviour, thermal properties and physical changes fire conditions. The results are only applicable to a certain type of VIPs, described in chapter 6.3.2. Further investigations should be done with different kinds of core and envelope solutions. Especially important

would be the investigations of VIPs with flammable core (porous EPS and PUR foams).

The presented tests focus on a fully developed enclosure fire stage so it did not investigate toxicity of VIPs combustion product. Toxicity is a major issue in fire situations and should be considered. Usage of PUR in VIPs solutions might increase toxicity risk but it can be expected that the mass of the toxic materials in VIPs might be negligible if other materials and building content is considered.

Furthermore, VIPs should be investigated in more realistic arrangements, considering protective layers of gypsum boards, steel sheets, other wall components and possible voids between them. It is expected that this would improve their behaviour. The performed tests should be considered as a worst case.

7 Conclusions

Lately the building development has been driven by a requirement of energy-efficiency. This thesis discusses the design measures, applied to reach this goal, and their impact to fire safety during the fully-developed fire stage. Potential for fire spread between the compartments by destruction of structural elements or convection of the unburned fuel volatiles through the existing openings is used as a basis to evaluate the fire safety.

More advanced building thermal insulation and increased air-tightness are the fundamental measures to decrease the heat flow out and into the building. New materials and solutions are introduced for building thermal insulation. It is important to evaluate performance and behavior of these materials in fire conditions. The thermal properties of room boundaries might influence the gas temperatures within the fire compartment, as described with the energy balance concept. Assessing temperature dependent properties of wall and ceiling materials would allow making more precise estimates on expected thermal loading to structures. The importance of temperature dependent boundary properties is shown in chapter 5.5.5 of this thesis.

Very important factor, which contributes to the fire development and the room temperatures, is the burning characteristics of materials. Combustible insulation can increase the fire load in the compartment and provide means of fire spread. The thesis discusses potential fire safety issues regarding to usage of vacuum insulation panels (VIPs) in buildings. Bench-scale tests are performed with VIP samples, consisting of incombustible core and combustible protective layer. Some surface burning is observed for the tested VIPs. Results of these tests show lower maximum HRR and total energy release values, if compared to combustible insulation foams. VIPs might offer more efficient and safe alternative to combustible insulation foams. Performed tests with VIP samples are presented in chapter 6 of this thesis.

Additional measures include glazing and space optimization. Increasing glazing areas allows benefiting from the solar heat and natural light in the buildings. Large open floor areas allow more effective usage of the natural light and ventilation. Both of these measures however increase non-uniformity of the compartment gas temperatures in the case of the fire. This might be potentially dangerous, because used fire safety codes require determining the fire resistance of the structural elements under the uniform heating conditions. Uniform temperature distribution assumption is valid for ventilation controlled fires within relatively small compartments with almost quadratic shape. This arrangement is not representative for many new buildings.

Other measures include advanced ventilation and air conditioning systems, overhangs for windows and heat extraction methods (solar panels etc.). These design solutions are not discussed in this thesis.

The pursuit for efficiency in building sector is still ongoing. Potential fire risks are created, because designers are still experimenting with the building design. On the

other hand, fire safety codes do not develop so rapidly and they are not flexible enough to be used in all the design cases. Performance-based fire safety engineering should be applied to deal with each building that has innovative features. Energy efficiency is an important goal to reach, and fire safety professionals should not break down this process. Instead, they should follow new design trends and apply their knowledge to minimize fire risks, considering the proposed design features.

8 Acknowledgements

First of all, I wish to express my gratitude to the thesis supervisor Prof. Patrick van Hees. Thank you for guidance, responsiveness and optimism!

I would like to thank to the following people for their input: research engineer Sven-Ingvar Granmark, PhD candidate Agustin Majdalani, Marc Mölter, Masters student Oriol Rios, PhD candidate Jonathan Wahlqvist and others who have shared their ideas and opinions. Also I wish to thank to company "Va-q-tec AG" for the provided VIP samples.

This thesis is the final achievement after 2 years of study in the educational programme IMFSE. My gratitude goes to all the people involved in the development of this programme: Prof. Robert Jönnson (Lund University), Prof. Bart Merci (Ghent University), Prof. José Torero (University of Edinburgh), all the professors and administrative staff. Also, I wish to thank my study mates. I have learned a lot from you!

9 References

1. Report of the World commission on Environment and development: Our common future. 1983.
2. M. Hamdy, A. Hasan, K. Siren: Applying a multi – objective optimization approach for Design of low-emission cost-effective dwellings. Building and Environment, vol. 46, 2011, 109-123.
3. T. Z. Harmathy: Overview of impact of energy conservation on firesafety. Fire technology vol.19, 1983.
4. T. Z. Harmathy: Some overlooked aspects of severity of compartment fires. Fire safety journal vol.3, 1981, 261-271.
5. http://www.our-energy.com/low_energy_passive_and_zero_energy_houses.html. February, 2012.
6. H. Simmler et al.: Study on VIP-component and Panels for Service life predictions of VIP in building applications (subtask A). 2005.
7. Buildings energy databook: http://buildingsdatabook.eren.doe.gov/default.aspx. April, 2012.
8. M. Alam, H. Singh, M. C. Limbachiya: Vacuum Insulation Panels (VIPs) for building construction industry – a review of the contemporary developments and future directions. Applied energy vol.88 issue 11, 2011, 3592-3602.
9. Dr. S. Hagan: A snake in the grass: Ethics vs. aesthetics in sustainable architecture. World renewable energy congress VI, 2000.
10. P. Heiselberg: Low energy building concepts. http://www.dtu.dk/upload/centre/lave/del-strategier/low%20energy%20building%20concepts.pdf. Downloaded in January, 2012.
11. E. Abel: Low-energy buildings. Energy and Buildings vol.21, 1994, 169-174.
12. M. L. Persson, A. Roos, M. Wall: Influence of window size on the energy balance of low energy houses. Energy and buildings vol.38 issue 3, 2006, 181-188.
13. T. Weber: Low-energy houses – Vision and reality- a statistical survey on a real energy consumption in 400 Swedish and German houses. Kungl Tekniska Hogskolan, division of Building technology, Stockholm, 2002.
14. Company Rockwool web page: www.rockwool.com. February, 2012.

15. C. J. Wieczorek: Fire safety: an integral part of sustainability. Fire protection engineering, 4th quarter 2011.

16. S. Dent: Fire protection engineering and sustainable design. Fire protection engineering, 2011.

17. Encyclopaedia Britannica: LEED standards. http://www.britannica.com.ludwig.lub.lu.se/EBchecked/topic/1382484/LEED-standards . March, 2012.

18. W. D. Walton, P. H. Thomas: Estimating Temperatures in compartment fires. SFPE handbook 3th edition. 2002.

19. D. Drysdale: An introduction to fire dynamics, 2nd edition. 1998.

20. A. H. Majdalani, J. L. Torero: Compartment fire analysis for modern infrastructure. 2011.

21. B. Karlsson, J. G. Quintiere: Enclosure fire dynamics. 1999.

22. S. E. Magnusson and S. Thelandersson: Temperature-time curves of complete process of fire development (theoretical study of wood fuel fires in enclosed spaces). 1970.

23. P. H. Thomas: Modelling of compartment fires. Fire safety journal vol.5, 1983, 181-190.

24. T. E. Waterman: Room Flashover- criteria and synthesis. Fire technology vol.4, 1968, 25-31.

25. J. Stern-Gottfried, G. Rein, L.A. Bisby, J. L. Torero: Experimental review of homogeneous temperature assumption in post-flashover compartment fires. Fire Safety Journal vol.45 issue 4, 2010, 249-261.

26. EN1991-1-2:2002 informative annex A. 2002.

27. K. McGrattan, S. Hostikka, J. Floyd, H. Baum, R. Rehm: Fire Dynamics Simulator (version5) Technical reference guide. NIST, 2007.

28. S. Li, Z. Yan, R. Zong, B. Sunden, G. Liao: Numerical modelling of flashover in experimental compartment fires. 8th International Conference on Performance-Based codes and Fire Safety design Methods. 2010.

29. Ch. Younes, C. A. Shdid, G. Bitsuamlak: Air infiltration through building envelopes: A review. Journal of Building physics vol.35(3), 2011, 267-302.

30. J. H. Klote: Smoke control. SFPE handbook 3rd edition.

31. M. L. Persson, A.Roos, M.Wall: Influence of window size on the energy balance of low energy houses. Energy and Buildings vol.38, 2006, 181-188.

32. J. Shields, G.W.H. Silcock, F.Flood: Behaviour of double glazing in corner fires. Fire Technology vol.41, 2005, 37-65.

33. A. Jonsdottir, G. Rein: Out of range. Fire Risk Management, dec. 2009, 14-17.

34. J. J. Murphy, J. Tidwell: Green Building challenges for fire service. Fire Engineering vol.164 issue1, 2011, 41-55.

35. H. Poirazis: Double skin Facades for office buildings, literature review. Department of construction and architecture, Lund University, 2004.

36. E. Gratia, A. De Herde: Greenhouse effect in double-skin facade. Energy and Buildings vol.39, 2007, 199-211.

37. H. Manz, Th. Frank: Thermal simulation of buildings with double-skin facades. Energy and Buildings vol.37 issue 11, 2005, 1114-1121.

38. P. Arnold: Energy conservation in the modern office building, Property Management vol.8, 2007 number 1, 2007, 28-33.

39. B. Gustin: Firefighting in modern office buildings. Fire Engineering, 2005, 59-66.

40. B. Bohm, S. Hadvig: Nonconventional fully developed Polyethylene and wood compartment fires. Flame and Combustion vol.44, 1982, 201-221.

41. S. Welch , A. Jowsey, S. Deeny, R. Morgan, J. L. Torero: BRE large compartment fire tests – Characterising post-flashover fires for model validation. Fire Safety Journal vol.42, 2007, 548-567.

42. K. A. M. Moinuddin, I.R. Thomas: An experimental study of fire development in deep enclosures and a new HRR-time-position model for a deep enclosure based on ventilation factor. Fire and Materials vool.33, 2009, 157-185.

43. J. Stern-Gottfried: Travelling fires for structural design. University of Edinburgh, 2011.

44. A. Law, J. Stern-Gottfried, M. Gillie, G. Rein: The influence of travelling fires on a concrete structure, Engineering Structures vol.33, 2011, 1635-1642.

45. Dr. Mohammad S. Al-Homoud: Performance characteristics and practical applications of common building thermal insulation materials. Building and Environment vol.40, 2005, 353-366.

46. European insulation association web page: http: //www.eurima.org/u-values-in-europe/ . April 2012.

47. A. Lyons: Materials for architects and builders. 2006.

48. B.P. Jelle: Traditional, state-of-the-art and future thermal building insulation materials and solutions – Properties, requirements and possibilities. Energy and Buildings vol.43, 2011, 2549-2563.

49. U. Krause, W. Grosshandler, L. Gritzo: The international Forum of fire research directors: A Position paper on sustainability and fire safety. Fire Safety Journal vol.49, 2012, 79-81.

50. S. Doroudiani, H. Omidia: Environmental, health and safety concerns of decorative mouldings made of expanded polystyrene in buildings. Building and Environment vol.45, 2010, 647-654.

51. M. Rossi, G. Camino, M.P. Luda: Characterisation of smoke in expended polystyrene combustion. Polymer Degradation and Stability vol.74, 2001, 507-512.

52. M. Modesti, A. Lorenzetti, F. Simioni, M. Checchin: Influence of different flame retardants on fire behaviour of modified PIR/PUR polymers. Polymer Degradation and Stability vol.74, 2001, 475-479.

53. M. Modesti, A. Lorenzetti: Flame retardancy of polyisocyanurane-polyurethane foams: use of different charring agents. Polymer Degradation and Stability vol.78, 2002, 341-347.

54. G. Matuschek: Thermal degradation of different fire retardant polyurethane foams. Thermochimica Acta vol. 263, 1995, 59-71.

55. M. Checchin, C.Cecchini,B.Cellarose, F.O.Sam: Use of cone calorimeter for evaluating fire performances of polyurethane foams. Polymer Degradation and Stability vol.64, 1999, 573-576.

56. A. Tewarson: Generation of heat and chemical compounds in fires. SFPE handbook 3th edition;

57. Federation of European Rigid Polyurethane Foam association: Thermal insulation materials made of rigid polyurethane foam (PIR/PUR). Report no.1. 2006.

58. D.J. Hopkin, T. Lennon, J. El-Rimawi, V. Silberschmidt: Full-scale natural fire tests on gypsum lined structural insulated panel (SIP) and engineered floor joist assemblies. Fire Safety Journal vol.46 issue 8, 2011, 528-542.

59. S. L. Manzello, R. G. Gann, S. R. Kukuck, D. B. Lenhert: Influence of gypsum board type (X or C) on real fire performance of partition assemblies. Fire and Materials vol.31 issue 7, 2007, 425-442.

60. J. Fricke, U. Heinemann, H. P. Ebert: Vacuum insulation panels – from research to market. Vacuum vol.82, 2008, 680-690.

61. www.vip-bau.de. April, 2012.

62. www.promatec.com. April, 2012.

63. P. R. N. Childs: Practical temperature measurement. 2001.

64. ISO 5660-1:2002.

65. M. L. Janssens: Measuring rate of heat release by oxygen consumption. Fire Technology vol.27, 1991, 234-249.

66. J. P. Holman: Heat transfer, 10th edition. 2010.

67. Kristopher Overholt web-site: Fire protection engineering notes, tools, and projects. http://www.koverholt.com/. May, 2012.

68. Company "va-Q-tec AG" website: www.va-q-tec.com.

10 Appendices

Appendix A: The input text files for FDS simulations (chapter 5.5.5)

CASE 1:

```
Free burning - ISO9705Room_all_surfaces_VIP_cRamp1_5cm
&HEAD CHID='VIP',TITLE='free burning propane'/
&MESH IJK=100,60,60,XB=0.0,5.0,0.0,3.0,0.0,3.0/ 5 cm grid
&TIME T_END=2400.0/
&MISC SURF_DEFAULT='INERT'/
&RADI NUMBER_RADIATION_ANGLES=1000/

&SURF ID='BURNER',HRRPUA=1000.,COLOR='SILVER'/
&OBST XB=1.2,3.2,1.0,2.0,0.0,0.1 SURF_IDS='BURNER','INERT','INERT'/
&REAC ID='PROPANE'
SOOT_YIELD=0.015
C=3.
H=8.
HEAT_OF_COMBUSTION=46450
IDEAL=.TRUE./

&MATL ID='VIP'
CONDUCTIVITY_RAMP='k_VIP'
SPECIFIC_HEAT_RAMP='c_VIP'
DENSITY=192/
&RAMP ID='k_VIP', T=20.,F=0.004/
&RAMP ID='k_VIP', T=900.,F=0.0075/
&RAMP ID='c_VIP', T=43.,F=0.726/
&RAMP ID='c_VIP', T=178.,F=0.915/

&SURF ID='VIP_WALL'
BACKING='EXPOSED'
MATL_ID = 'VIP'
THICKNESS = 0.02
COLOR='GREEN'/

&OBST XB=0.4,0.4,0.3,2.7,0.0,2.4, SURF_IDS='VIP_WALL', 'VIP_WALL', 'VIP_WALL'/
&OBST XB=0.4,4.0,0.3,0.3,0.0,2.4, SURF_IDS='VIP_WALL', 'VIP_WALL', 'VIP_WALL'/
&OBST XB=4.0,4.0,0.3,2.7,0.0,2.4, SURF_IDS='VIP_WALL', 'VIP_WALL', 'VIP_WALL'/
&OBST XB=0.4,4.0,2.7,2.7,0.0,2.4, SURF_IDS='VIP_WALL', 'VIP_WALL', 'VIP_WALL'/
&OBST XB=0.4,4.0,0.3,2.7,2.4,2.4, SURF_IDS='VIP_WALL', 'VIP_WALL', 'VIP_WALL'/
&OBST XB=0.0,5.0,0.0,3.0,0.0,0.0, SURF_IDS='VIP_WALL', 'VIP_WALL', 'VIP_WALL'/
&HOLE XB=3.99,4.01,0.9,2.1,0.0,1.5/
&HOLE XB=0.39,0.41,0.7,2.3,0.5,1.5/
&VENT XB=0.0,0.0,0.0,3.0,0.0,3.0, SURF_ID='OPEN' /
&VENT XB=0.0,5.0,0.0,0.0,0.0,3.0, SURF_ID='OPEN' /
&VENT XB=5.0,5.0,0.0,3.0,0.0,3.0, SURF_ID='OPEN' /
&VENT XB=0.0,5.0,3.0,3.0,0.0,3.0, SURF_ID='OPEN' /
&VENT XB=0.0,5.0,0.0,3.0,3.0,3.0 SURF_ID='OPEN' /

&DEVC ID='TC11', QUANTITY='TEMPERATURE', XYZ=0.5,0.4,0.3/
&DEVC ID='TC12', QUANTITY='TEMPERATURE', XYZ=0.5,0.4,0.8/
&DEVC ID='TC13', QUANTITY='TEMPERATURE', XYZ=0.5,0.4,1.3/
&DEVC ID='TC14', QUANTITY='TEMPERATURE', XYZ=0.5,0.4,1.8/
&DEVC ID='TC15', QUANTITY='TEMPERATURE', XYZ=0.5,0.4,2.3/
&DEVC ID='TC21', QUANTITY='TEMPERATURE', XYZ=3.9,0.4,0.3/
&DEVC ID='TC22', QUANTITY='TEMPERATURE', XYZ=3.9,0.4,0.8/
&DEVC ID='TC23', QUANTITY='TEMPERATURE', XYZ=3.9,0.4,1.3/
&DEVC ID='TC24', QUANTITY='TEMPERATURE', XYZ=3.9,0.4,1.8/
&DEVC ID='TC25', QUANTITY='TEMPERATURE', XYZ=3.9,0.4,2.3/
&DEVC ID='TC31', QUANTITY='TEMPERATURE', XYZ=2.2,0.4,0.3/
&DEVC ID='TC32', QUANTITY='TEMPERATURE', XYZ=2.2,0.4,0.8/
&DEVC ID='TC33', QUANTITY='TEMPERATURE', XYZ=2.2,0.4,1.3/
&DEVC ID='TC34', QUANTITY='TEMPERATURE', XYZ=2.2,0.4,1.8/
&DEVC ID='TC35', QUANTITY='TEMPERATURE', XYZ=2.2,0.4,2.3/
&TAIL/
```

CASE 2:

```
Free burning - ISO9705Room_all_surfaces_VIP_kRamp2
&HEAD CHID='VIP',TITLE='free burning propane'/
&MESH IJK=100,60,60,XB=0.0,5.0,0.0,3.0,0.0,3.0/ 5 cm grid
&TIME T_END=2400.0/
&MISC SURF_DEFAULT='INERT'/
&RADI NUMBER_RADIATION_ANGLES=1000/

&SURF ID='BURNER',HRRPUA=1000.,COLOR='SILVER'/
&OBST XB=1.2,3.2,1.0,2.0,0.0,0.1 SURF_IDS='BURNER','INERT','INERT'/
&REAC ID='PROPANE'
SOOT_YIELD=0.015
C=3.
H=8.
HEAT_OF_COMBUSTION=46450
IDEAL=.TRUE./

&MATL ID='VIP'
CONDUCTIVITY_RAMP='k_VIP'
SPECIFIC_HEAT_RAMP='c_VIP'
DENSITY=192/

&RAMP ID='k_VIP', T=20.,F=0.004/
&RAMP ID='k_VIP', T=900.,F=0.5/
&RAMP ID='c_VIP', T=43.,F=0.726/
&RAMP ID='c_VIP', T=178.,F=0.915/

&SURF ID='VIP_WALL'
BACKING='EXPOSED'
MATL_ID = 'VIP'
THICKNESS = 0.02
COLOR='GREEN'/

&OBST XB=0.4,0.4,0.3,2.7,0.0,2.4, SURF_IDS='VIP_WALL', 'VIP_WALL', 'VIP_WALL'/
&OBST XB=0.4,4.0,0.3,0.3,0.0,2.4, SURF_IDS='VIP_WALL', 'VIP_WALL', 'VIP_WALL'/
&OBST XB=4.0,4.0,0.3,2.7,0.0,2.4, SURF_IDS='VIP_WALL', 'VIP_WALL', 'VIP_WALL'/
&OBST XB=0.4,4.0,2.7,2.7,0.0,2.4, SURF_IDS='VIP_WALL', 'VIP_WALL', 'VIP_WALL'/
&OBST XB=0.4,4.0,0.3,2.7,2.4,2.4, SURF_IDS='VIP_WALL', 'VIP_WALL', 'VIP_WALL'/
&OBST XB=0.0,5.0,0.0,3.0,0.0,0.0, SURF_IDS='VIP_WALL', 'VIP_WALL', 'VIP_WALL'/
&HOLE XB=3.99,4.01,0.9,2.1,0.0,1.5/
&HOLE XB=0.39,0.41,0.7,2.3,0.5,1.5/
&VENT XB=0.0,0.0,0.0,3.0,0.0,3.0, SURF_ID='OPEN' /
&VENT XB=0.0,5.0,0.0,0.0,0.0,3.0, SURF_ID='OPEN' /
&VENT XB=5.0,5.0,0.0,3.0,0.0,3.0, SURF_ID='OPEN' /
&VENT XB=0.0,5.0,3.0,3.0,0.0,3.0, SURF_ID='OPEN' /
&VENT XB=0.0,5.0,0.0,3.0,3.0,3.0 SURF_ID='OPEN' /

&DEVC ID='TC11',  QUANTITY='TEMPERATURE', XYZ=0.5,0.4,0.3/
&DEVC ID='TC12',  QUANTITY='TEMPERATURE', XYZ=0.5,0.4,0.8/
&DEVC ID='TC13',  QUANTITY='TEMPERATURE', XYZ=0.5,0.4,1.3/
&DEVC ID='TC14',  QUANTITY='TEMPERATURE', XYZ=0.5,0.4,1.8/
&DEVC ID='TC15',  QUANTITY='TEMPERATURE', XYZ=0.5,0.4,2.3/
&DEVC ID='TC21', QUANTITY='TEMPERATURE', XYZ=3.9,0.4,0.3/
&DEVC ID='TC22', QUANTITY='TEMPERATURE', XYZ=3.9,0.4,0.8/
&DEVC ID='TC23', QUANTITY='TEMPERATURE', XYZ=3.9,0.4,1.3/
&DEVC ID='TC24', QUANTITY='TEMPERATURE', XYZ=3.9,0.4,1.8/
&DEVC ID='TC25', QUANTITY='TEMPERATURE', XYZ=3.9,0.4,2.3/
&DEVC ID='TC31', QUANTITY='TEMPERATURE', XYZ=2.2,0.4,0.3/
&DEVC ID='TC32', QUANTITY='TEMPERATURE', XYZ=2.2,0.4,0.8/
&DEVC ID='TC33', QUANTITY='TEMPERATURE', XYZ=2.2,0.4,1.3/
&DEVC ID='TC34', QUANTITY='TEMPERATURE', XYZ=2.2,0.4,1.8/
&DEVC ID='TC35', QUANTITY='TEMPERATURE', XYZ=2.2,0.4,2.3/

&TAIL/
```

CASE 3:

```
Free burning - ISO9705Room_all_surfaces_VIP_kRamp3
&HEAD CHID='VIP',TITLE='free burning propane'/
&MESH IJK=100,60,60,XB=0.0,5.0,0.0,3.0,0.0,3.0/ 5 cm grid
&TIME T_END=2400.0/
&MISC SURF_DEFAULT='INERT'/
&RADI NUMBER_RADIATION_ANGLES=1000/ 118 page user manual

&SURF ID='BURNER',HRRPUA=1000.,COLOR='SILVER'/
&OBST XB=1.2,3.2,1.0,2.0,0.0,0.1 SURF_IDS='BURNER','INERT','INERT'/
&REAC ID='PROPANE'
SOOT_YIELD=0.015
C=3.
H=8.
HEAT_OF_COMBUSTION=46450
IDEAL=.TRUE./   skatiit 25 lpp in user manual

&MATL ID='VIP'
CONDUCTIVITY_RAMP='k_VIP'
SPECIFIC_HEAT_RAMP='c_VIP'
DENSITY=192/
&RAMP ID='k_VIP', T=20.,F=0.004/
&RAMP ID='k_VIP', T=900.,F=1.0/
&RAMP ID='c_VIP', T=43.,F=0.726/
&RAMP ID='c_VIP', T=178.,F=0.915/

&SURF ID='VIP_WALL'
BACKING='EXPOSED'
MATL_ID = 'VIP'
THICKNESS = 0.02
COLOR='GREEN'/

&OBST XB=0.4,0.4,0.3,2.7,0.0,2.4, SURF_IDS='VIP_WALL', 'VIP_WALL', 'VIP_WALL'/
&OBST XB=0.4,4.0,0.3,0.3,0.0,2.4, SURF_IDS='VIP_WALL', 'VIP_WALL', 'VIP_WALL'/
&OBST XB=4.0,4.0,0.3,2.7,0.0,2.4, SURF_IDS='VIP_WALL', 'VIP_WALL', 'VIP_WALL'/
&OBST XB=0.4,4.0,2.7,2.7,0.0,2.4, SURF_IDS='VIP_WALL', 'VIP_WALL', 'VIP_WALL'/
&OBST XB=0.4,4.0,0.3,2.7,2.4,2.4, SURF_IDS='VIP_WALL', 'VIP_WALL', 'VIP_WALL'/
&OBST XB=0.0,5.0,0.0,3.0,0.0,0.0, SURF_IDS='VIP_WALL', 'VIP_WALL', 'VIP_WALL'/
&HOLE XB=3.99,4.01,0.9,2.1,0.0,1.5/
&HOLE XB=0.39,0.41,0.7,2.3,0.5,1.5/
&VENT XB=0.0,0.0,0.0,3.0,0.0,3.0, SURF_ID='OPEN' /
&VENT XB=0.0,5.0,0.0,0.0,0.0,3.0, SURF_ID='OPEN' /
&VENT XB=5.0,5.0,0.0,3.0,0.0,3.0, SURF_ID='OPEN' /
&VENT XB=0.0,5.0,3.0,3.0,0.0,3.0, SURF_ID='OPEN' /
&VENT XB=0.0,5.0,0.0,3.0,3.0,3.0 SURF_ID='OPEN' /

&DEVC ID='TC11', QUANTITY='TEMPERATURE', XYZ=0.5,0.4,0.3/
&DEVC ID='TC12', QUANTITY='TEMPERATURE', XYZ=0.5,0.4,0.8/
&DEVC ID='TC13', QUANTITY='TEMPERATURE', XYZ=0.5,0.4,1.3/
&DEVC ID='TC14', QUANTITY='TEMPERATURE', XYZ=0.5,0.4,1.8/
&DEVC ID='TC15', QUANTITY='TEMPERATURE', XYZ=0.5,0.4,2.3/
&DEVC ID='TC21', QUANTITY='TEMPERATURE', XYZ=3.9,0.4,0.3/
&DEVC ID='TC22', QUANTITY='TEMPERATURE', XYZ=3.9,0.4,0.8/
&DEVC ID='TC23', QUANTITY='TEMPERATURE', XYZ=3.9,0.4,1.3/
&DEVC ID='TC24', QUANTITY='TEMPERATURE', XYZ=3.9,0.4,1.8/
&DEVC ID='TC25', QUANTITY='TEMPERATURE', XYZ=3.9,0.4,2.3/
&DEVC ID='TC31', QUANTITY='TEMPERATURE', XYZ=2.2,0.4,0.3/
&DEVC ID='TC32', QUANTITY='TEMPERATURE', XYZ=2.2,0.4,0.8/
&DEVC ID='TC33', QUANTITY='TEMPERATURE', XYZ=2.2,0.4,1.3/
&DEVC ID='TC34', QUANTITY='TEMPERATURE', XYZ=2.2,0.4,1.8/
&DEVC ID='TC35', QUANTITY='TEMPERATURE', XYZ=2.2,0.4,2.3/

&TAIL/
```

CASE 4:

```
Free burning - ISO9705Room_all_surfaces_VIP_kRamp4
&HEAD CHID='VIP',TITLE='free burning propane'/
&MESH IJK=100,60,60,XB=0.0,5.0,0.0,3.0,0.0,3.0/ 5 cm grid
&TIME T_END=2400.0/
&MISC SURF_DEFAULT='INERT'/
&RADI NUMBER_RADIATION_ANGLES=1000/

&SURF ID='BURNER',HRRPUA=1000.,COLOR='SILVER'/
&OBST XB=1.2,3.2,1.0,2.0,0.0,0.1 SURF_IDS='BURNER','INERT','INERT'/
&REAC ID='PROPANE'
SOOT_YIELD=0.015
C=3.
H=8.
HEAT_OF_COMBUSTION=46450
IDEAL=.TRUE./   skatiit 25 lpp in user manual

&MATL ID='VIP'
CONDUCTIVITY_RAMP='k_VIP'
SPECIFIC_HEAT_RAMP='c_VIP'
DENSITY=192/
&RAMP ID='k_VIP', T=20.,F=0.004/
&RAMP ID='k_VIP', T=500.,F=0.05/
&RAMP ID='k_VIP',T=900.,F=60.0/
&RAMP ID='c_VIP', T=43.,F=0.726/
&RAMP ID='c_VIP', T=178.,F=0.915/

&SURF ID='VIP_WALL'
BACKING='EXPOSED'
MATL_ID = 'VIP'
THICKNESS = 0.02
COLOR='GREEN'/

&OBST XB=0.4,0.4,0.3,2.7,0.0,2.4, SURF_IDS='VIP_WALL', 'VIP_WALL', 'VIP_WALL'/
&OBST XB=0.4,4.0,0.3,0.3,0.0,2.4, SURF_IDS='VIP_WALL', 'VIP_WALL', 'VIP_WALL'/
&OBST XB=4.0,4.0,0.3,2.7,0.0,2.4, SURF_IDS='VIP_WALL', 'VIP_WALL', 'VIP_WALL'/
&OBST XB=0.4,4.0,2.7,2.7,0.0,2.4, SURF_IDS='VIP_WALL', 'VIP_WALL', 'VIP_WALL'/
&OBST XB=0.4,4.0,0.3,2.7,2.4,2.4, SURF_IDS='VIP_WALL', 'VIP_WALL', 'VIP_WALL'/
&OBST XB=0.0,5.0,0.0,3.0,0.0,0.0, SURF_IDS='VIP_WALL', 'VIP_WALL', 'VIP_WALL'/
&HOLE XB=3.99,4.01,0.9,2.1,0.0,1.5/
&HOLE XB=0.39,0.41,0.7,2.3,0.5,1.5/
&VENT XB=0.0,0.0,0.0,3.0,0.0,3.0, SURF_ID='OPEN' /
&VENT XB=0.0,5.0,0.0,0.0,0.0,3.0, SURF_ID='OPEN' /
&VENT XB=5.0,5.0,0.0,3.0,0.0,3.0, SURF_ID='OPEN' /
&VENT XB=0.0,5.0,3.0,3.0,0.0,3.0, SURF_ID='OPEN' /
&VENT XB=0.0,5.0,0.0,3.0,3.0,3.0 SURF_ID='OPEN' /

&DEVC ID='TC11', QUANTITY='TEMPERATURE', XYZ=0.5,0.4,0.3/
&DEVC ID='TC12', QUANTITY='TEMPERATURE', XYZ=0.5,0.4,0.8/
&DEVC ID='TC13', QUANTITY='TEMPERATURE', XYZ=0.5,0.4,1.3/
&DEVC ID='TC14', QUANTITY='TEMPERATURE', XYZ=0.5,0.4,1.8/
&DEVC ID='TC15', QUANTITY='TEMPERATURE', XYZ=0.5,0.4,2.3/
&DEVC ID='TC21', QUANTITY='TEMPERATURE', XYZ=3.9,0.4,0.3/
&DEVC ID='TC22', QUANTITY='TEMPERATURE', XYZ=3.9,0.4,0.8/
&DEVC ID='TC23', QUANTITY='TEMPERATURE', XYZ=3.9,0.4,1.3/
&DEVC ID='TC24', QUANTITY='TEMPERATURE', XYZ=3.9,0.4,1.8/
&DEVC ID='TC25', QUANTITY='TEMPERATURE', XYZ=3.9,0.4,2.3/
&DEVC ID='TC31', QUANTITY='TEMPERATURE', XYZ=2.2,0.4,0.3/
&DEVC ID='TC32', QUANTITY='TEMPERATURE', XYZ=2.2,0.4,0.8/
&DEVC ID='TC33', QUANTITY='TEMPERATURE', XYZ=2.2,0.4,1.3/
&DEVC ID='TC34', QUANTITY='TEMPERATURE', XYZ=2.2,0.4,1.8/
&DEVC ID='TC35', QUANTITY='TEMPERATURE', XYZ=2.2,0.4,2.3/

&TAIL/
```

Appendix B: Heating of the steel I section under the different temperature regimes: case 1 to case 4

	Case 1			Case 2			Case 3			Case 4		
FDS Time, s	Gas temperature,° C	Δ T, °C (steel)	T, °C (steel)	Gas temperature,° C	Δ T, °C (steel)	T, °C (steel)	Gas temperature, C	Δ T, °C (steel)	T, °C (steel)	Gas temperature, C	Δ T,°C (steel)	T,° C (steel)
0.00	20.00	0.00	20.00	20.00		20.00	20.00		20.00	20.00		20.00
2.40	130.51	0.10	20.10	124.86	0.09	20.09	125.48	0.09	20.09	127.68	0.10	20.10
4.80	551.23	0.65	20.75	568.80	0.69	20.78	552.26	0.65	20.74	502.59	0.55	20.64
7.20	744.93	1.24	21.98	697.21	1.06	21.84	684.90	1.01	21.76	713.60	1.12	21.76
9.60	839.09	1.69	23.67	762.52	1.31	23.15	716.24	1.13	22.88	753.44	1.27	23.03
12.00	799.42	1.48	25.15	650.77	0.90	24.05	649.60	0.90	23.78	723.16	1.15	24.19
14.40	802.12	1.49	26.65	696.88	1.05	25.11	635.68	0.86	24.64	740.88	1.22	25.40
16.80	829.95	1.63	28.28	682.17	1.00	26.11	617.86	0.81	25.45	702.47	1.07	26.48
19.20	844.03	1.71	29.99	630.43	0.84	26.95	660.98	0.93	26.38	719.05	1.13	27.61
21.60	825.56	1.61	31.60	730.05	1.17	28.12	649.76	0.90	27.28	705.63	1.08	28.69
24.00	838.31	1.67	33.27	719.02	1.13	29.25	693.03	1.04	28.31	710.30	1.10	29.79
26.40	842.56	1.70	34.97	720.33	1.13	30.39	667.10	0.95	29.26	718.50	1.13	30.91
28.80	839.71	1.68	36.65	683.62	1.00	31.39	644.20	0.88	30.14	775.66	1.36	32.28
31.20	804.28	1.49	38.14	700.88	1.06	32.45	701.01	1.06	31.20	763.49	1.31	33.58
33.61	805.93	1.50	39.64	684.89	1.00	33.45	686.05	1.01	32.21	752.25	1.26	34.84
36.00	813.57	1.54	41.18	720.45	1.13	34.58	683.70	1.00	33.21	745.76	1.23	36.07
38.41	826.18	1.60	42.78	741.28	1.21	35.80	687.85	1.01	34.23	756.95	1.28	37.35
40.80	831.56	1.63	44.41	708.18	1.08	36.88	682.94	1.00	35.22	759.09	1.28	38.63
43.20	853.79	1.75	46.16	728.88	1.16	38.04	699.73	1.05	36.28	768.32	1.32	39.95
45.60	858.34	1.78	47.93	697.67	1.04	39.08	660.35	0.92	37.20	719.76	1.12	41.08
48.00	817.96	1.55	49.49	749.94	1.24	40.33	654.27	0.90	38.10	735.03	1.18	42.26
50.40	835.73	1.64	51.13	723.68	1.14	41.46	673.98	0.96	39.06	727.98	1.15	43.41
52.80	822.82	1.57	52.71	722.71	1.13	42.60	709.41	1.08	40.14	736.31	1.18	44.59
55.20	817.02	1.54	54.25	734.65	1.18	43.77	683.43	0.99	41.14	736.17	1.18	45.78
57.60	818.02	1.55	55.80	749.47	1.24	45.01	698.71	1.04	42.18	718.09	1.11	46.89
60.00	847.57	1.71	57.50	731.47	1.16	46.18	695.07	1.03	43.21	741.42	1.20	48.09
62.40	827.80	1.60	59.10	734.63	1.17	47.35	701.53	1.05	44.26	755.23	1.26	49.35
64.80	827.21	1.59	60.69	712.53	1.09	48.44	694.83	1.03	45.29	791.43	1.42	50.77
67.20	840.14	1.66	62.35	751.95	1.24	49.68	700.70	1.05	46.34	742.19	1.20	51.97

69.60	843.74	1.68	64.02	744.94	1.21	50.90	705.19	1.06	47.40	767.91	1.31	53.28
72.00	830.60	1.60	65.63	720.33	1.12	52.01	754.81	1.26	48.66	767.55	1.31	54.59
74.41	833.99	1.62	67.25	750.04	1.23	53.24	701.10	1.05	49.71	771.27	1.32	55.91
76.80	864.32	1.79	69.04	726.93	1.14	54.38	706.50	1.06	50.77	757.79	1.26	57.17
79.20	852.63	1.72	70.76	737.69	1.18	55.56	714.36	1.09	51.86	789.79	1.40	58.57
81.60	864.45	1.79	72.55	734.63	1.17	56.73	689.34	1.00	52.87	798.63	1.45	60.02
84.00	852.44	1.72	74.27	715.31	1.09	57.82	682.07	0.98	53.84	814.64	1.52	61.55
86.40	823.49	1.56	75.83	762.92	1.28	59.10	701.80	1.04	54.89	807.25	1.49	63.03
88.80	821.59	1.55	77.37	753.28	1.24	60.34	735.34	1.17	56.06	820.74	1.55	64.58
91.20	832.95	1.61	78.98	744.89	1.20	61.55	705.45	1.06	57.11	816.11	1.53	66.11
93.61	805.44	1.46	80.44	723.66	1.12	62.67	706.12	1.06	58.17	818.19	1.54	67.65
96.00	812.14	1.49	81.94	729.93	1.14	63.81	712.56	1.08	59.25	822.37	1.56	69.21
98.40	845.90	1.67	83.61	799.77	1.45	65.25	737.89	1.18	60.43	820.05	1.54	70.75
100.80	847.96	1.68	85.29	757.85	1.25	66.51	713.64	1.08	61.51	812.83	1.51	72.26
103.20	834.25	1.61	86.90	732.66	1.15	67.66	713.08	1.08	62.59	781.13	1.35	73.61
105.60	854.91	1.72	88.61	738.14	1.17	68.83	691.09	1.00	63.59	809.08	1.48	75.09
108.00	872.90	1.82	90.44	747.92	1.21	70.04	719.20	1.10	64.68	781.61	1.35	76.44
110.40	859.03	1.74	92.18	762.92	1.27	71.31	714.15	1.08	65.76	802.93	1.45	77.90
112.80	823.49	1.54	93.72	746.82	1.20	72.51	709.36	1.06	66.83	789.85	1.39	79.28
115.20	824.82	1.55	95.27	762.35	1.27	73.78	697.48	1.02	67.84	801.87	1.44	80.73
117.60	834.48	1.60	96.87	724.99	1.11	74.89	695.29	1.01	68.85	794.54	1.41	82.13
120.00	842.43	1.64	98.51	727.33	1.12	76.01	713.79	1.07	69.93	814.07	1.50	83.63
122.40	844.50	1.65	100.16	750.45	1.21	77.22	746.88	1.20	71.13	781.52	1.34	84.98
124.80	848.77	1.67	101.83	786.59	1.37	78.60	730.73	1.14	72.27	780.71	1.34	86.32
127.20	847.00	1.66	103.49	733.53	1.14	79.74	729.14	1.13	73.40	781.69	1.34	87.66
129.60	846.77	1.66	105.15	749.91	1.21	80.95	693.43	1.00	74.40	809.60	1.47	89.13
132.00	823.36	1.53	106.68	782.55	1.35	82.30	705.60	1.04	75.44	800.62	1.43	90.56
134.40	855.26	1.70	108.38	755.76	1.23	83.53	730.92	1.13	76.57	770.35	1.29	91.85
136.80	840.84	1.62	110.00	740.52	1.17	84.69	719.42	1.09	77.66	762.65	1.25	93.10
139.20	859.46	1.73	111.73	741.63	1.17	85.86	745.23	1.19	78.85	777.55	1.32	94.41
141.60	822.56	1.52	113.25	774.11	1.31	87.17	724.25	1.11	79.95	794.45	1.39	95.81
144.00	811.00	1.46	114.71	770.18	1.29	88.46	720.34	1.09	81.04	773.60	1.30	97.10
146.40	825.14	1.53	116.24	754.07	1.22	89.67	725.81	1.11	82.15	777.49	1.31	98.42
148.80	832.21	1.57	117.80	754.18	1.22	90.89	708.17	1.04	83.20	767.02	1.26	99.68
151.2	848.5	1.66	119.4	753.0	1.21	92.10	728.3	1.12	84.31	765.5	1.26	100.9

0	6		6	4			6			3		4
153.60	861.54	1.73	121.19	748.10	1.19	93.29	715.78	1.07	85.38	767.58	1.26	102.20
156.00	829.47	1.55	122.74	746.91	1.18	94.47	719.60	1.08	86.46	747.43	1.18	103.38
158.40	821.79	1.51	124.24	747.49	1.18	95.66	727.31	1.11	87.57	766.40	1.26	104.64
160.80	833.57	1.57	125.81	752.68	1.21	96.86	702.08	1.02	88.59	745.83	1.17	105.81
163.20	862.10	1.73	127.54	763.47	1.25	98.11	732.39	1.13	89.72	763.94	1.24	107.05
165.60	842.38	1.61	129.15	767.39	1.27	99.38	725.60	1.10	90.82	738.55	1.14	108.19
168.00	820.30	1.49	130.64	772.70	1.29	100.67	754.97	1.22	92.04	746.85	1.17	109.36
170.40	826.99	1.53	132.17	759.92	1.23	101.90	721.30	1.08	93.12	766.66	1.25	110.61
172.80	851.25	1.66	133.82	766.38	1.26	103.16	729.71	1.11	94.24	765.38	1.25	111.86
175.20	821.30	1.49	135.32	755.28	1.21	104.37	717.42	1.07	95.30	750.62	1.18	113.04
177.60	819.49	1.48	136.80	787.20	1.35	105.72	716.82	1.06	96.36	757.75	1.21	114.25
180.01	843.78	1.61	138.41	764.80	1.25	106.97	717.96	1.07	97.43	785.98	1.34	115.59
182.40	821.33	1.49	139.90	732.73	1.11	108.08	759.41	1.23	98.66	779.04	1.30	116.89
184.80	857.71	1.69	141.59	739.15	1.14	109.22	751.32	1.20	99.86	779.98	1.31	118.20
187.20	872.62	1.78	143.37	761.43	1.23	110.45	778.68	1.32	101.18	770.51	1.26	119.46
189.60	827.80	1.52	144.88	779.81	1.31	111.76	736.14	1.13	102.31	785.38	1.33	120.79
192.00	817.09	1.46	146.35	764.53	1.24	113.00	717.99	1.06	103.37	757.15	1.20	121.99
194.40	834.75	1.55	147.90	759.72	1.22	114.22	735.12	1.13	104.49	776.74	1.29	123.28
196.80	850.04	1.64	149.54	771.74	1.27	115.49	732.83	1.12	105.61	777.14	1.29	124.56
199.20	841.58	1.59	151.12	786.51	1.34	116.83	744.60	1.16	106.77	764.40	1.23	125.79
201.60	856.21	1.67	152.79	772.66	1.27	118.11	730.54	1.11	107.88	756.31	1.19	126.99
204.00	856.71	1.67	154.46	779.89	1.30	119.41	716.71	1.05	108.93	748.40	1.16	128.15
206.40	845.13	1.60	156.07	781.10	1.31	120.72	726.44	1.09	110.02	780.91	1.30	129.45
208.80	830.59	1.52	157.59	779.63	1.30	122.02	747.00	1.17	111.19	785.61	1.32	130.77
211.20	826.83	1.50	159.09	758.59	1.21	123.23	764.32	1.24	112.43	775.02	1.27	132.04
213.60	842.90	1.59	160.68	744.73	1.15	124.38	749.92	1.18	113.61	766.00	1.23	133.27
216.00	821.80	1.47	162.15	791.32	1.35	125.73	739.12	1.13	114.74	796.35	1.37	134.64
218.40	854.83	1.65	163.80	745.86	1.15	126.88	692.46	0.96	115.70	777.32	1.28	135.92
220.80	855.08	1.65	165.45	761.80	1.22	128.09	748.97	1.17	116.87	806.38	1.42	137.33
223.20	833.01	1.53	166.98	766.58	1.24	129.33	731.35	1.10	117.97	791.64	1.34	138.67
225.61	850.26	1.62	168.60	762.89	1.22	130.55	755.62	1.20	119.17	808.70	1.42	140.10
228.00	842.07	1.57	170.17	781.85	1.30	131.85	730.51	1.09	120.26	766.01	1.22	141.32
230.40	847.78	1.60	171.78	755.79	1.19	133.04	738.86	1.13	121.39	791.20	1.34	142.66
232.80	849.94	1.61	173.39	773.21	1.26	134.30	760.63	1.22	122.60	783.27	1.30	143.96

235.20	874.36	1.76	175.15	781.82	1.30	135.60	758.91	1.21	123.81	764.30	1.21	145.17
237.60	834.61	1.53	176.68	803.50	1.40	137.00	769.12	1.25	125.06	786.28	1.31	146.48
240.00	832.99	1.52	178.19	812.42	1.44	138.44	731.01	1.09	126.15	808.80	1.42	147.90
242.40	853.39	1.63	179.82	784.60	1.31	139.75	739.38	1.12	127.27	770.02	1.23	149.13
244.80	849.40	1.60	181.42	809.96	1.43	141.18	735.48	1.11	128.38	770.43	1.23	150.36
247.20	842.95	1.57	182.99	754.03	1.17	142.35	744.12	1.14	129.52	769.96	1.23	151.60
249.60	863.81	1.68	184.68	770.63	1.24	143.59	760.35	1.21	130.73	767.86	1.22	152.82
252.00	875.63	1.75	186.43	783.10	1.30	144.89	753.15	1.18	131.90	764.08	1.20	154.02
254.40	860.43	1.66	188.09	796.47	1.36	146.25	766.39	1.23	133.14	774.04	1.25	155.26
256.80	855.50	1.63	189.72	752.75	1.16	147.41	762.86	1.22	134.35	773.08	1.24	156.51
259.20	851.06	1.60	191.33	765.69	1.21	148.62	783.98	1.31	135.66	765.70	1.21	157.71
261.60	846.14	1.58	192.90	775.88	1.26	149.88	759.48	1.20	136.86	788.37	1.31	159.02
264.00	833.34	1.50	194.41	754.34	1.16	151.05	729.52	1.07	137.93	751.46	1.14	160.16
266.40	833.40	1.50	195.91	775.93	1.26	152.30	742.45	1.13	139.06	760.73	1.18	161.34
268.80	819.64	1.43	197.33	766.05	1.21	153.52	750.41	1.16	140.22	787.52	1.30	162.65
271.20	839.53	1.53	198.87	776.30	1.26	154.77	738.20	1.11	141.32	756.33	1.16	163.81
273.60	859.29	1.64	200.51	768.11	1.22	155.99	755.61	1.18	142.50	765.68	1.20	165.01
276.00	854.05	1.61	202.12	794.97	1.34	157.33	762.03	1.20	143.70	776.39	1.25	166.25
278.40	842.20	1.54	203.67	766.53	1.21	158.54	751.92	1.16	144.86	730.50	1.05	167.30
280.80	845.51	1.56	205.23	751.36	1.14	159.69	734.31	1.09	145.95	736.35	1.07	168.38
283.20	829.26	1.47	206.69	773.91	1.24	160.93	754.80	1.17	147.12	754.73	1.15	169.53
285.60	834.67	1.50	208.19	800.41	1.36	162.29	727.20	1.06	148.17	724.27	1.02	170.55
288.00	861.18	1.65	209.84	772.76	1.23	163.52	722.50	1.04	149.21	736.13	1.07	171.62
290.40	867.64	1.68	211.52	778.79	1.26	164.78	769.38	1.23	150.44	762.38	1.18	172.80
292.80	842.99	1.54	213.06	781.77	1.27	166.05	756.41	1.17	151.61	741.62	1.09	173.89
295.20	853.03	1.59	214.65	798.04	1.35	167.40	709.88	0.99	152.60	727.04	1.03	174.92
297.60	883.28	1.77	216.42	767.56	1.20	168.60	741.89	1.11	153.71	715.39	0.99	175.90
300.00	863.05	1.65	218.07	782.32	1.27	169.87	734.67	1.08	154.78	703.29	0.94	176.85
302.40	858.38	1.62	219.69	777.49	1.25	171.12	728.45	1.05	155.84	718.66	1.00	177.84
304.80	833.46	1.48	221.17	767.63	1.20	172.32	750.21	1.14	156.98	751.64	1.13	178.97
307.20	830.39	1.46	222.63	772.73	1.22	173.55	796.49	1.35	158.33	743.32	1.09	180.06
309.60	842.58	1.53	224.16	786.79	1.29	174.83	737.32	1.09	159.41	757.40	1.15	181.21
312.00	826.94	1.44	225.60	774.13	1.23	176.06	719.48	1.02	160.43	712.06	0.97	182.18
314.40	822.06	1.41	227.01	770.60	1.21	177.27	728.90	1.05	161.48	670.76	0.82	183.00
316.8	833.8	1.47	228.4	778.8	1.25	178.5	767.2	1.21	162.6	705.8	0.94	183.9

0	8		8	5		2	0		9	6		4
319.20	849.60	1.56	230.04	777.11	1.24	179.75	752.21	1.14	163.83	679.96	0.85	184.79
321.60	841.18	1.51	231.55	776.08	1.23	180.99	721.60	1.02	164.85	689.39	0.88	185.68
324.00	838.30	1.49	233.04	789.53	1.29	182.28	743.81	1.11	165.96	697.23	0.91	186.59
326.40	827.11	1.43	234.48	767.99	1.19	183.47	755.42	1.15	167.11	704.16	0.93	187.52
328.80	853.11	1.57	236.05	764.26	1.18	184.65	763.42	1.19	168.30	721.93	1.00	188.52
331.20	851.12	1.56	237.61	795.55	1.32	185.96	751.99	1.14	169.43	721.09	0.99	189.51
333.60	864.47	1.64	239.25	774.87	1.22	187.18	728.00	1.04	170.47	710.04	0.95	190.47
336.00	852.26	1.56	240.81	788.79	1.28	188.47	732.16	1.05	171.53	681.22	0.85	191.32
338.40	812.71	1.35	242.16	771.29	1.20	189.67	737.90	1.08	172.60	678.48	0.84	192.16
340.80	812.72	1.35	243.51	767.00	1.18	190.85	730.61	1.05	173.65	709.38	0.95	193.10
343.20	830.66	1.44	244.95	775.74	1.22	192.07	731.39	1.05	174.70	698.85	0.91	194.01
345.60	827.27	1.42	246.37	756.71	1.13	193.21	712.52	0.98	175.67	696.20	0.90	194.91
348.00	836.12	1.47	247.83	798.63	1.32	194.53	744.21	1.10	176.77	711.37	0.95	195.86
350.40	855.72	1.58	249.41	760.66	1.15	195.68	712.25	0.97	177.74	694.65	0.89	196.75
352.80	821.09	1.38	250.79	763.91	1.16	196.84	745.92	1.10	178.84	697.59	0.90	197.65
355.20	842.96	1.50	252.29	797.90	1.32	198.16	746.08	1.10	179.95	698.97	0.90	198.56
357.60	852.29	1.55	253.84	771.92	1.20	199.36	765.42	1.18	181.13	709.38	0.94	199.50
360.00	845.97	1.51	255.36	776.99	1.22	200.57	729.03	1.03	182.16	680.79	0.84	200.34
362.40	815.67	1.35	256.71	766.35	1.17	201.74	759.80	1.16	183.32	739.16	1.05	201.39
364.80	800.33	1.27	257.98	764.15	1.16	202.90	729.30	1.03	184.35	753.04	1.11	202.50
367.20	833.56	1.44	259.42	783.35	1.24	204.14	733.14	1.05	185.40	718.46	0.97	203.48
369.60	839.10	1.47	260.89	792.86	1.29	205.43	757.48	1.14	186.54	703.57	0.92	204.39
372.00	846.51	1.51	262.40	815.98	1.40	206.83	721.52	1.00	187.54	694.32	0.88	205.27
374.40	856.14	1.56	263.96	788.30	1.26	208.09	773.32	1.21	188.75	706.60	0.92	206.20
376.80	825.87	1.39	265.35	778.57	1.22	209.31	769.06	1.19	189.94	699.53	0.90	207.10
379.20	859.48	1.58	266.93	779.10	1.22	210.53	740.54	1.07	191.01	728.92	1.01	208.10
381.60	854.25	1.55	268.48	777.34	1.21	211.73	787.75	1.27	192.29	688.04	0.86	208.96
384.00	863.27	1.60	270.08	758.39	1.12	212.86	769.37	1.19	193.48	702.93	0.91	209.87
386.40	852.69	1.54	271.61	818.78	1.41	214.27	741.00	1.07	194.54	680.34	0.83	210.70
388.80	875.13	1.67	273.28	812.69	1.37	215.64	742.30	1.07	195.62	702.84	0.91	211.60
391.20	873.82	1.66	274.94	805.39	1.34	216.98	727.25	1.01	196.63	703.11	0.91	212.51
393.60	848.91	1.51	276.45	809.51	1.36	218.33	728.70	1.02	197.64	722.34	0.98	213.49
396.00	827.20	1.39	277.83	790.78	1.26	219.60	716.92	0.97	198.61	732.64	1.02	214.50
398.40	833.26	1.42	279.25	789.51	1.26	220.85	747.11	1.09	199.70	698.29	0.89	215.39

400.80	828.34	1.39	280.64	769.90	1.16	222.02	726.35	1.00	200.71	700.60	0.89	216.28
403.20	801.14	1.25	281.89	819.12	1.40	223.42	711.33	0.95	201.65	687.01	0.85	217.13
405.60	820.79	1.35	283.24	818.80	1.40	224.82	736.75	1.04	202.70	675.94	0.81	217.93
408.01	805.82	1.27	284.51	790.26	1.25	226.07	767.94	1.17	203.87	675.25	0.80	218.74
410.40	814.17	1.31	285.83	769.51	1.16	227.23	748.27	1.09	204.96	714.47	0.94	219.68
412.80	856.53	1.54	287.37	767.56	1.15	228.38	755.56	1.12	206.08	689.94	0.85	220.53
415.20	828.52	1.38	288.75	838.53	1.50	229.87	763.10	1.15	207.23	686.47	0.84	221.37
417.60	844.79	1.47	290.22	827.18	1.43	231.31	718.28	0.97	208.19	687.78	0.84	222.21
420.00	852.68	1.51	291.74	781.80	1.21	232.52	741.51	1.06	209.25	707.85	0.91	223.13
422.40	848.26	1.49	293.22	792.52	1.26	233.78	753.18	1.10	210.35	694.27	0.86	223.99
424.80	843.89	1.46	294.68	773.28	1.17	234.94	754.56	1.11	211.46	693.33	0.86	224.85
427.20	881.07	1.68	296.36	781.81	1.21	236.15	739.34	1.04	212.51	690.70	0.85	225.70
429.60	846.18	1.47	297.83	770.65	1.15	237.30	750.12	1.09	213.59	704.92	0.90	226.60
432.00	875.90	1.64	299.48	783.00	1.21	238.51	735.71	1.03	214.62	717.42	0.94	227.54
434.40	845.22	1.46	300.94	795.97	1.27	239.78	747.90	1.08	215.70	676.20	0.80	228.34
436.80	821.56	1.33	302.27	795.03	1.26	241.04	756.46	1.11	216.81	683.14	0.82	229.16
439.20	821.69	1.33	303.60	787.11	1.22	242.27	752.05	1.09	217.90	696.98	0.87	230.03
441.60	844.61	1.45	305.05	772.85	1.16	243.42	762.38	1.13	219.04	717.58	0.94	230.97
444.00	851.35	1.49	306.54	787.96	1.23	244.65	738.88	1.04	220.07	692.48	0.85	231.82
446.40	846.79	1.46	308.01	786.05	1.22	245.86	724.27	0.98	221.05	686.43	0.83	232.65
448.80	815.67	1.29	309.30	764.68	1.12	246.98	764.70	1.14	222.19	662.42	0.75	233.40
451.20	837.49	1.41	310.71	767.17	1.13	248.11	741.43	1.04	223.23	676.84	0.79	234.19
453.60	856.80	1.52	312.22	763.95	1.11	249.22	700.17	0.88	224.12	719.89	0.95	235.14
456.00	836.72	1.40	313.62	768.97	1.13	250.35	726.84	0.98	225.10	676.67	0.79	235.93
458.40	838.25	1.41	315.03	804.19	1.30	251.65	755.06	1.10	226.20	690.17	0.84	236.77
460.80	851.32	1.48	316.51	770.15	1.14	252.79	761.18	1.12	227.32	703.67	0.88	237.65
463.20	856.01	1.50	318.01	765.01	1.11	253.90	751.69	1.08	228.40	694.65	0.85	238.50
465.60	834.11	1.38	319.39	785.44	1.20	255.10	719.54	0.95	229.35	715.38	0.93	239.43
468.00	852.00	1.48	320.87	792.75	1.24	256.34	761.71	1.12	230.47	691.32	0.84	240.26
470.40	838.81	1.40	322.27	774.02	1.15	257.49	725.07	0.97	231.44	732.68	0.99	241.25
472.80	861.43	1.53	323.80	791.36	1.23	258.71	744.70	1.05	232.49	683.26	0.81	242.06
475.21	846.53	1.44	325.25	815.79	1.35	260.06	762.17	1.12	233.60	703.36	0.88	242.94
477.60	851.49	1.47	326.71	771.78	1.13	261.19	753.69	1.08	234.69	698.97	0.86	243.80
480.00	856.20	1.49	328.21	779.34	1.17	262.36	728.36	0.98	235.67	717.43	0.93	244.73
482.4	832.8	1.36	329.5	806.6	1.30	263.6	730.2	0.98	236.6	712.2	0.91	245.6

0	9		7	1		6	6		5	2		4
484.81	827.09	1.33	330.90	772.95	1.14	264.79	738.25	1.02	237.67	717.49	0.93	246.56
487.20	845.99	1.43	332.33	742.68	1.01	265.80	742.36	1.03	238.70	757.66	1.09	247.65
489.60	829.42	1.34	333.67	775.79	1.15	266.95	729.68	0.98	239.68	678.59	0.79	248.43
492.00	843.77	1.41	335.08	764.21	1.09	268.04	793.09	1.25	240.93	690.08	0.82	249.26
494.40	865.23	1.54	336.62	748.68	1.03	269.07	809.82	1.33	242.26	690.13	0.82	250.08
496.80	845.80	1.42	338.04	775.96	1.14	270.21	752.20	1.07	243.33	726.24	0.95	251.04
499.20	848.12	1.43	339.48	781.80	1.17	271.38	766.87	1.13	244.46	746.27	1.03	252.07
501.61	835.04	1.36	340.84	778.27	1.15	272.53	773.13	1.16	245.62	740.27	1.01	253.08
504.00	834.55	1.36	342.19	786.01	1.19	273.72	728.12	0.97	246.58	704.70	0.87	253.95
506.40	863.61	1.52	343.71	775.76	1.14	274.86	752.67	1.07	247.65	680.64	0.79	254.74
508.80	855.81	1.47	345.18	778.38	1.15	276.01	731.60	0.98	248.63	680.49	0.79	255.52
511.21	849.88	1.44	346.62	816.19	1.33	277.34	706.39	0.88	249.51	691.54	0.82	256.35
513.60	853.12	1.45	348.07	806.97	1.28	278.62	739.65	1.01	250.52	701.29	0.86	257.20
516.00	832.70	1.34	349.41	804.37	1.27	279.89	756.70	1.08	251.60	668.64	0.74	257.94
518.40	830.22	1.32	350.73	758.17	1.05	280.95	736.13	0.99	252.59	701.06	0.85	258.80
520.80	825.04	1.29	352.02	784.73	1.17	282.12	765.51	1.11	253.70	789.53	1.22	260.02
523.20	865.27	1.52	353.54	818.12	1.33	283.45	726.39	0.95	254.66	715.02	0.90	260.92
525.60	846.10	1.40	354.94	759.71	1.06	284.51	720.47	0.93	255.58	667.43	0.74	261.65
528.00	874.50	1.57	356.51	757.79	1.05	285.56	734.49	0.98	256.57	683.66	0.79	262.44
530.40	824.66	1.28	357.79	790.10	1.19	286.75	742.32	1.01	257.58	694.46	0.83	263.27
532.80	834.95	1.34	359.13	783.88	1.16	287.91	724.13	0.94	258.52	702.42	0.85	264.12
535.20	839.74	1.36	360.49	778.84	1.14	289.05	781.00	1.18	259.69	714.27	0.90	265.02
537.61	842.71	1.38	361.87	789.59	1.19	290.24	738.97	1.00	260.69	670.61	0.74	265.76
540.01	844.67	1.39	363.26	785.66	1.17	291.40	719.45	0.92	261.61	661.44	0.71	266.47
542.40	831.06	1.31	364.57	771.38	1.10	292.50	742.76	1.01	262.62	697.30	0.83	267.30
544.81	847.00	1.40	365.96	792.57	1.20	293.70	740.60	1.00	263.62	687.49	0.80	268.10
547.20	828.82	1.29	367.26	787.47	1.17	294.87	738.58	0.99	264.61	682.05	0.78	268.88
549.60	828.06	1.29	368.54	779.07	1.13	296.00	738.98	0.99	265.60	691.31	0.81	269.68
552.00	847.01	1.39	369.93	766.98	1.08	297.08	763.79	1.09	266.69	651.18	0.68	270.36
554.40	847.23	1.39	371.32	785.04	1.16	298.23	734.30	0.97	267.66	666.66	0.72	271.08
556.80	856.09	1.44	372.76	790.05	1.18	299.41	741.64	1.00	268.66	701.62	0.84	271.93
559.20	820.81	1.24	374.01	753.84	1.02	300.43	768.88	1.11	269.77	651.02	0.67	272.60
561.60	831.37	1.30	375.30	753.42	1.01	301.44	747.77	1.02	270.79	693.52	0.81	273.41
564.00	844.09	1.37	376.67	783.91	1.15	302.58	753.01	1.04	271.83	730.32	0.95	274.36

566.40	869.10	1.51	378.18	806.83	1.26	303.84	751.68	1.04	272.87	732.03	0.95	275.31
568.80	854.00	1.42	379.60	784.47	1.15	304.99	763.09	1.08	273.95	696.75	0.82	276.13
571.20	853.30	1.41	381.01	799.84	1.22	306.20	729.67	0.94	274.90	697.79	0.82	276.95
573.60	852.82	1.41	382.42	769.64	1.08	307.28	751.89	1.03	275.93	720.02	0.90	277.86
576.00	861.07	1.45	383.87	800.89	1.22	308.50	741.77	0.99	276.92	707.65	0.86	278.71
578.40	846.00	1.36	385.23	790.11	1.17	309.67	754.24	1.04	277.96	669.48	0.72	279.44
580.80	851.42	1.39	386.63	779.49	1.12	310.79	741.51	0.99	278.95	673.62	0.74	280.18
583.20	834.43	1.30	387.93	747.06	0.97	311.76	721.87	0.91	279.86	695.38	0.81	280.99
585.60	845.09	1.35	389.28	779.60	1.11	312.87	756.78	1.05	280.90	712.72	0.87	281.86
588.00	874.30	1.52	390.80	781.43	1.12	314.00	774.29	1.12	282.03	715.97	0.88	282.74
590.40	855.69	1.41	392.21	778.38	1.11	315.10	723.26	0.91	282.94	728.78	0.93	283.67
592.80	851.01	1.38	393.60	778.94	1.11	316.21	725.50	0.92	283.86	718.65	0.89	284.56
595.20	845.95	1.35	394.95	763.75	1.04	317.25	740.53	0.98	284.83			
597.60	837.66	1.30	396.25	768.93	1.06	318.31	746.80	1.00	285.84			
600.00	834.77	1.29	397.54	799.51	1.20	319.51						
602.40	830.88	1.26	398.80									
604.80	842.86	1.33	400.13									
607.20	854.09	1.39	401.52									
609.60	861.73	1.43	402.95									
612.00	844.55	1.33	404.28									
614.40	840.66	1.31	405.59									
616.80	846.19	1.34	406.92									
619.20	856.25	1.39	408.32									
621.60	855.45	1.39	409.70									
624.00	814.99	1.16	410.87									
626.40	839.13	1.29	412.16									
628.80	831.53	1.25	413.40									
631.20	835.67	1.27	414.67									
633.60	862.06	1.41	416.08									
636.01	843.69	1.31	417.39									

Appendix C: The temperature measurements of the exposed surface of VIP samples.

The temperature measurements for the exposed surface are presented in the following graphs. Temperature on the exposed surfaces is measured with thermocouples 6, 7, 8, 9 and 10 (see figure 6.2.). Thermocouple nr.6 is located at the middle of the test sample. Several thermocouples had lost their positions during burning of the protective envelope, measurements of these thermocouples are not presented.

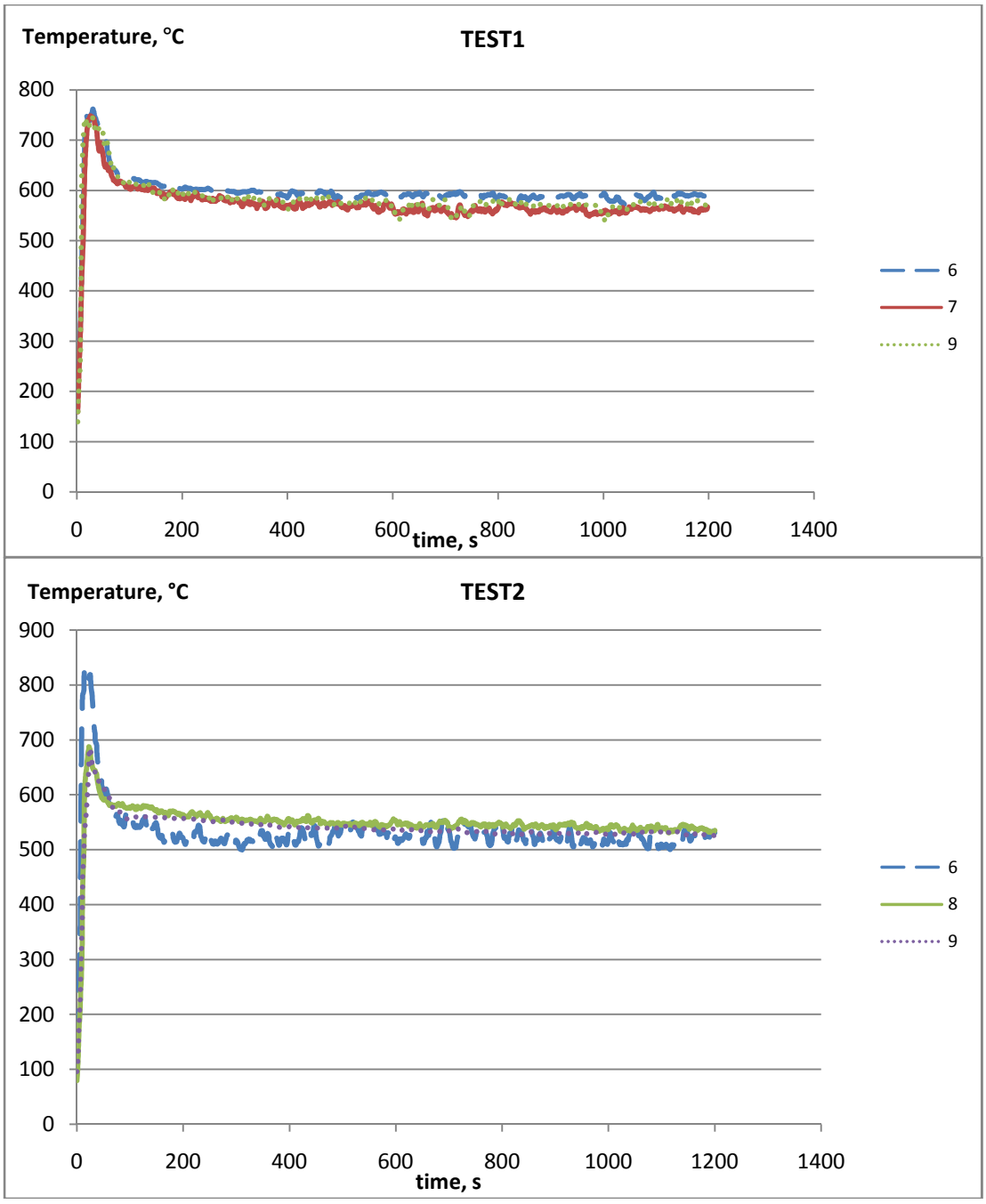

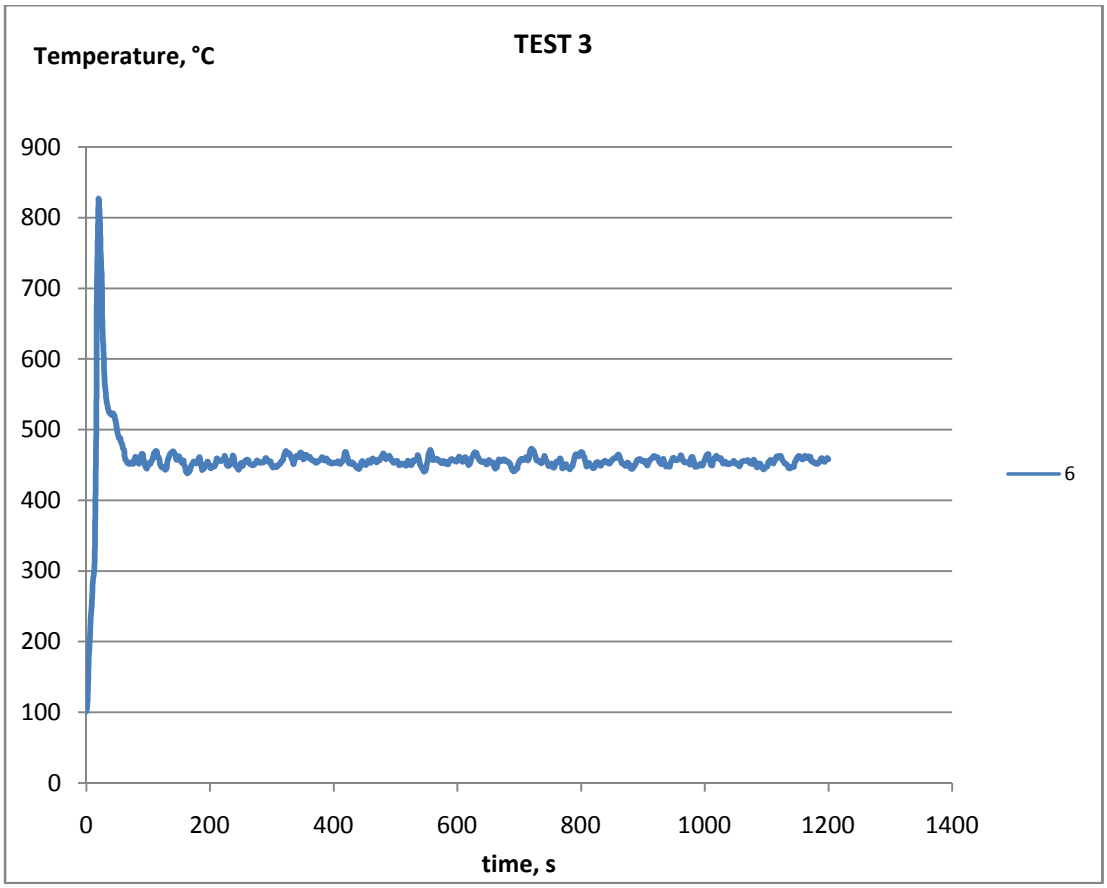
TEST 3
Temperature, °C
900
800
700
600
500
400
300
200
100
0
0
200
400
600
800
1000
1200
1400
time, s
6

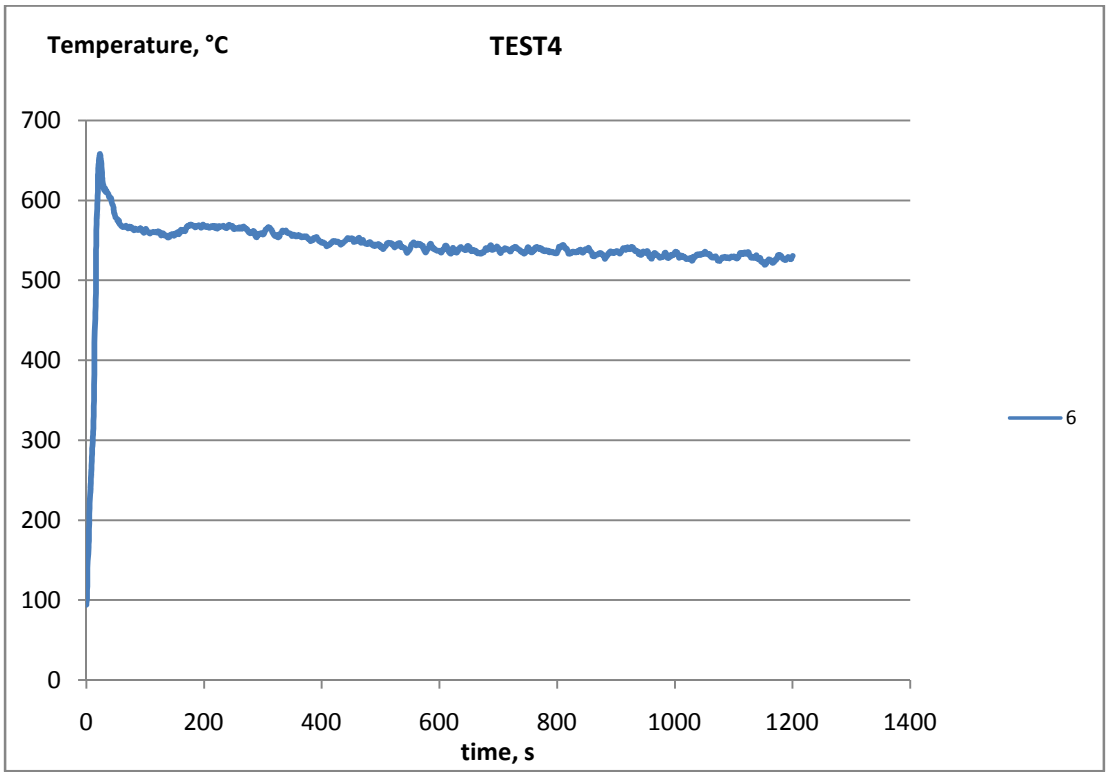
TEST4
Temperature, °C
700
600
500
400
300
200
100
0
0
200
400
600
800
1000
1200
1400
time, s
6

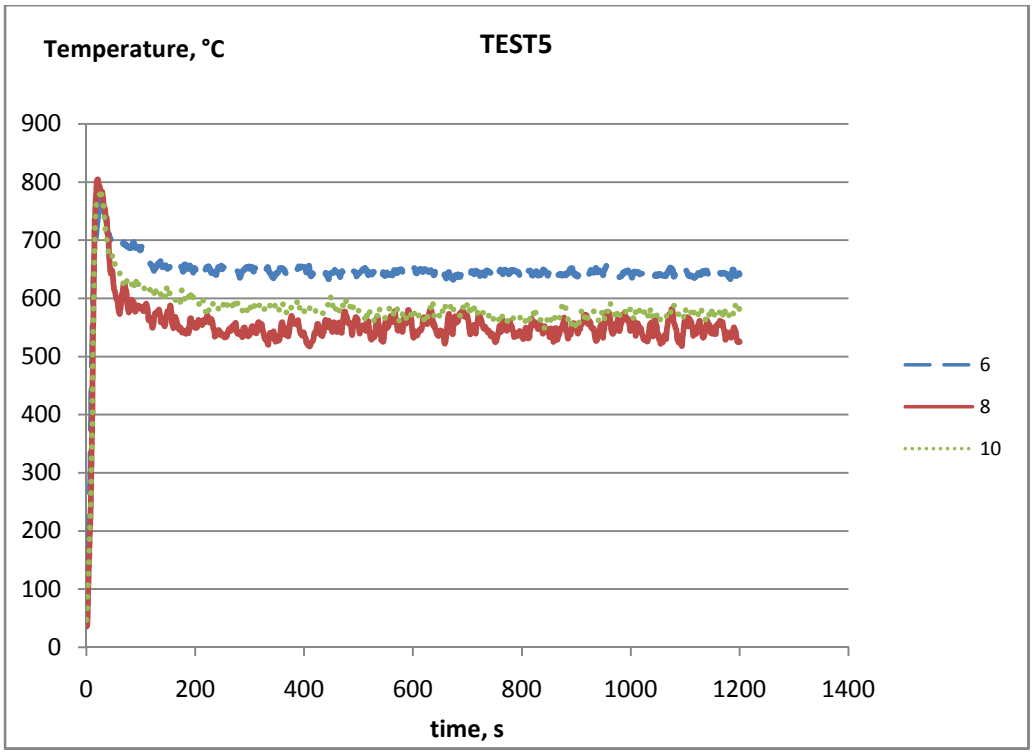
Temperature, °C
TEST5
900
800
700
600
500
400
300
200
100
0
0
200
400
600
800
1000
1200
1400
time, s
6
8
10

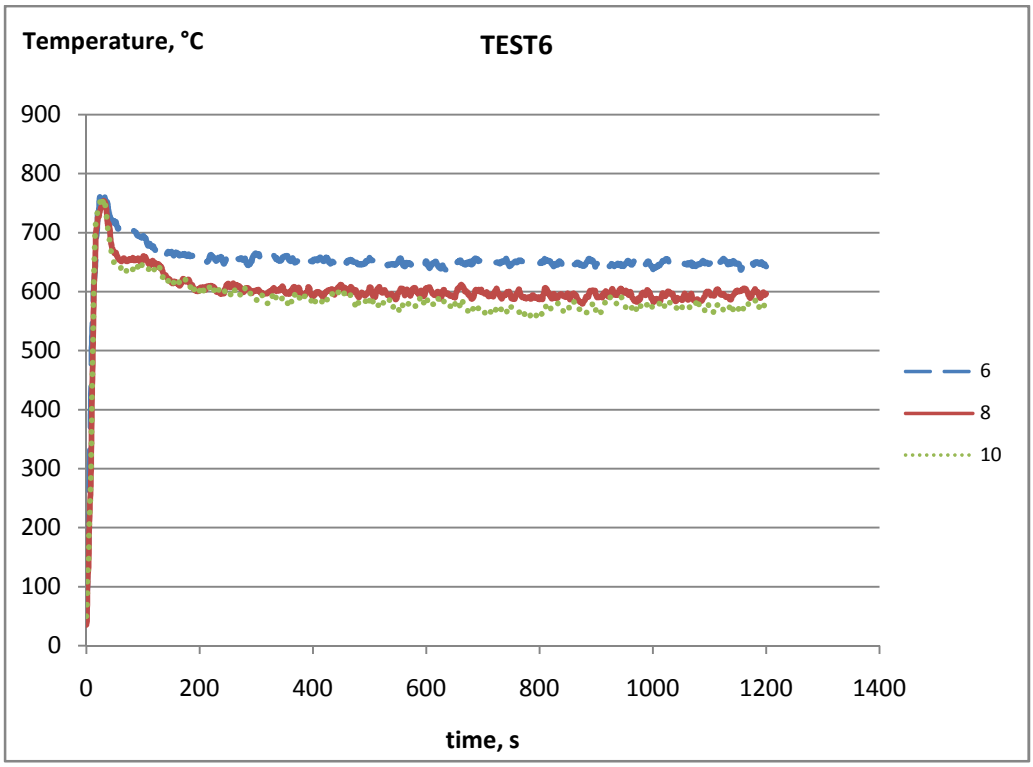
Temperature, °C
TEST6
900
800
700
600
500
400
300
200
100
0
0
200
400
600
800
1000
1200
1400
time, s
6
8
10

Appendix D: The temperature measurements of all the surfaces of the VIP sample.

The temperature measurements for all the surfaces are presented in following graphs. The graphs include:

- ✓ Exposed side average – average measured temperature of all the thermocouples located on the exposed side of the test samples. Several thermocouples had lost their positions during the test and the measurements of these thermocouples are not taken in account;
- ✓ Unexposed side average – average measured temperature from all the thermocouples located on the unexposed side of the sample;
- ✓ Exposed side middle – thermocouple nr.6 measurement (see figure 6.2);
- ✓ Unexposed side middle – thermocouple nr.1 measurement (see figure 6.2);
- ✓ Side thermocouple 11 – thermocouple nr.11 measurements (see figure 6.2);
- ✓ Side thermocouple 12 – thermocouple nr.12 measurements (see figure 6.2).

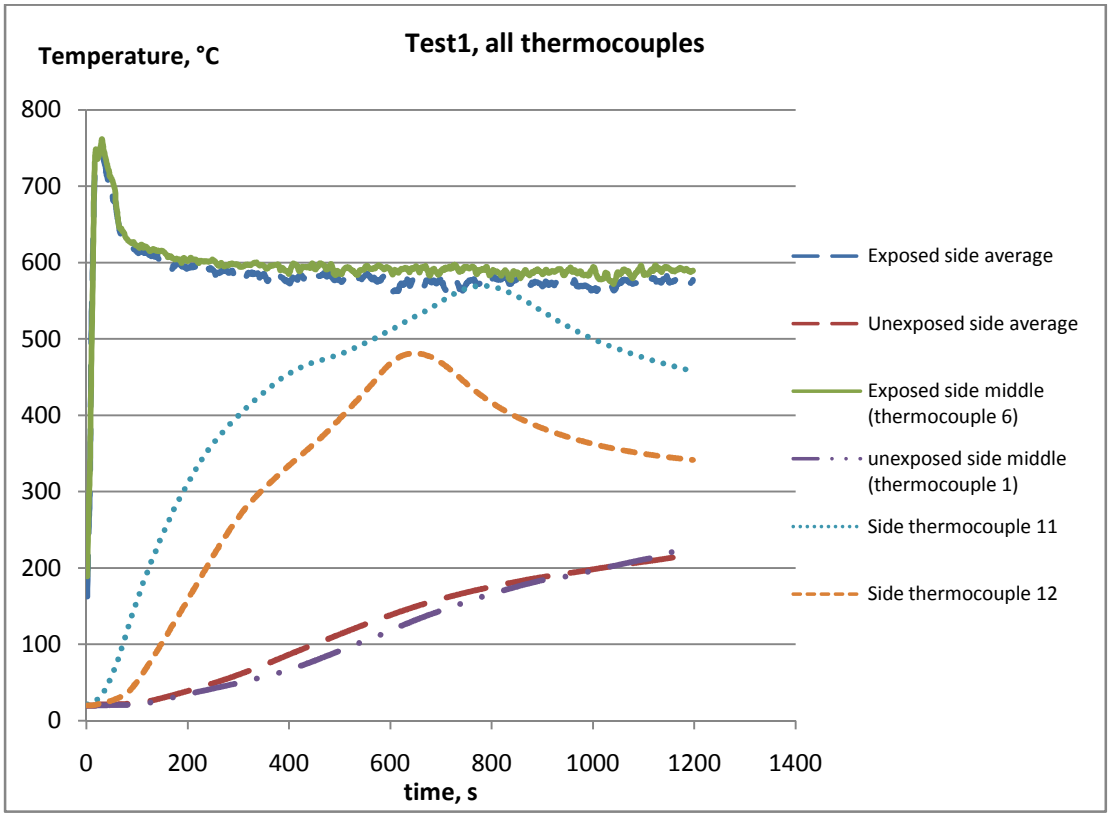

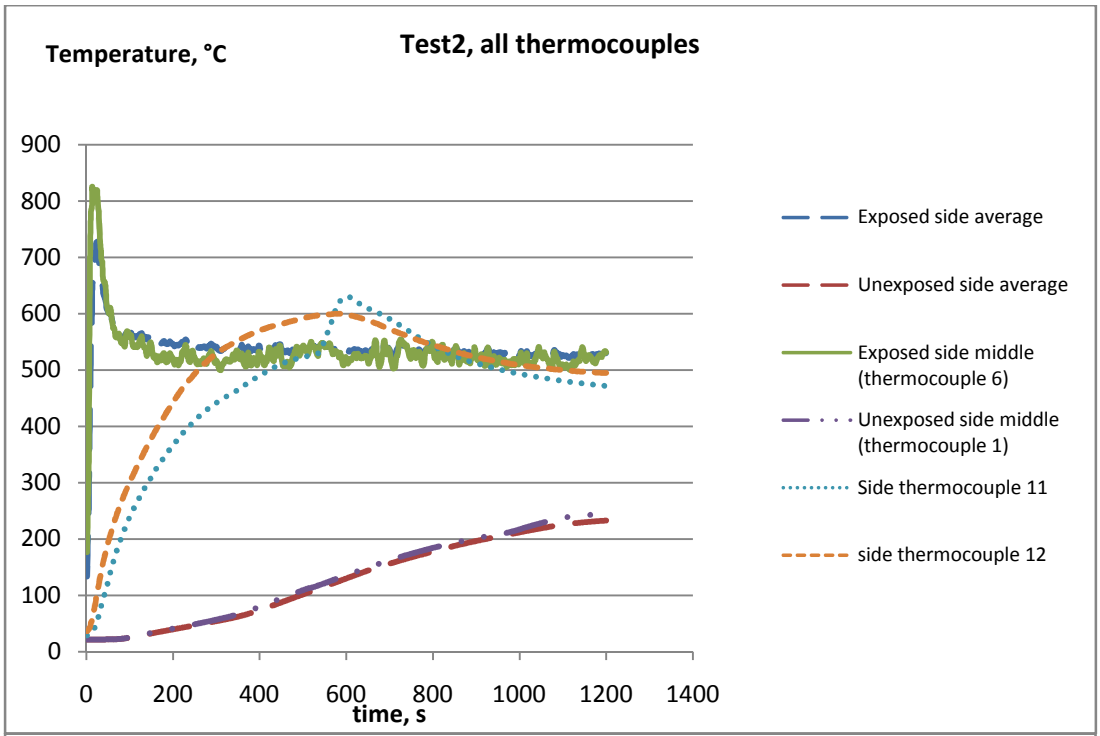
Temperature, °C
Test2, all thermocouples
900
800
700
600
500
400
300
200
100
0
0
200
400
600
800
1000
1200
1400
time, s
Exposed side average
Unexposed side average
Exposed side middle (thermocouple 6)
Unexposed side middle (thermocouple 1)
Side thermocouple 11
side thermocouple 12

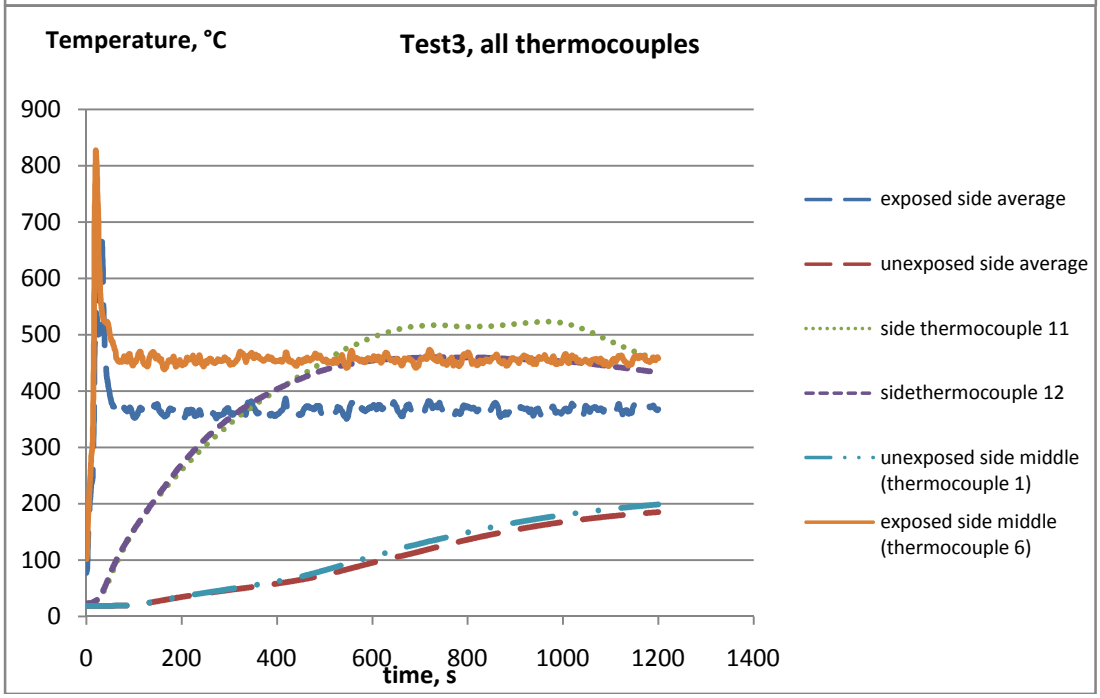
Temperature, °C
Test3, all thermocouples
900
800
700
600
500
400
300
200
100
0
0
200
400
600
800
1000
1200
1400
time, s
exposed side average
unexposed side average
side thermocouple 11
sidethermocouple 12
unexposed side middle (thermocouple 1)
exposed side middle (thermocouple 6)

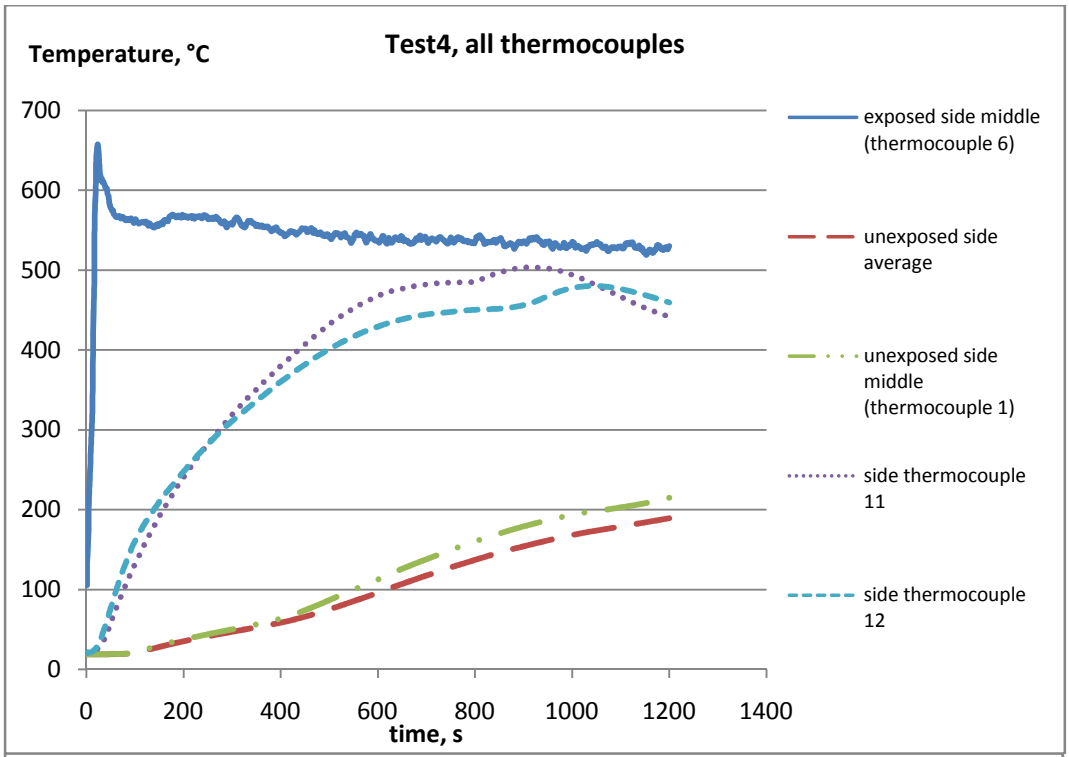
Test4, all thermocouples
Temperature, °C
700
600
500
400
300
200
100
0
0
200
400
600
800
1000
1200
1400
time, s
exposed side middle (thermocouple 6)
unexposed side average
unexposed side middle (thermocouple 1)
side thermocouple 11
side thermocouple 12

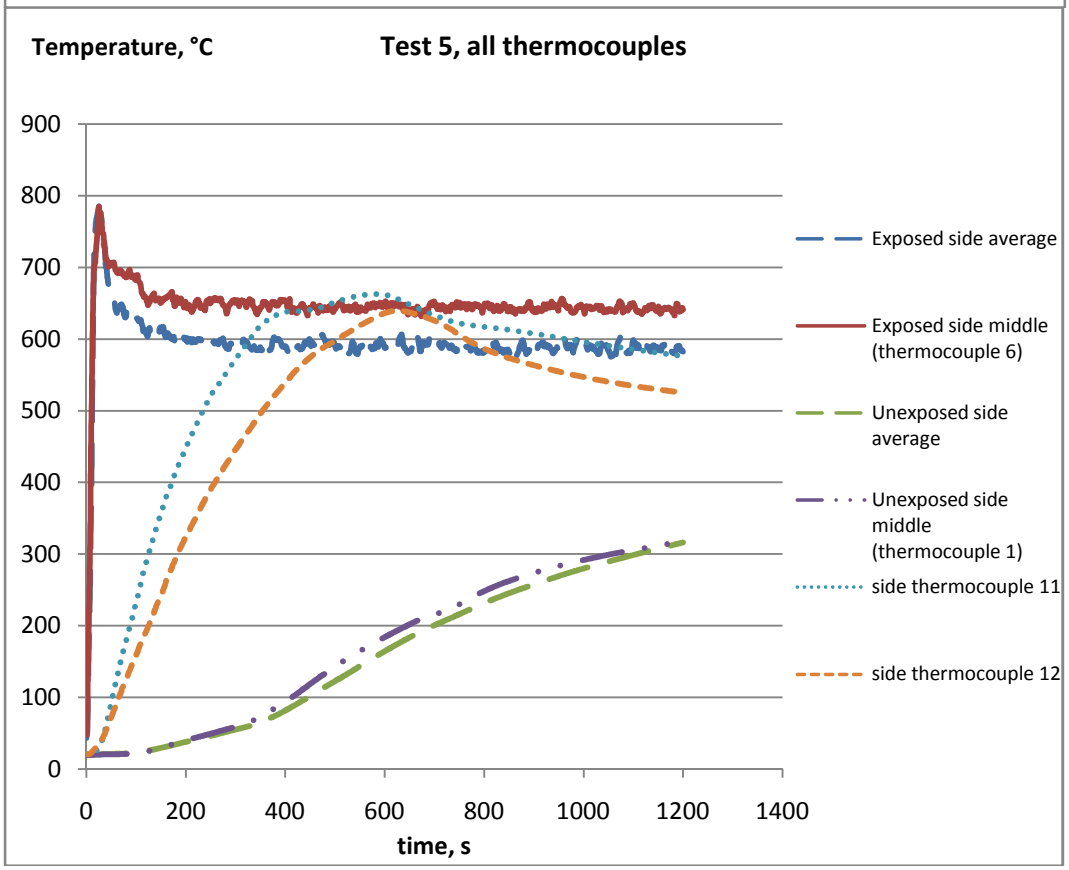
Test 5, all thermocouples
Temperature, °C
900
800
700
600
500
400
300
200
100
0
0
200
400
600
800
1000
1200
1400
time, s
Exposed side average
Exposed side middle (thermocouple 6)
Unexposed side average
Unexposed side middle (thermocouple 1)
side thermocouple 11
side thermocouple 12

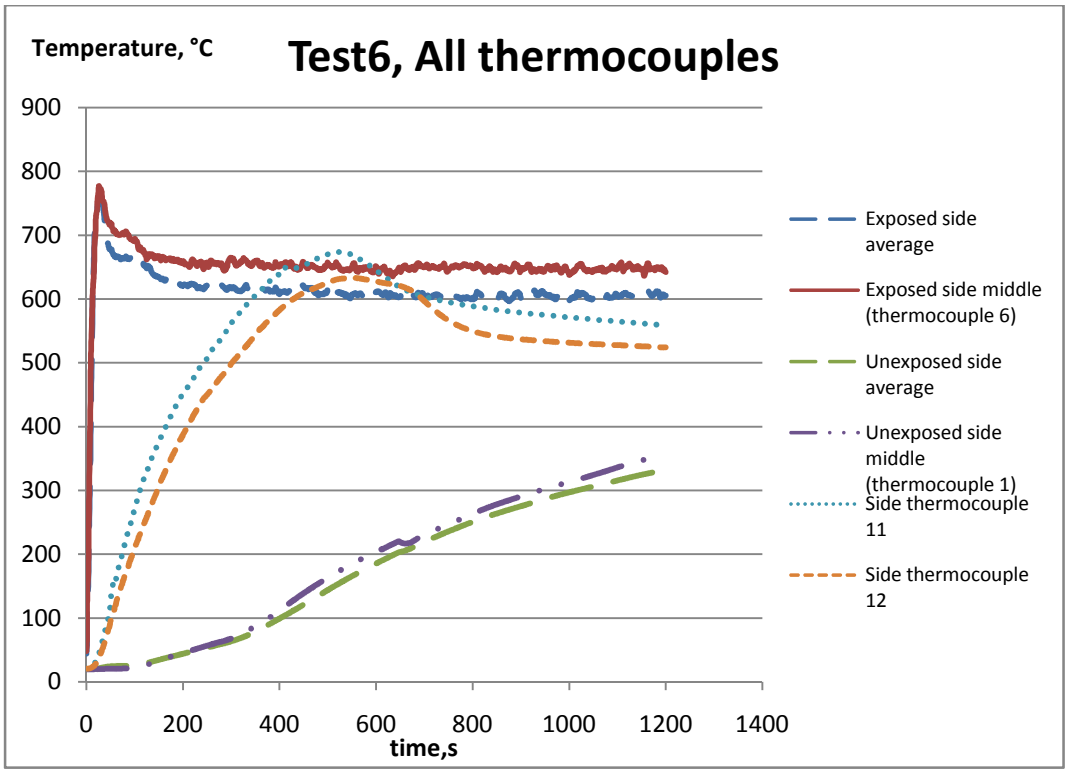
Temperature, °C
Test6, All thermocouples
900
800
700
600
500
400
300
200
100
0
0
200
400
600
800
1000
1200
1400
time,s
Exposed side average
Exposed side middle (thermocouple 6)
Unexposed side average
Unexposed side middle (thermocouple 1)
Side thermocouple 11
Side thermocouple 12

Appendix E: The temperature measurements of the unexposed surface of the VIP samples.

The temperature measurements for the unexposed surface are presented in following graphs. The temperature on the unexposed surface is measured with thermocouples 1, 2, 3, 4 and 5 (see figure 6.2.). Thermocouple nr.1 is located at the middle of the test sample. During test6 thermocouple nr.4 had failed and therefore it is not presented.

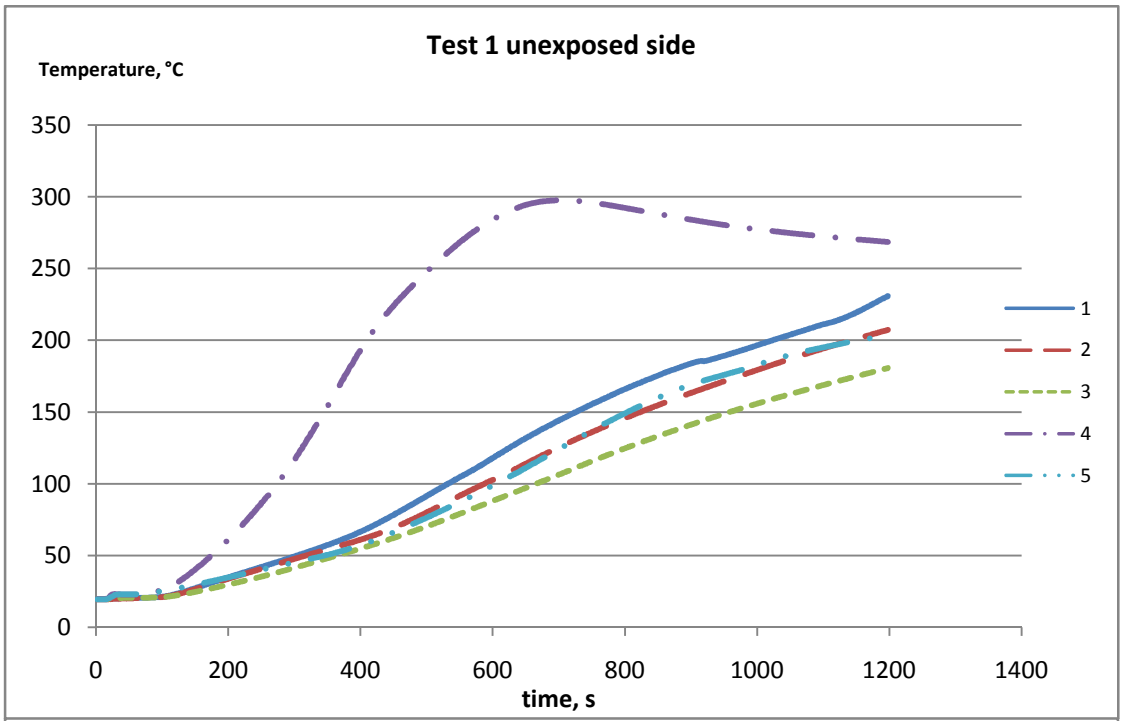

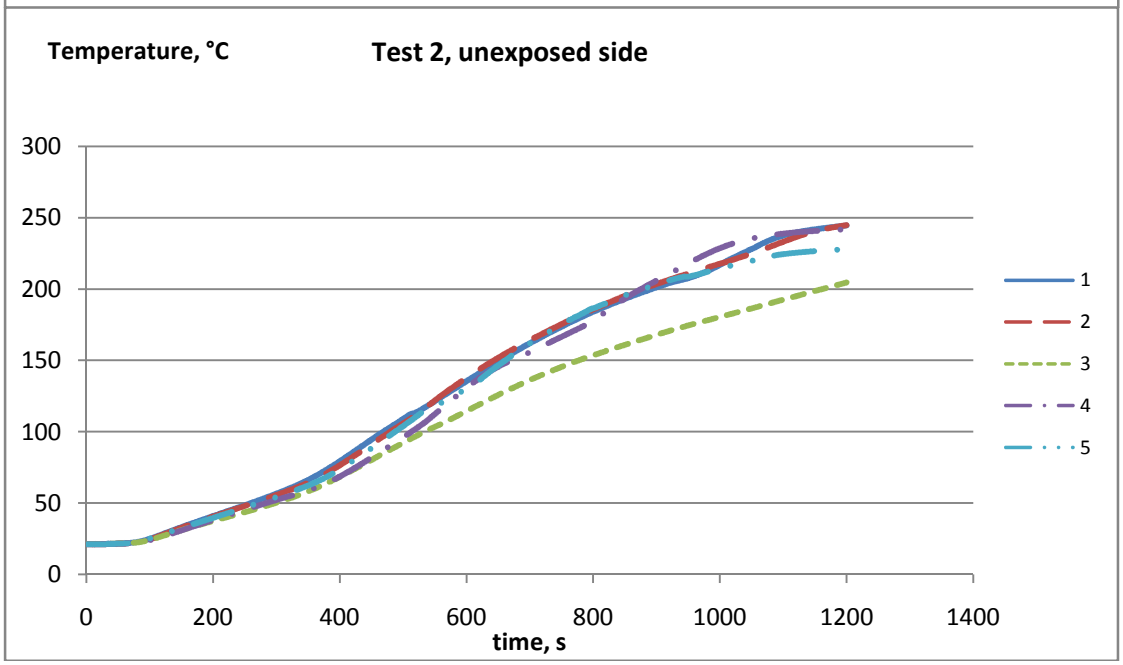

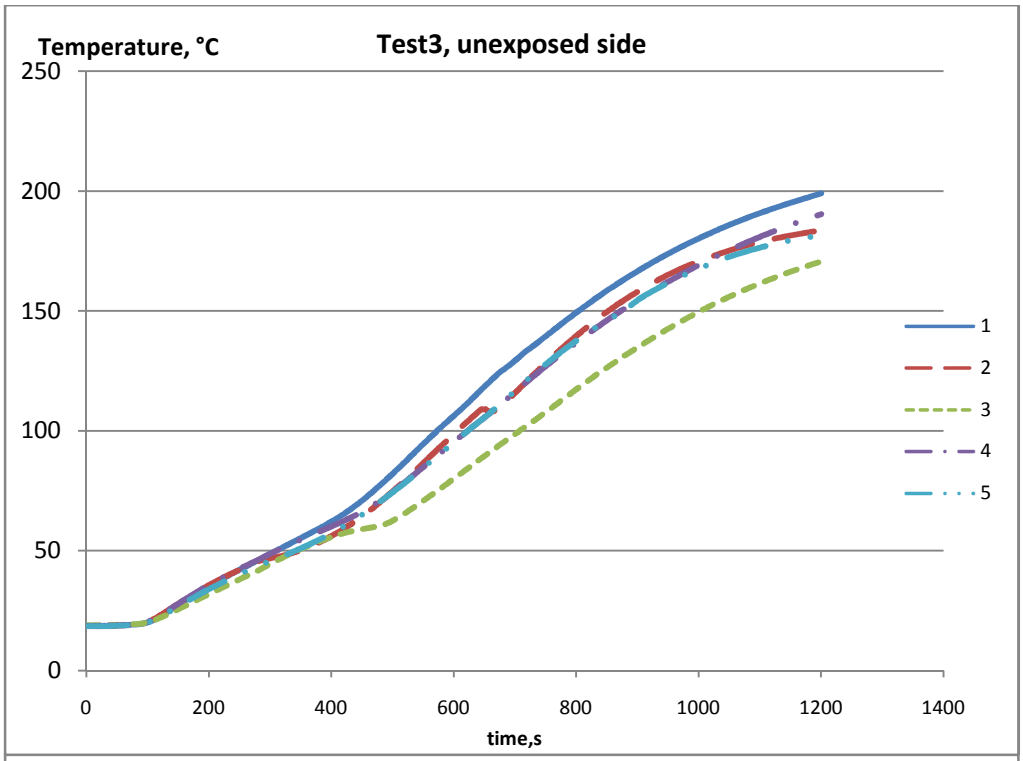
Test3, unexposed side
Temperature, °C
250
200
150
100
50
0
0
200
400
600
800
1000
1200
1400
time,s
1
2
3
4
5

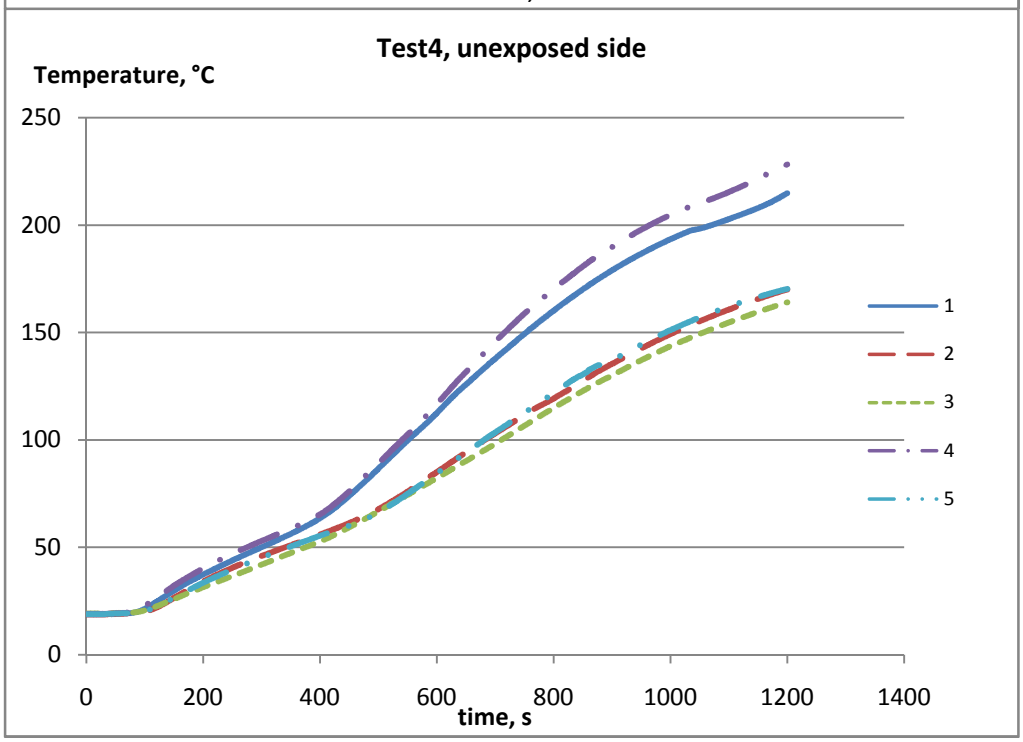
Test4, unexposed side
Temperature, °C
250
200
150
100
50
0
0
200
400
600
800
1000
1200
1400
time, s
1
2
3
4
5

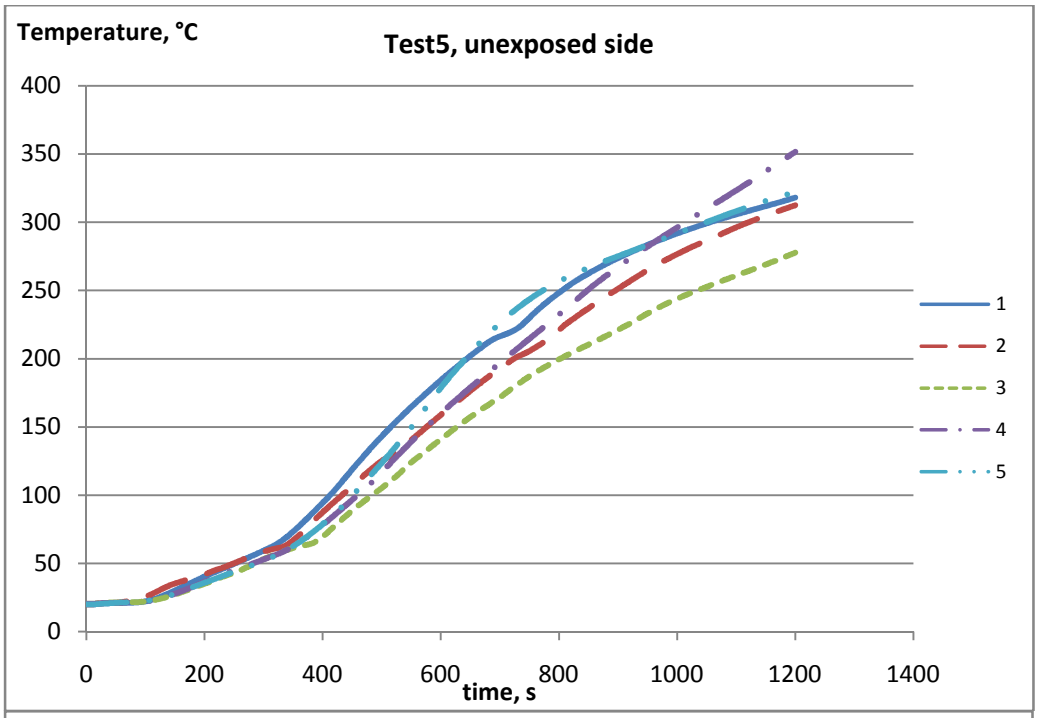
Temperature, °C
Test5, unexposed side
400
350
300
250
200
150
100
50
0
0
200
400
600
800
1000
1200
1400
time, s
1
2
3
4
5

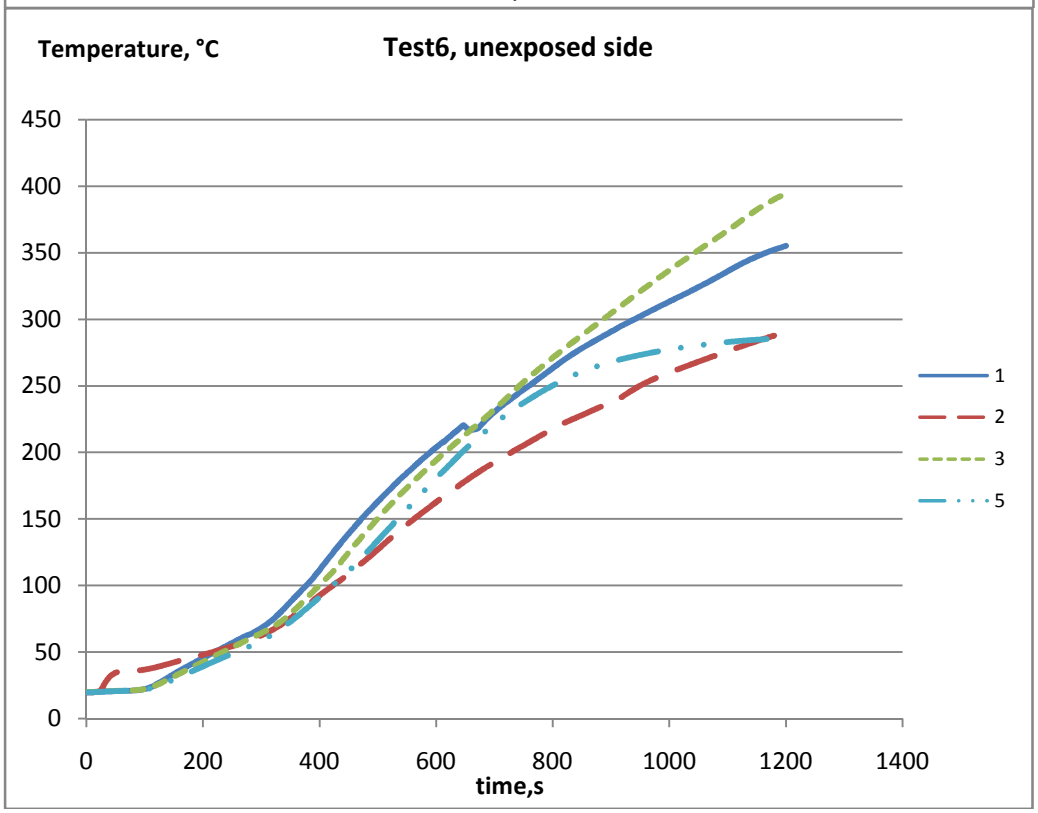
Temperature, °C
Test6, unexposed side
450
400
350
300
250
200
150
100
50
0
0
200
400
600
800
1000
1200
1400
time,s
1
2
3
5